Spectrotemporal processing and intrinsic functional connectivity in human auditory cortex

Kuwook Cha

Doctor of Philosophy

Integrated Program in Neuroscience

McGill University

Montréal, QC

December 15th, 2016

A thesis submitted to McGill University in partial fulfillment of the requirements of the degree of Doctor of Philosophy

Acknowledgements

My supervisors, Robert Zatorre and Marc Schönwiesner, made essential contribution to this thesis with their advice for the entire course of research and careful examinations of the results and the text. The MRI technicians, David Costa, Ron Lopez, and Louise Marcotte, and the core research assistants, Mike Ferreira and Ilana Leppert, at the McConnell Brain Imaging Center helped me running the experiments with their state-of-art support for relatively novel imaging technique, interleaved silent steady state imaging. A McGill undergraduate student, Bowen Li, enthusiastically assisted the experiments. Philippe Albouy and Pascal Kropf helped to translate the abstract of the thesis to French.

As I believe that good science comes out of becoming a good man of science and building a good community of science, I must acknowledge that an enormous number of people supported me and my work for this thesis – not only for me to give birth to the present work but to become a better man and community member of science. I thank Robert and Marc again for being excellent examples of scientific minds and communications. They have positive minds to find out at least one good thing from any results which I myself would have regarded only disappointing. Despite their solidity and high standard in research, they never lose humility to be open to new, and yet unexplainable findings, which can bring us better questions. These two men are not only good scientists but good persons – therefore, good men of science – so to have taught me how important it is to be a good person as a scientist and to have a good work-life balance. I cannot thank them enough for their care for my well-being and personhood, without which all this work would not have come out to this world.

Speaking of being a good person, there are many folks, inside and outside scientific circles, who played significant roles in my academic and personal growth. My lab colleagues have not only intellectually inspired me but emotionally supported me. My first Canadian neuroscientist friend and former lab colleague, Martha Shiell who had helped me feel home in the new culture and the graduate program before she encouraged me to join the lab when I almost dropped out of my PhD studies. She was also a model student to me in many ways. Friends from my former lab at McGill and the MNI 7th Floor folks also gave me solidarity throughout a horrible time I was going through. I also

remember my very first lab colleauges back in South Korea, including my former supervisor Sang-Hun Lee who exemplified dedication and enthusiasm for better research and all the lab mates who struggled together to make our dreams in science come true. I never forget Choongil Lee, my first model neuroscientist in my college time, whose intellectual gracefulness convinced me to study neuroscience.

My 'framily bros', Sujaya Neupane and Pascal Kropf, as well as the Plateau neighbors and the 'Ranch' members: I was certainly thinking of them when I said to myself "Though, I have such wonderful friends." on one cold winter night after a long frustrating work. Pascal should receive credits for spending his time on discussing theoretical implications of my work with me. I must mention my spiritual family in St. Peter's Anglican Church and Mennonite Fellowship of Montreal: their community support for this foreign person out of unconditional love and care without which I would have given up this journey. I thank Chris Barrigar and Jean Baptiste Mukiza for their humble Christian brotherhood which held science, faith and humanity altogether in my integrity. My fellow dancers and encounters at Cat's Corner and Harlem Shout kept me in good vibe especially at the stage of thesis writing which many people often warned me must be depressing (it would have been so without anticipating every week to dance with you!).

I certainly feel blessed to have been in the great scientific community of Montreal. I thank my advisory committee members, Sylvain Baillet, Etienne de Villers Sidani, and Pierre Bellec, for their academic support and personal care. My gratitude also goes to many inspiring neuroscientists in Montreal including Paul Cisek, Andrea Green, Adrian Peyrache, Chris Pack, Brenda Miller, and late Donald Hebb. All of these people aspired me to value building a good scientific community. The legacy must continue!

Lastly, I am immensely grateful for my mother 안선옥, sister 차영미, brother-in-law 허민 and brother 차봉주, for their love and support, and fathomless respect for my scientific journey at cost of missing their youngest. Kids in my family, 허진영, 차민영, 허재영, and 차민지, were my best reasons to stop crying and continue the journey. I also thank my extended family, 박희순, 황경애, Gabriele, Ruby and Peter Thielmann, and Sunisha, Sunita and Shanta Neupane for their readily kindness and generosity in my time of need. Justine Hansen was among the angelic encounters, holding me to see the hope and joy I have.

Contribution of Authors

I am the primary author of the two manuscripts presented in the current thesis (chapters 2 and 3). The studies are conducted with my two supervisors, Robert Zatorre and Marc Schönwiesner. In study 1 (chapter 2), I designed the study, analyzed the data, and wrote the manuscript with advice from RZ and MS. In study 2 (chapter 3), I designed the study, conducted the experiments, analyzed the data, and wrote the manuscript with advice from RZ and MS.

Abstract

Studying the interaction and connectivity between neurons is important to understanding human perception and behaviors. Functional connectivity, defined as temporal coherence between recordings of neural activity in different locations, is a promising paradigm to study intrinsic dynamics of brain activity. In mammalian sensory cortices, intrinsic functional connectivity revealed by recording spontaneous activity has been positively correlated to sensory tuning similarities of neurons. Human functional magnetic resonance imaging (fMRI) studies have also demonstrated similar patterns with respect to retinotopy and somatotopy. Such coherent spontaneous activity have also been reported to be associated with behavior and perception. This thesis seeks to understand the nature of coherent spontaneous activity, that is, intrinsic functional connectivity, in human auditory cortex in relation to its spectrotemporal processing.

In Study 1, we obtained fMRI responses to pure tone stimuli and estimated best (preferred) frequencies of individual voxels in human auditory cortex. Intrinsic functional connectivity was computed by correlating residual activity, which was obtained by subtracting stimulus effects from fMRI responses, between every pair of voxels, and their correlations were sorted by difference in best frequencies. This analysis revealed that intrinsic functional connectivity decreases as the difference in best frequencies of paired voxels increases. This effect was consistent within and across hemispheres, and within and across regions of core and belt areas. The effect was preserved even after correcting functional connectivity for distance between voxels. Functional connectivity of the right core area had particularly high frequency preference specificity compared to the other three areas. Consistent results were observed when resting-epoch data were used.

Study 2 was designed not only to generalize the tuning specificity of functional connectivity to spectrotemporal tuning properties, but to address functional implications of having tuning-specific functional connectivity. The cortical activity measured in fMRI in response to 72 natural sounds were analyzed to characterize spectrotemporal modulation transfer functions (MTFs) of individual voxels that are parameterized by characteristic frequency, spectral density and modulation rate. These tuning functions

provided enough information to classify novel sounds from separate test datasets. Intrinsic functional connectivity was computed by correlating residual activity taken from auditory responses and resting-state activity from a separate run. Functional connectivity from both activity types was specific to the three tuning parameters. To examine the implication of functional connectivity on spectrotemporal processing, we built a model that combines spectrotemporal tuning functions and functional connectivity to predict voxel activity, and tested whether single-trial stimulus identification based on this model is improved compared to the model which uses the tuning functions. When functional connectivity was incorporated into the model, single-trial decoding performance was better than when only the tuning functions are used. The effect was preserved across primary and non-primary auditory cortex in both hemispheres. The results were also confirmed when maximum likelihood decoders with covariance estimated from residual or resting-state activity were used.

The findings in the above studies suggest that functional connectivity in human auditory cortex is associated with its functional and anatomical architecture, and that tuning-specifically coherent spontaneous activity is functionally important to neural encoding and decoding mechanisms.

Résumé

L'étude des interactions neuronales et de la connectivité corticale est importante pour comprendre les mécanismes qui sous-tendent la perception et les comportements humains. La connectivité fonctionnelle, définie comme la cohérence temporelle de l'activité neuronale provenant de régions distinctes, est une approche prometteuse pour étudier la dynamique intrinsèque de l'activité spontanée ainsi que son influence sur les interactions neuronales extrinsèques. Dans les cortex sensoriels des mammifères, il a été démontré que la connectivité fonctionnelle intrinsèque, révélée par l'enregistrement de l'activité spontanée, peut prédire positivement les profils de réponse des neurones sensoriels. L'activité cérébrale spontanée cohérente semble donc avoir un rôle fonctionnel dans le traitement de l'information neuronale. Ce travail de thèse cherche à comprendre la nature de l'activité spontanée cohérente, c'est-à-dire la connectivité fonctionnelle intrinsèque, dans le cortex auditif humain en relation avec le traitement spectro-temporel.

Dans l'étude 1, nous avons mesuré l'activité IRMf en réponse à des tons purs et nous avons estimé les profils de réponses préférentiels de voxels individuels en fonction de ces fréquences dans le cortex auditif humain. La connectivité fonctionnelle intrinsèque a été calculée en corrélant l'activité résiduelle de chaque paire de voxels, et les corrélations entre voxels ont été triées en fonction des différences dans des fréquences préférentielles. Cette analyse a révélé que la connectivité fonctionnelle intrinsèque diminue lorsque la différence dans les préférences fréquentielles des voxels appariés augmente. Cet effet était cohérent au sein et entre les hémisphères, et au sein et entre les régions du noyau et les aires périphériques (ceinture) du cortex auditif. Cet effet a été préservé après correction pour la distance entre les voxels. La connectivité fonctionnelle au sein du noyau auditif droit était dotée d'un profil spécifique de réponse préférentiel pour les hautes fréquences par rapport aux trois autres zones. Des résultats similaires ont été observés lors de l'utilisation des données de repos.

L'étude 2 a été conçue dans le but de généraliser la tuning-spécificité des profils de connectivité fonctionnelle et permet aussi d'estimer les implications fonctionnelles de

connectivité fonctionnelle. L'activité corticale, mesurée par IRMf, en réponse à 72 sons naturels a été analysée dans le but de caractériser les fonctions de transfert de modulation spectro-temporels de voxels individuels. La connectivité fonctionnelle intrinsèque a été estimée en corrélant l'activité résiduelle des réponses auditives et l'activité de repos provenant d'une série de données distincte. Le profil de connectivité fonctionnelle lors des deux était spécifique aux trois propriétés spectro-temporelles. Pour examiner l'implication de la connectivité fonctionnelle sur le traitement spectrotemporel, nous avons construit un modèle qui combine les fonctions d'accord spectrotemporel et la connectivité fonctionnelle pour prédire l'activité du voxel et a testé si l'identification du stimulus d'un seul essai basée sur ce modèle est améliorée par rapport au modèle qui utilise l'accord les fonctions. Lorsque la connectivité fonctionnelle a été incorporée dans le modèle, les performances de décodage à un essai étaient meilleures que lorsque seules les fonctions de réglage sont utilisées. Ces résultats ont également été confirmés lorsque nous avons utilisé des décodeurs à leur maximum de vraisemblance avec une covariance estimée à partir de l'activité résiduelle ou de l'activité de repos.

Les résultats des études ci-dessus suggèrent que la connectivité fonctionnelle dans le cortex auditif humain est associée à son architecture fonctionnelle et anatomique et que la connectivité fonctionnelle est aussi informative que la corrélation avec le bruit, les deux mesures pouvant être utilisées afin de décoder l'activité neuronale.

Table of Contents

General Introduction

1.1. Functional connectivity: A connectionist's window to the mind and behavior

One of the central questions in neuroscience is how neurons interact each other, which is necessarily also linked to how they interconnect with each other. Advances in simultaneous recording techniques such as multi-microelectrode array and functional magnetic resonance imaging (fMRI), along with development of multivariate analyses methods has facilitated the pursuit of answering this question for the last few decades. While localization of neural correlates of cognition and behavior as exemplified in extreme form with the infamous 'grandmother cells' is still critical to understand brain function (Barlow, 2009; Quian Quiroga and Kreiman, 2010), no neuroscientist of this day can imagine studying the brain without considering the orchestrated patterns of neural activity.

The idea of neural coding and computation by a population of neurons mediated by anatomical connections must be dated back to the theoretical postulation of Hebb, one of the most insightful neuroscientists in history. His theory is often summarized as "Cells that fire together wire together" (Löwel and Singer, 1992), and the emphasis on correlated activity to create neural representation has inspired the earliest experimental findings of correlations in neural activity during the 1960's in animals (Perkel et al., 1967a, 1967b; Gerstein and Perkel, 1969). Later, in the 1990's, correlations in neural activity began to be studied in humans using brain imaging techniques, at which point functional connectivity was formally and explicitly defined as temporal correlations between two spatially distinct neurophysiological recordings (Friston et al., 1993; Friston, 1994).

Although the definition of functional connectivity is simple and technical, the ultimate purpose of studying functional connectivity is not to describe the pattern of correlations per se but to understand cognition and behavior, as Hebb's connectionist vision was not only a conceptual abstraction of neural organizations but also aimed at understanding of *The Organization of Behavior* (Hebb, 1949). The studies presented in

this thesis represent a step along the journey of understanding the brain, mind and behavior altogether in light of functional connectivity, specifically with respect to how correlations in spontaneous and stimulus-evoked activity are related to sensory encoding. The current thesis primarily focuses on functional magnetic resonance imaging studies on human auditory cortex, but the mechanistic basis and the implications are discussed in the broader context of systems and cognitive neurophysiology across recording techniques, species, and sensory systems.

1.1.1. Studying functional connectivity: historical development

The number of peer-reviewed journal publications on brain functional connectivity has exponentially increased for the last 2 decades since its introduction to the field of brain imaging (Friston et al., 1993; Friston, 2011; Raichle, 2015). Functional connectivity in brain imaging has then extended its impact to resting-state functional connectivity (Biswal et al., 1995; Raichle, 2015), identification of functional networks (Beckmann et al., 2005; Damoiseaux et al., 2006), regional parcellation (Kim et al., 2010; Kahnt et al., 2012) and developing clinical applications (Rosazza and Minati, 2011). Despite its recent popularity especially in human brain imaging, the interest in studying correlations in neural activity was not new to neurophysiologists at the advent of functional imaging as mentioned above. For instance, Gerstain and Perkel published in 1969 their seminal report of correlations in simultaneously recorded neurons (Gerstain and Perkel, 1969), which was a decade before the term functional connectivity appears in neuroscience literature (Anderson, 1979). Since then, neurophysiologists have endeavored to elucidate how the brain encode and transfer information through temporal correlations and synchrony. However, the term functional connectivity is less frequently used in animal electrophysiology than human brain imaging. It is possibly due to the terminological non-specificity (Horwitz, 2003) considering that there are various ways of analyzing temporal dependence in electrophysiological data; and it may reflect the distinct historic routes in paradigm development and lack of cross-talk between the two communities. Integration between such distinct disciplines and modalities of studies on

functional connectivity has recently begun (Kohn et al., 2009), and this thesis is a contribution along the line of such a pursuit.

1.1.2. Definitions of functional connectivity and other related terms

Functional connectivity can have different operational meanings and scientific implications depending on the measure or the underlying activity. For example, functional connectivity may imply a continuous measure such as correlation coefficient to indicate the strength, whereas it can also mean a binary statistical decision on the presence of connectivity made by thresholding the continuous measure (Rubinov and Sporns, 2010). Depending on the temporal resolution of neurophysiological measures, one can compute cross-correlation to look at the detailed temporal dynamics such as lags or time constants (Kohn and Smith, 2005; Jermakowicz et al., 2009). When temporal resolution of the signal allows, coherence, i.e., cross-spectral density, is also used in order to examine a frequency-dependent relationship between the recorded signals (Leopold et al., 2003). There is also an increasing number of studies that address temporal dynamics or stochasticity of functional connectivity (Luczak et al., 2009; Bharmauria et al., 2016). Despite the variety of measures, functional connectivity means statistical dependency between two time series recordings without exception. Importantly, functional connectivity does not imply directionality of the influence between two neural systems, which is rather referred to as *effective connectivity* (Friston, 1994, 2011).

It is also important to distinguish *intrinsic* functional connectivity from *stimulus-* or *task-dependent* functional connectivity. Functional connectivity is inferred to be intrinsic when the correlated activity does not relate to a stimulus or task, that is, a common extrinsic drive of the correlated activity. This does not mean that one cannot estimate intrinsic functional connectivity from stimulus- or task-evoked activity, because the confounding effects of the stimulus or task to functional connectivity can be regressed out. In fact, the earliest functional connectivity in brain imaging literature was computed in such experimental setting (Friston et al., 1993; Friston, 1994), only after which the well-known *resting-state* functional connectivity began to get rigorous attention (Biswal et al., 1995; Raichle, 2010; Friston, 2011). Resting-state functional connectivity, named

after the very experimental condition where the subject is not given any stimulus or task but asked to stay at rest, is rather a special case of intrinsic functional connectivity. Intrinsic functional connectivity can be also computed from activity measured during resting epochs within a stimulus- or task-based experiment (Fair et al., 2007).

In contrast, stimulus- or task-dependent functional connectivity is inferred when correlations in activity are observed in the presence of the extrinsic drivers of neural activity (Friston et al., 1997; Kohn and Smith, 2005). For instance, areas A and B may not show functional connectivity in the absence of a stimulus but correlations in their activity can appear as a stimulus is being presented. This is sometimes called *psychophysiological interaction* in brain imaging literature because one would seek the interactive effect of psychological and/or physiological conditions and brain activity of one area on another area (Friston et al., 1997). Animal electrophysiologists have also known that functional connectivity can be altered by a stimulus, and discussed its implication on neural encoding and decoding (Kohn and Smith, 2005; Ponce-Alvarez et al., 2013; Franke et al., 2016; Zylberberg et al., 2016).

Correlations in neural activity have, in fact, been of great interest to animal electrophysiologists in different terms such as *neural synchrony* and *noise correlation* with emphasis on different implications. Neural synchrony can either mean spike train synchrony in discrete signals or spike signal synchrony in continuous signals (Singer and Gray, 1995). In both cases, synchrony emphasizes temporally precise coincidence of neural events or phase-locked oscillations. On the other hand, noise correlation refers to correlation in neural activity after being corrected for the stimulus effect, with emphasis on co-variability in trial-to-trial response variations to an identical stimulus (Shadlen and Newsome, 1998; Bair et al., 2001; Cohen and Kohn, 2011). While human brain imaging studies on functional connectivity are mostly concerned with the spatial patterns of those interactions, investigations on neural synchrony and noise correlations in animal electrophysiological studies have been conducted rather to answer questions on neural information coding and transfer, behavioral or neural variability, and binding problems (Zohary et al., 1994; Shadlen and Newsome, 1998; Abbott and Dayan, 1999; Singer, 1999; Bair et al., 2001; Averbeck et al., 2006).

1.2. Coherent spontaneous activity in fMRI

In 1995, Biswal and colleagues published their seminal study of correlated activity in the resting brain in sensorimotor-associated regions (Biswal et al., 1995). They found that fMRI activity in the finger-hand motor region of the left hemisphere is significantly correlated with the homologous region of the other hemisphere when the participant is at rest without performing any particular task. Also, the topography of the voxels that showed correlated activity in the resting brain was very similar to the activation map obtained by a bilateral finger tapping task. The results suggest that the cortex maintains correlated spontaneous activity among regions that are functionally related or that would be co-activated during a task performance (Fox et al., 2006b; Sadaghiani et al., 2010).

Spatially organized coherence in the resting-state brain activity has been consistently replicated in many other functional networks beside the motor cortex, and resting-state functional connectivity has become one of the most prevailing methods used in human brain imaging to study functional integration and connectivity (Raichle, 2009; Friston, 2011). The advantages of studying large-scale networks in the brain without having to develop a particular experimental setup and its applicability to special populations who are not able to conduct certain tasks have attracted neuroscientists and clinicians together, and resting-state functional connectivity has become an important part of brain connectome studies (Behrens and Sporns, 2012; Jbabdi et al., 2013).

It should be noted here that the activity in the resting brain is often called *intrinsic* or *spontaneous activity*. Although these terms are often regarded as interchangeable, there is subtle nuance: resting-state activity emphasizes the specific state or experimental condition whereas intrinsic or spontaneous activity regards the origin or source of the activity. In other words, the latter can arise independently of a certain state or experimental condition, and neural responses can be thought of as a mixture of intrinsic or spontaneous activity, and extrinsic or evoked activity (Fox et al., 2006b, 2007; Sadaghiani et al., 2009; Saka et al., 2010; Becker et al., 2011). For this reason, it is sometimes called on-going activity (Arieli et al., 1996; Kenet et al., 2003; Hesselmann et al., 2008a; Becker et al., 2011; Leopold and Maier, 2012).

1.2.1. Functional organization of coherent spontaneous activity in sensory cortices: tuning-specific functional connectivity

Early human resting-state fMRI made its success to identify functional organizations of spontaneous activity mostly on a larger scale: Beginning with coherent resting-state activity in the motor cortex (Biswal et al., 1995), regions that have related functions such as visual (Lowe et al., 1998; Cordes et al., 2000) and auditory (Cordes et al., 2000) areas, the hippocampus (Rombouts et al., 2003; Vincent et al., 2006), the default mode network (Greicius et al., 2003) and the attentional systems (Laufs et al., 2003; Fox et al., 2006a) have been identified by analyzing the coherent pattern of resting-state spontaneous activity. More recent human brain imaging studies have stretched the scale down into topographic organizations of functional connectivity within sensory cortices. For example, Heinzle and colleagues (2011) showed that fMRI voxels whose activity encodes close locations in retinotopic space have higher resting-state functional connectivity than voxels that have distant receptive field locations (Figure 1C). Similar findings have been replicated in the somatotopic areas (van den Heuvel and Hulshoff Pol, 2010; Cauda et al., 2011).

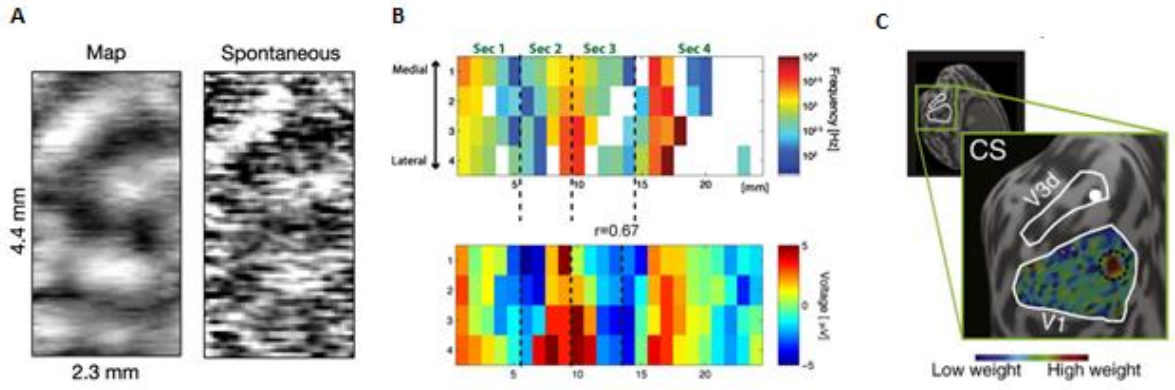

Figure 1. Tuning-specific coherence in spontaneous activity.
A. A snapshot of spontaneous activity (right) measured by voltage-sensitive dye imaging in cat visual cortex which is correlated with the orientation preference map (left). Adapted from Kenet et al. (2003). B. A snapshot of spontaneous activity (bottom) measured by electrocorticography in macaque auditory cortex which is correlated with the frequency preference map (top). Adapted from Fukushima et al. (2012). C. Resting-state functional connectivity map in human primary visual cortex (V1) for a seed voxel in

V3 (white dot). The seed voxel has the same voxel receptive field location with the voxels in V1 that show the highest functional connectivity (dotted black circle).

Such fine-scale delineation of functional connectivity has importance for linking human functional connectivity studies to animal electrophysiological studies that have consistently documented organized spatiotemporal patterns in spontaneous activity (Arieli et al., 1995; Nauhaus et al., 2009; Rothschild et al., 2010; Saitoh et al., 2010). These patterns are not only topographical but associated with sensory representation. For instance, Kenet and colleagues (2003) demonstrated that the spatial organization of spontaneous activity measured by voltage sensitive dye imaging in the cat visual cortex is coherent with the spatial pattern of visually-evoked activity in response to oriented stimuli (Figure 1A). Similarly, spontaneous activity in the guinea pig auditory cortex resembles the spatiotemporal pattern of tone-evoked activity which suggests spontaneous activity is organized along the topography of frequency selectivity (Saitoh et al., 2010). These studies suggest that when two neurons prefer similar sensory features, they would have coherent spontaneous activity, i.e., functional connectivity. Such positive relation between functional connectivity and sensory tuning properties has been replicated across species and sensory modalities (Brosch and Schreiner, 1999; Fukushima et al., 2012; Farley and Noreña, 2013). Despite the difference in the scale, these human brain imaging studies share the same principle with the above findings in animal neurophysiology: functionally related neurons or neuronal populations have coherent activity with one another in the absence of stimuli or tasks.

Despite the observation that spatial patterns of spontaneous activity are similar between animal neurophysiology and human brain imaging, the temporal scales of the two signals are very different. Whereas resting-state functional connectivity in fMRI is most prevalent at a very low frequency range from 0.01 to 0.1 Hz (Fox and Raichle, 2007), coherence measured in electrophysiological signals usually lies at 1 Hz or higher (Kohn et al., 2009). Is functional connectivity in fMRI due to temporal aliasing of the higher-frequency fluctuations in electrophysiological signals or are they both manifestation of neuronal fluctuations in different time scales? Leopold and colleagues

(Leopold et al., 2003) first sought to answer this question by analyzing spontaneous fluctuations in band limited power of local field potential signals in monkey visual cortex using multi-electrode recording; and they found that spectral power of the local field potential at various bands recorded from different electrodes fluctuates coherently at very low frequency (<0.1 Hz). In other words, fast oscillations of population activity recorded from different electrodes are nested in coherent slow fluctuations of activity. The coherence was particularly high in the high gamma band (50 ~ 100 Hz) power signal, which also showed the longest spatial extent of coherence between electrodes compared to other frequency bands. Similar findings were replicated by other groups when multi-electrode and fMRI activity were simultaneously recorded in the monkey visual cortex (Shmuel and Leopold, 2008; Schölvinck et al., 2010). These results suggest that the slow fluctuations in resting-state fMRI has a neuronal origin at a different time scale than the faster fluctuations of spontaneous activity which seems to be tightly linked to the slow fluctuations (Kohn et al., 2009; Leopold and Maier, 2012). Particularly, coherent power modulation of gamma oscillations between distant neurons might be a substrate of the coherent slow fluctuations that can be detected in fMRI (Shmuel and Leopold, 2008).

How are coherent patterns in spontaneous activity related to anatomical connectivity? Although it is natural to infer that neural activity patterns are constrained by anatomical connections, elucidation of the detailed relation is not trivial. Some of the first evidence for the link between resting-state fMRI and anatomical projections was sought by Vincent and colleagues (Vincent et al., 2007). They recorded resting-state fMRI activity in the macaque monkey brain and obtained a functional connectivity map using seed regions in oculomotor regions such as frontal eye fields and lateral intraparietal area. The spatial pattern of the connectivity was significantly correlated with the map of anatomical projections obtained by retrograde tracer injection to the lateral intraparietal area. This result indicates that resting-state functional connectivity arises along anatomical projections. However, functional connectivity was not restricted to direct projections: they found that foveal V1/V2 was functionally connected with the foveal V1/V2 in the opposite hemisphere, which lacks direct interhemispheric connections except along the vertical meridian (Van Essen et al., 1982). Therefore,

coherent fluctuations of spontaneous fMRI activity are likely mediated by polysynaptic connections rather than direct projections.

Quantification of the association between functional and anatomical connectivity is rather a complex matter. First of all, there is no documentation for how many polysynaptic connections can mediate functional connectivity. Furthermore, researchers have not come to a consensus on which statistical procedures to detect functional connectivity are precise and which are the confounding signals that affect functional connectivity (i.e., globally correlated activity) (Murphy et al., 2009; Jo et al., 2010; Saad et al., 2012; Jbabdi et al., 2013). An alternative way of evaluating functional connectivity is to measure it as a continuous variable rather than a binary statistical decision (Jbabdi et al., 2013). Even in this case, it has yet to be resolved whether and how much the number of projections and/or synaptic efficacy play a role to determine the strength of functional connectivity. Therefore, the best knowledge to date on relation between functional and anatomical connectivity is only that the general patterns or organizational principles (e.g., retinotopic connectivity) are overlapped and polysynaptic projections can yield statistically significant functional connectivity.

1.2.2. Functional roles of coherent spontaneous activity

One of the intriguing facts about spontaneous activity is that it makes the brain consume 20% of the oxygen that we take in although the volume of the brain is only 5% of the body (Raichle et al., 2001). Also, the magnitude of the metabolic consumption (Fukunaga et al., 2008) as well as of the activity fluctuation (Arieli et al., 1995) is comparable to that of evoked activity. If one considers only these two facts, spontaneous activity without any functional contribution would appear to be very wasteful. Do the organized spatiotemporal patterns of spontaneous activity reflect merely shared noise mediated by anatomical connections, or does it have functional roles? Considering the large metabolic costs (Raichle et al., 2001; Fukunaga et al., 2008) and the significant magnitude of the fluctuations as aforementioned, it would be more sensible for it to have functional benefits.

A number of human fMRI studies have addressed the relation between fluctuations in spontaneous brain activity and variability in perception or behavior. Fox and colleagues (Fox et al., 2007) demonstrated that fMRI activity in the left and right motor cortex preceding right finger press explained variance in the pressure exerted during the task performance. Similarly, Boly and colleagues (2007) reported that somatosensory detection performance was improved in the trials when brain regions responsible for task-related activations showed higher pre-stimulus activity. They also found that poorer performance was associated with high pre-stimulus activity in the areas that are known to be deactivated during task engagement. Other studies reported that the perception of ambiguous figures, such as Rubin's vase-face picture was correlated with pre-stimulus activity in the right fusiform face area (Hesselmann et al., 2008a), and that coherent motion perception was associated with the pre-stimulus activity in the right motion-sensitive occipito-temporal cortex (hMT+) (Hesselmann et al., 2008b). Such a positive relation between percept of figure-ground and pre-stimulus activity has also been found in macaque primary visual cortex (Supèr et al., 2003).

These results, taken together, support a hypothesis that spontaneous activity is the neurophysiological basis of trial-to-trial variability in neural responses (Arieli et al., 1996; Saka et al., 2010, 2012; Becker et al., 2011) as well as behaviors (Bair et al., 2001). However, the positive relation between spontaneous activity and variability in neural responses and behavior does not necessarily demonstrate the functional benefits of maintaining spontaneous activity. One may even infer that spontaneous activity rather contributes to unreliability of neural responses and behavioral performance as a source of noise. Namely, spontaneous activity reflects internal sensory noise, as the signal detection theory describes, that biases perceptual or behavioral outputs (Ringach, 2009; Hesselmann et al., 2010).

Sadaghiani and collaborators (2010), however, suggest to pay attention to the interaction, i.e., non-linear relation, between spontaneous activity and evoked activity that varies according to percept. For instance, correlation between pre-stimulus activity and peak activity in the fusiform face area was decreased on trials when the participants perceived faces compared to when they report a vase (Hesselmann et al., 2008a).

Similarly, correlation between pre-stimulus and peak activity in hMT+ was also lower when the observer reported a coherent motion percept (Hesselmann et al., 2008b). The interaction between ongoing and evoked activity can be explained by predictive coding (Friston et al., 2009) which predicts that when spontaneous activity is high and more coherent with the incoming stimuli, the amplitude of evoked activity would be low because the prediction by spontaneous activity is accurate. This account is, however, in question: In the studies of Hesselmann and colleagues, the pre-stimulus baseline activity is temporally remote from the peak response, and the authors only address the effect of magnitude of baseline activity rather than correlated patterns in spontaneous activity.

A prominent hypothesis for the functional role of spontaneous activity is the replay hypothesis. In this account, spontaneous activity is involved in rehearsal of representations that have been learnt, or memory consolidation (Fukushima et al., 2012). The replay hypothesis was originally proposed to explain a phenomenon that the coordinated activity or sequential trace of activity patterns across neurons reverberates both in hippocampus and sensory cortex during sleep (Wilson and McNaughton, 1994; Ji and Wilson, 2007). Later, such activity patterns were observed also in awake or quasi-awake state (Han et al., 2008; Carr et al., 2011). The coordinated pattern in resting-state or ongoing spontaneous activity can be a special case of this phenomenon. This hypothesis is particularly linked to the recently emerged concept of dynamic functional connectivity which refers to change in functional connectivity according to experiences or mental state (Hutchison et al., 2013; Liu and Duyn, 2013; Stevens and Spreng, 2014). However, it does not address the possibility of an immediate role for processing a concurrent stimulus.

In contrast, a group of authors hypothesize that spontaneous activity is involved in sensory gating for immediate stimulus information processing (Luczak et al., 2009, 2013, 2015). This hypothesis is based on the observations that the activity of individual cortical neurons show consistent temporal patterns with respect to the coherent population activity, called ‘activity packets’, measured by multi-unit activity or local field potential recording (Luczak et al., 2009, 2013). The temporal relation between activity packets and spiking timing was consistent either when a stimulus is presented or not (Luczak et al.,

2013). However, the probability of incidence of activity packet was higher at stimulus onset than sustained stimulus presentation or silent period. The results suggest that the cortex sporadically generates activity packets, which are coherent fluctuations of population activity, and neurons broadcast their messages in relation to the packets.

Fiser and co-authors (2010) attempt to propose a unified framework using the notion of Bayesian learning and inference. They suggest that spontaneous activity represents the prior probability distribution regarding the internal model about the environment that the brain has previously learnt, and the sensory input provides new evidence to compute the posterior probability distribution. While the learning process is relevant to memory consolidation in the replay hypothesis, the inference based on the already learnt internal model is in accordance with the sensory gating hypothesis. The notion of internal model and the emphasis on Bayesian inference and learning are in line with the predictive coding theory (Friston et al., 2009). However, this framework does not necessarily predict a negative interaction between spontaneous and evoked activity as proposed by other researchers mentioned above (e.g., Hesselmann et al., 2010).

1.2.3. Correlations in spontaneous activity and trial-to-trial response variation

As briefly introduced in the above section, spontaneous cortical activity both in humans and other animals is tuning-specifically organized. This pattern is consistent with correlations in trial-to-trial variation in stimulus/task-evoked activity, i.e., noise correlations: noise correlations tend to be high when neurons have similar feature preferences (Petersen et al., 2001; Averbeck and Lee, 2003; Averbeck et al., 2006; Rothschild et al., 2010). Such similarity in the pattern of correlations of the two sources of signals, together with the fact that neural response variability is accounted for by spontaneous activity (Arieli et al., 1996; Fox et al., 2006b), may be important to understanding the functional implication of spontaneous activity because a large body of research has discussed the impact of noise correlations on neural encoding and decoding (Abbott and Dayan, 1999; Bair et al., 2001; Schneidman et al., 2003; Shamir and Sompolinsky, 2004; Latham and Nirenberg, 2005; Averbeck et al., 2006).

The problem of noise correlations originated from an old assumption that noise in neural activity, which is measured as trial-to-trial variability, can be cancelled out by averaging activity across many neurons (Pouget et al., 2000). This assumption is problematic because noise cannot be cancelled when the noise is correlated between recording channels (Abbott and Dayan, 1999). Averaging signals across neurons could rather result in significant information loss. Numerous studies have discussed the impact of noise correlations in neural information processing and the matter is still under debate. However, there is rough consensus. Firstly, theoretical studies using information-theoretic measures suggest that the presence of noise correlation can lead to coding inefficiency (Abbott and Dayan, 1999; Schneidman et al., 2003; Averbeck et al., 2006). Especially, certain conditions of noise correlations, such as being positively correlated with tuning similarity of neurons, are more likely detrimental than otherwise, and this disadvantage can exponentially increase as the population size becomes large (Shamir and Sompolinsky, 2004; Averbeck et al., 2006; Moreno-Bote et al., 2014). Secondly, ignoring noise correlations leads to information loss in decoding unless noise is independent across neurons (Averbeck et al., 2006; Graf et al., 2011) or small enough to be ignored (Nirenberg and Latham, 2003; Latham and Nirenberg, 2005).

As mentioned above, most empirical evidence strongly indicates that neural response variability is correlated across neurons that are tuned to similar stimulus features. For this reason, the redundancy and apparent inefficiency in coding with correlated noise has intrigued researchers (Barlow, 2001; Latham and Nirenberg, 2005; Bharmauria et al., 2014; Schneidman, 2016) and motivated an alternative view to emphasize reliability and learnability of the neural code supported by correlated noise (Fiser et al., 2010; Jeanne et al., 2013; Miller et al., 2014; Schneidman, 2016). At the same time, the importance of incorporating the information of noise correlation into decoding has been both theoretically and empirically demonstrated (Nirenberg and Latham, 2003; Latham and Nirenberg, 2005; Graf et al., 2011). Importantly, this point has begun to be made also in human brain imaging thanks to the introduction of multivoxel pattern analysis: a multivoxel analysis in general takes into account the co-variability of voxel activity, and it is capable to capture different patterns responsible for

distinct cognitive processes which cannot be detected by univariate analysis or averaging voxel activity (Kriegeskorte and Bandettini, 2007; Kriegeskorte, 2011; Serences and Saproo, 2012). Therefore, noise correlation is very important to neural information processing, and studying the relation between spontaneous activity and neural response variabilities, especially the correlations that reside in both types of activity might be essential for exploring possible mechanisms and functional roles of spontaneous activity.

1.3. Spectrotemporal processing and tuning-specific functional connectivity in auditory cortex

The hypotheses and supporting findings introduced in the previous section indicate that coherent spontaneous activity influences neural information processing and behavior. However, they do not address the relation between coherent spontaneous activity and detailed encoding or tuning properties of the sensorimotor systems unless implicitly at best. As introduced above, there is increasing evidence that coherence in spontaneous activity is organized with respect to tuning functions of neurons. Therefore, explicitly incorporating this pattern to understanding the functional implications of coherent spontaneous activity would be an essential step. Understanding correlations in spontaneous activity can also have importance in understanding correlations in evoked activity, whether in signal or noise, as the above hypotheses point out. The current thesis addresses these issues by relating spontaneous activity particularly to spectrotemporal processing in human auditory cortex. This section provides is a brief introduction on what has been known about spectrotemporal processing and coherent spontaneous activity in auditory cortex.

1.3.1. Spectrotemporal representation of a sound in the central auditory nervous system

A sound, in the physical sense, is a change in air pressure over time, which implies the original domain of the variation is only time. The auditory system in the brain, however, transforms them into a frequency representation that is the basis of pitch perception (Moore, 2003). Two mechanisms are involved in this transformation: place code and temporal code. Place code represents spectral magnitude in different places in the neural system whereas temporal code is realized by periodic temporal patterns of

neural activity directly. Place code is first implemented in the cochlear where the mechanical vibrations are transduced to neural signals along the basilar membrane to decompose different frequencies. The auditory nerve outputs from the cochlear can be represented as temporal envelopes of these frequency channels, each of which corresponds to 'preferred' or 'characteristic' frequency of a nerve cell (Chi et al., 2005). This auditory nerve output representation of a sound over (characteristic) frequency and time is referred to as auditory spectrogram. In this 2-dimensional space, a sound can be represented as envelope modulation jointly in time and frequency. In the downstream stages such as the inferior colliculus, medial geniculate body and the auditory cortex, neurons become specialized to certain forms of spectrotemporal modulations a center frequency and a latency, which is referred to as spectrotemporal receptive, or response, field (Atlas and Shamma, 2003; Chi et al., 2005). Although acoustic properties that drive cortical responses can be numerous, a spectrotemporal receptive field can capture the most important features including characteristic frequency, latency, spectral bandwidth and modulation (also called spectral density), and temporal modulation (Kowalski et al., 1996a, 1996b; Depireux et al., 1998). The above understanding of the auditory system is established mostly based on electrophysiological studies of non-human mammalian brain.

1.3.2. Spectrotemporal processing in human auditory cortex

Studies on spectrotemporal representations in human auditory cortex are relatively sparse due to methodological limitations, but topographical representation of preferred frequency has been relatively well studied compared to other auditory features. It is not only thanks to its gross topography that can be captured even in the coarse spatial resolution of brain imaging techniques but its functional importance. As described above, frequency is the most fundamental feature domain for the representation of a sound, and the spatial organization of preferred frequency, called tonotopy or cochleotopy, is an auditory example of the principal topographic organizations of sensorimotor cortices such as retinotopy and somatotopy.

Human fMRI studies have attested that there are multiple tonotopic fields on the supratemporal plane around Heschl's gyrus, an anatomical landmark of location of the

primary auditory cortex (Langers and van Dijk, 2012; Moerel et al., 2012; Saenz and Langers, 2014; Schönwiesner et al., 2014). In fact, the exact location and orientation of tonotopic axis of the primary auditory cortex is a matter of debate (Humphries et al., 2010; Da Costa et al., 2011; Moerel et al., 2014). A classical configuration is that the tonotopic progression runs along the long axis of Heschl's gyrus (Lauter et al., 1985; Wessinger et al., 1997; Langers et al., 2007) but some researchers have proposed that the tonotopic axis of primary auditory cortex is perpendicular (Humphries et al., 2010; Da Costa et al., 2011) to Heschl's gyrus, while others believe that it is an oblique or V-shaped configuration (Humphries et al., 2010; Langers and van Dijk, 2012). It is commonly believed that the primary auditory cortex has at least two tonotopic progressions mirroring each other (A1 and R), and some add another tonotopic field RT in the anterior extension (Baumann et al., 2013; Moerel et al., 2014; Saenz and Langers, 2014). The area surrounding the primary auditory cortex is defined as the secondary auditory cortex and it shares the tonotopic gradients with the primary auditory cortex (Kaas and Hackett, 2000; Moerel et al., 2014). Because of this surrounding geography, the primary and secondary auditory cortices are often called the core and belt (fields) areas, respectively (Kaas and Hackett, 2000; Baumann et al., 2013). Another tonotopic region that still shares the tonotopic gradients and runs along the lateral part of the belt area is identified as the parabelt area (Kaas and Hackett, 2000; Baumann et al., 2013). While the core, belt and parabelt areas are all tonotopic, their physiological properties and anatomical connectivity differ in primate studies. For instance, the core area prefers a narrower spectral band (Read et al., 2001; Moerel et al., 2012; Schönwiesner et al., 2014) and they receive more thalamocortical projections compared to the other areas (Hackett, 2011).

Temporal representations of auditory stimuli in the human cortex have been much less studied than spectral representation but still available. Frequency modulation was found to activate Heschl's gyrus, anterolateral and posterolateral parts of superior temporal gyrus, and superior temporal sulcus more strongly than unmodulated stimuli (Hall et al., 2002). In another study, the representation of amplitude modulation was located in primary and non-primary areas (Giraud et al., 2000). Hart and colleagues

(2003) also found activation by amplitude and frequency modulations in widely spread regions of the human auditory cortex (Hart et al., 2003). They also found greater activation in lateral Heschl's gyrus and planum temporale than other regions, which implies hierarchical processing, and the response to amplitude is stronger in the right hemisphere than the left.

The joint spectrotemporal tuning functions in human auditory cortex have been studied by a few research groups. Langers and colleagues (2003) used dynamic ripple sounds which are known to optimally drive neuronal responses with respect to their spectrotemporal receptive fields (Depireux et al., 2001; Langers et al., 2003). They were able to demonstrate topography of preference in spectral density, temporal modulation rate and drift direction, separately. However, it was Schönwiesner and Zatorre (2009) who characterized the joint spectrotemporal receptive fields or modulation transfer functions of individual voxels for the first time in the human cortex (Schönwiesner and Zatorre, 2009). Finally, Santoro and colleagues (2014) used natural sounds rather than artificial dynamic ripple sounds and a neurophysiologically-based spectrotemporal receptive field model of auditory cortical neurons (Chi et al., 2005) to estimate joint modulation transfer functions of individual voxels with respect to characteristic frequency, spectral density and modulation rate (Santoro et al., 2014).

An interesting aspect in spectral and temporal processing of the human auditory cortex is its functional asymmetry (Zatorre et al., 2002): the left hemisphere is proposed to be more specialized to analyze speech and temporal features and the right is suggested to better process music and spectral information. This model is based on asymmetry in macro- and micro- anatomy such as myelination (Anderson et al., 1999), volumetrics (Zatorre et al., 2002) and minicolumn structure (Galuske et al., 2000), as well as functional asymmetry evidenced by the findings that lesions in the left temporal cortex that lead to impairments in speech processing and ones in the right that degrade music processing. Several human brain imaging studies also support this idea. For example, Zatorre and Belin (2001) manipulated the temporal rate and spectral separation of pure tone stimuli which modulated activations in positron emission tomography in human auditory cortex. They found that the left Heschl's gyrus and supratemporal sulcus is more

strongly modulated in response to temporal rate changes while the right counter parts, to spectral variations (Zatorre and Belin, 2001). Schönwiesner and colleagues (2005) reported similar findings that parametrically changing temporal complexity in stimuli modulates fMRI responses more strongly in the left antero-lateral belt area while spectral complexity varies responses in the equivalent region in the right hemisphere. While Zatorre and colleagues (2002) propose that this lateralization is due to spectrotemporal trade-off, some other studies showed that temporal integration over longer time is rather lateralized to the right planum temporale (Overath et al., 2008) or that spectrotemporal lateralization is minimal (Overath et al., 2012). In summary, cortical neurons in human auditory cortex seem to have spectrotemporal response field properties as in animals and there are certain regional biases and hemispheric asymmetry in resolving spectral and temporal features. Such functional specialization yields distinct activation patterns to respond to different spectrotemporal components although the exact mechanism needs to be elucidated in order to resolve inconsistent results across studies.

1.3.3. Tuning-specific functional connectivity in auditory cortex

As mentioned above, increasing evidence has pointed out that spontaneous activity is coherent when tuning properties of neurons are similar, and that it can have functional importance. However, this question has not been addressed in human auditory cortex. There have been a few studies that examined the relation between auditory tuning functions and coherent spontaneous activity in non-human mammals. Saito and colleagues (2010) recorded neural activity in the auditory cortex of guinea pigs using voltage sensitive dye imaging both during pure tone presentation and at rest. They found that spatiotemporal traveling wave of spontaneous activity resembles that of tone-evoked activity, which spreads along iso-frequency strips. In another study using voltage-sensitive dye imaging on the same species, phase coherence of spontaneous slow-wave activity in delta-theta band gradually decreased as the difference in preferred frequency of the recording sites within and between the core and belt areas increases (Farley and Noreña, 2013). This relationship was preserved both within and between the core and belt areas, and there was consistent phase difference when the coherence was computed

between the core and belt areas, which was preserved when multi-tone stimuli were presented. Similar findings were reported in a macaque monkey study using electrocorticography (Fukushima et al., 2012): fluctuations of gamma band power in spontaneous activity was spatially coherent with the tonotopic map obtained by tone-evoked activity across the core and belt areas. The relation between temporal feature representation in the auditory cortex and spontaneous activity has been reported by only one study where correlations in spontaneous activity varied with similarity in the onset, offset and temporal pattern of response of cell pairs recorded in the cat primary auditory cortex (Brosch and Schreiner, 1999). These findings are consistent with the notion that functional connectivity reflects or is constrained by the pattern of anatomical connectivity because thalamocortical (McMullen and de Venecia, 1993; Hashikawa et al., 1995; Miller et al., 2001; Kimura et al., 2003; Lee et al., 2004b) and corticocortical (Read et al., 2001; Lee et al., 2004b) projections are tonotopically organized.

Studies on the relation between functional connectivity and other auditory stimulus features are rare. Brosch and others (1999) computed cross-correlograms of spontaneous activity in pairs of neurons in cat primary auditory cortex to evaluate how correlation strength, i.e., peak cross-correlation, and correlation width in terms of similarity of many tuning properties including spectral overlap, characteristic frequency, response onset/offset/pattern and binaural interaction (Brosch and Schreiner, 1999). The similarity of all tuning properties varied with either correlation strength or width. Although this study indicates that tuning-specific functional connectivity is a generic organizational principle in the cortex regardless of any tuning properties, it has never been investigated whether the similarity of spectrotemporal response field properties of spectral density and modulation rate is related to the pattern of coherent spontaneous activity. Also, the anatomical projection patterns with respect to the above tuning properties have never been reported in contrast to tonotopic axonal projections. Therefore, testing tuning-specific functional connectivity with respect to various tuning properties including spectral density and modulation rate in human auditory cortex is essential to understand the functional organization of human auditory cortex and it can serve as a basis to predict anatomical projection patterns considering the correlation

between functional and anatomical connectivity patterns (Vincent et al., 2007; Honey et al., 2009).

1.4. Proposal of the thesis: studying spectrotemporal processing and spontaneous activity in human auditory cortex using fMRI

To summarize the previous sections, the following points were introduced: (1) Functional connectivity has long been of interest to the field of neuroscience especially for understanding the brain through neuronal interactions; (2) the definition of functional connectivity is simply 'temporal coherence between neural events in spatially distinct locations', but the types of functional connectivity can be various; (3) resting-state fMRI functional connectivity reflects the functional architecture of the brain including gross functional networks and the organization of sensory tuning properties; (4) coherent spontaneous activity can have functional roles such as memory consolidation, sensory gating and/or prior probability representation; (5) correlations in spontaneous activity and noise correlations commonly have tuning-specificity which indicates possible involvement of spontaneous activity in information processing; (6) spectrotemporal processing in the human brain has been studied with respect to single-voxel tuning functions and specialization in regional and hemispheric levels; and finally (7) various auditory tuning functions have been related to coherent spontaneous activity in animals but there have been no human studies in this regard.

The above studies lead to three major questions about the relation between spectrotemporal processing and spontaneous activity in human auditory cortex: (1) whether functional connectivity in human auditory cortex is specific to spectrotemporal tuning, (2) if so, whether tuning-specific functional connectivity is associated with gross functional architecture such as functional asymmetry, and (3) what would be functional implications of functional connectivity in auditory cortex. To address these questions, two following studies are conducted.

Study 1 is designed to address the following hypotheses: first, functional connectivity is specific to frequency preference in human auditory cortex, within and across core and non-core fields, and also across hemispheres; second, frequency tuning-

specific functional connectivity reflects known functional architecture of human auditory cortex such as functional asymmetry. To test the hypotheses, best frequencies of individual fMRI voxels in human auditory cortex are estimated from fMRI responses to pure tones of 8 frequencies. Then, functional connectivity, i.e., correlations in activity between every pair of voxels, is computed from two different sources of activity: residual activity and resting-epoch activity. Residual activity was obtained by regressing out stimulus effects from fMRI activity in response to the stimuli and resting-epoch activity was taken by sub-sampling the data only from the acquisitions 18 seconds apart from the last stimulus presentation. Functional connectivity is sorted according to the difference of best frequency of the paired voxels to evaluate the tuning-specificity of functional connectivity. The data will be also sorted with respect to the hemispheres and the distinction of core and non-core fields that are parcellated using a recently published technique (Schönwiesner et al., 2014). The tuning specificity is quantified and compared between the auditory regions to evaluate its relation to functional specialty of the regions and hemispheres.

In study 2, tuning-specific functional connectivity is investigated in a larger context: whether the tuning-specificity of functional connectivity can be generalized to other tuning properties such as spectral density and modulation rate; whether and to what extent resting-state functional connectivity and noise correlations are similar or different ; whether the existence of tuning-specific noise correlations is disadvantageous for decoding the information with the correlation ignored; and whether resting-state functional connectivity is relevant to stimulus processing in the cortex so that the information of resting-state functional connectivity can be useful for decoding a stimulus. For these questions, fMRI responses to 72 natural sounds in 6 categories and resting-state activity are measured. Using a spectrotemporal response model previously developed based on neurophysiological data (Chi et al., 2005), modulation transfer functions of individual voxels were estimated. Voxelwise functional connectivity is computed either from residual activity (trial-to-trial response variation) and resting-state activity, and sorted according to tuning similarity between paired voxels to evaluate tuning-specificity of functional connectivity. To evaluate the effect of response co-variability (i.e., noise

correlations) between voxels, single-trial stimulus decoding (identification) by the tuning model is applied to the original data and the data with residual activity, or noise, decorrelated by trial-by-trial shuffling. Finally, decoding with resting-state functional connectivity incorporated is performed in comparison to decoding without functional connectivity added.

Study 1: Preferred frequency selectivity of voxel-by-voxel functional connectivity in human auditory cortex

Study 1 is designed to reveal the relation between frequency preference and functional connectivity in human auditory cortex, which is predicted to have positive correlation according to previous studies in animals or other human sensory cortices. Also, it is investigated whether such preferred frequency selectivity in functional connectivity differs across areas or hemispheres so to reflect functional architecture of human auditory cortex such as functional asymmetry. This study is published in Cerebral Cortex in 2014 (Cha, K., Zatorre, R.J., Schönwiesner, M., 2014. Frequency Selectivity of Voxel-by-Voxel Functional Connectivity in Human Auditory Cortex. Cereb. Cortex 1–14).

Abstract

While functional connectivity in the human cortex has been increasingly studied, its relationship to cortical representation of sensory features has not been documented as much. We used functional magnetic resonance imaging to demonstrate that voxel-by-voxel intrinsic functional connectivity (FC) is selective to frequency preference of voxels in the human auditory cortex. Thus, FC was significantly higher for voxels with similar frequency tuning than for voxels with dissimilar tuning functions. Frequency-selective FC, measured via the correlation of residual hemodynamic activity, was not explained by generic FC that is dependent on spatial distance over the cortex. This pattern remained even when FC was computed using residual activity taken from resting epochs. Further analysis showed that voxels in the core fields in the right hemisphere have a higher frequency selectivity in within-area FC than their counterpart in the left hemisphere, or than in the non-core-fields in the same hemisphere. Frequency-selective FC is consistent with previous findings of topographically-organized FC in the human visual and motor cortices. The high degree of frequency selectivity in the right core area is in line with findings and theoretical proposals regarding the asymmetry of human auditory cortex for spectral processing.

2.1. Introduction

To understand complex computation in the brain, it is necessary to identify the pattern of functional interactions between different regions at various spatial and temporal scales. This requires an understanding of the pattern of temporal coherence of neural activity between individual neurons or different populations of neurons, beyond relating only the magnitude of neural responses to behavioral and cognitive variables. Temporal coherence in neural activity has been studied for decades in terms of synchrony in spiking activity (Phillips et al., 1984), synchronous oscillations of neural populations (Singer and Gray, 1995; Fries, 2005), and correlations in trial-to-trial variability (or 'noise' correlation) (Gawne and Richmond, 1993; Lee et al., 1998; Averbeck et al., 2006). Given the invasive nature of this line of research, such fine-scale temporal dynamics in human brains has not been studied much. However, temporal coherence in activity measured functional magnetic resonance imaging (fMRI), referred to as 'functional connectivity' (FC), has gained much attention and has provided significant information in the field of systems and cognitive neuroscience (Fox and Raichle, 2007; Behrens and Sporns, 2012). Although the fluctuations that yield coherent patterns in fMRI are rather very slow (<0.1Hz) than fast as those in neurophysiological studies, they seem to have a neuronal origin (Shmuel and Leopold, 2008; Schölvinck et al., 2010) as do evoked fMRI responses (Logothetis et al., 2001). It is also evident that coherent fast fluctuations or oscillations in neural activity observed in neurophysiological studies are embedded in very slow fluctuations in fMRI activity (Leopold et al., 2003; Shmuel and Leopold, 2008; Kohn et al., 2009; Leopold and Maier, 2012). Notably, FC, or temporal coherence in neural activity, in most of these studies is considered 'intrinsic' because it is obtained by correlating spontaneous activity in absence of a stimulus or a task, and thus it is not explained by external inputs or task demands.

While the functional roles of intrinsic neural activity are not yet well understood, there has been a line of research to relate it to cortical representation of sensory stimuli, both in animals and humans. For instance, a study using voltage-sensitive dye imaging in the cat visual cortex showed that temporally coherent spontaneous activity emerges in the spatial pattern of orientation maps (Tsodyks et al., 1999; Kenet et al., 2003). Nauhaus et

al. (2009) found that spontaneous spiking activity in monkey and cat primary visual cortex triggers spatiotemporal propagations of local field potentials that reflect the similarity of preferred orientation between recording sites. In the auditory domain, Fukushima et al. (2012) demonstrated that high gamma band spontaneous activity in the macaque auditory cortex is coherent with frequency tuning at recorded sites. Analogously, correlations of residual spiking activity (noise correlation) of two simultaneously recorded neurons in macaque primary motor cortex have been reported to be high when their tuning properties are similar (Lee et al., 1998). In fMRI studies, it has been demonstrated that topographically organized sensory and motor features are related via very slow coherent fluctuations of intrinsic activity. Heinzle et al. 2011 found that intrinsic FC measured by fMRI in visual cortex is retinotopically organized: activity of fMRI voxels in V1 in resting-state was better explained by activity of voxels in V3 when the voxels had similar receptive field locations than dissimilar locations. Other resting-state fMRI studies have shown somatotopic organization of intrinsic FC in human motor network (van den Heuvel and Hulshoff Pol, 2010; Cauda et al., 2011) and in monkey somatosensory cortex (Chen et al., 2011). These results agree with observations in the animal literature that neural populations with similar tuning share coherent intrinsic activity, although the gaps in sampling units, frequency ranges, and species have yet to be filled (Kohn et al., 2009).

An advantage of using fMRI to study the functional organization of the brain at large scale is that it samples activity in multiple brain regions simultaneously. This applies not only to conventional amplitude-based studies, but also to studies of FC. For example, in Heinzle et al. (2011), the authors additionally demonstrated that the pattern of intrinsic FC in the visual cortex reflects difference in inter-hemispheric connectivity depending on voxel receptive field locations: voxels whose receptive fields were located along the vertical meridian have significant FC across the hemispheres, while that is not the case for voxels that are responsive to the horizontal meridian. This pattern of FC reflects the pattern of callosal connectivity found in anatomical tracer studies (Kennedy et al., 1986). Haak et al. (2012) have shown that the spatial extent of FC in human visual cortex increases as the hierarchical order of visual areas increases. This pattern is

commensurate with the hierarchical structure of retinotopic connectivity in early visual areas (Lehky and Sejnowski, 1988; Angelucci et al., 2002). Their findings also support the notion of constant cortical extent of inter-areal projections in the early visual cortex that has been proposed in previous studies (Hubel and Wiesel, 1974; Motter, 2009; Kumano and Uka, 2010; Harvey and Dumoulin, 2011).

In the present study, we hypothesized that intrinsic activity of auditory neurons in humans is more correlated with each other when they have similar preferred frequencies than when dissimilar. This hypothesis can be tested using fMRI since fMRI is capable of sampling the activity of neurons with similar preferred frequency in a voxel, because of tonotopic organization (Merzenich and Brugge, 1973; Romani et al., 1982; Morel et al., 1993; Howard et al., 1996; Wessinger et al., 2001); intrinsic FC can then be estimated on a voxel-by-voxel basis as discussed above. We predicted that the intrinsic FC between fMRI voxels, which is not explained by stimulus inputs, would be higher between voxels with similar preferred frequencies than between voxels with dissimilar ones. To test this hypothesis, we first estimated preferred frequencies of individual voxels in human auditory cortex using fMRI, and then analyzed residual fMRI activity and resting-epoch activity to compute intrinsic FC with respect to preferred frequency.

We further investigated whether the degree of frequency selectivity in FC differs across core and non-core auditory cortex, and across the hemispheres, in order to relate the pattern of FC to two well-known principles of functional architecture of auditory cortex: hierarchical processing and functional asymmetry. In human auditory cortex, core fields have higher frequency selectivity than secondary fields (Wessinger et al., 2001; Moerel et al., 2012), as is also the case in other animals (Morel et al., 1993; Rauschecker et al., 1995). This hierarchy is thought to be due to integration of a broader range of frequency information and higher complexity of sensory representation in the secondary fields than the core (Rauschecker, 1998; Kaas et al., 1999; Wessinger et al., 2001; Kumar et al., 2007). Another important aspect in the functional organization of the human auditory cortex is that the auditory cortex in the right hemisphere has a higher spectral resolution than on the left, which instead is more sensitive to rapid temporal variations

(Zatorre et al., 2002). This model is supported by findings that right auditory areas show stronger modulations to spectral variations (Schönwiesner et al., 2005; Hyde et al., 2008).

One interesting question that we address with our paradigm is whether the extent of frequency selectivity in FC is reflective of the hierarchical and asymmetric patterns of response seen in other studies. If frequency selective FC is a byproduct of the selectivity in response amplitude to stimuli, or conversely, sharp frequency tuning in the core fields is explained by local FC within an area, then we would expect that FC would be more frequency-selective (1) in the core fields than in the non-core fields, and (2) in the right than in the left auditory cortices. However, if FC is not simply reflective of the pattern of response amplitude but rather provides additional information for hierarchy and asymmetry, the pattern of FC would differ from the pattern of frequency selectivity in response amplitude. We compare the degrees of frequency selectivity in FC across the core and non-core fields of both hemispheres and discuss the results in light of sensory encoding/decoding and hierarchical emergence of functional asymmetry.

2.2. Materials and Methods

2.2.1. Participants

Seven people (4 male, 25 ~ 32 years old) with normal hearing went through anatomical and functional MRI scans with informed consent after approval of the experimental procedure by the local ethics committee.

2.2.2. Stimuli

Eight different frequencies of pure tones were used to stimulate the pure-tone sensitive and tonotopic auditory areas of the participants. The frequencies were logarithmically spaced between 200 Hz and 8000 Hz (200, 338.8, 573.8, 971.9, 1646.2, 2788.4, 4723.1 and 8000 Hz). In order to minimize adaptation, frequency was slightly jittered within a range of a single semitone (1/12 octave) every 250 ms with 3/4 duty cycle during each 4-second long stimulus presentation of one of the eight frequencies. The System 3 hardware of Tucker Davis Technologies (Alachua, FL, USA) was used to generate the stimulus at 24.4 kHz sampling rate. In stimulus presentation, we added a

noise that has equal energy in each equivalent rectangular band (Moore and Glasberg, 1996) at a level of 40 dB below the tones in order to minimize the effect of different thresholds for different frequencies, inter-participant difference in hearing threshold, and the transfer function of the headphones. Subjects were able to adjust the loudness of the sounds at 70 to 80 dB SPL that were delivered binaurally via an MR-compatible high-fidelity headphone (MR Confon).

2.2.3. Procedure

A sparse imaging protocol (Belin et al., 1999; Hall et al., 1999) with 9-second long repetition time (TR) was applied (Figure 2.1). A block consisted of 4 epochs (corresponding to 4 TR's), each of which lasted for 9 seconds. During the initial 2 epochs of a block, a pure tone in one of the 8 frequency conditions was presented. Each epoch started with 4 seconds of stimulus presentation, followed by 1 second of image acquisition, and then 4 seconds of silence. Thus, the noise due to the functional image acquisition did not interfere with hearing the tone stimulus. The 2 epochs with pure tone sound presentation were followed by silence that lasted for the remaining 2 epochs. A long duration (18 sec) of silence was inserted in order to minimize the fMRI response undershoot effect between stimulus blocks (Hu et al., 2010; Olulade et al., 2011). Each frequency condition was presented 10 times for each run of functional imaging and each subject underwent two runs. The order of stimuli was pseudo-randomized with balanced transition probability. The subjects were instructed to passively listen to the stimuli while watching a silent nature documentary.

2.2.4. Imaging protocol

An echo-planar imaging sequence (gradient echo; repetition time: 9 seconds; echo time: 36 ms; flip angle: 90°; in-plane resolution: 1.5 x 1.5 mm^2; slice thickness: 2.5 mm; field of view: 192 mm) was used to acquire functional images on a 3 Tesla scanner (Trio, Siemens). The total number of volumes per subject was 322 including 1 initial dummy volume. Thirteen slices were oriented parallel to the lateral sulcus to cover Heschl's gyrus, planum temporale, planum polare and the superior temporal gyrus and sulcus. A high resolution (1 x 1 x 1 mm^3) MPRAGE image that covered the whole brain was

acquired for each subject in the same session for anatomical registration.

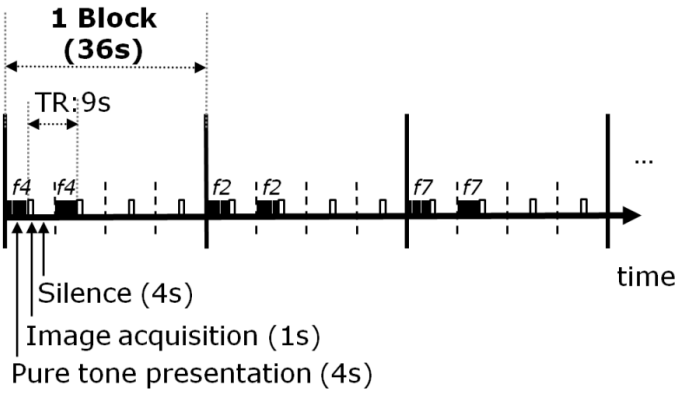

Figure 2.1. Stimulus presentation and fMRI sparse sampling.
Functional images were acquired every 9 seconds. Within a block of 4 acquisitions, each of the first two acquisitions was preceded by a 4-second stimulus sequence (pure tones 187 ms in duration presented every 250 ms). Frequency conditions of the pure tones were randomly changed across blocks as indicated herein as f4, f2 and f7 which correspond to 573.8, 338.8, and 4723.1 Hz.

2.2.5. Data preprocessing and the estimation of preferred frequency of voxels

Functional imaging data were preprocessed and the general linear model (GLM)-based estimation of response to the tone stimuli was conducted using SPM2 (www.fil.ion.ucl.ac.uk/spm). Preprocessing included motion-correction and high-pass filtering. No additional spatial smoothing or stereotaxic normalization was applied to minimize spatial autocorrelation. The gray matter (GM), the white matter (WM) and the cerebrospinal fluid were segmented using the segmentation tool of SPM2 (Ashburner and Friston, 1997). The segmented tissues were used to define the voxels/regions of interest and estimate correlations as a function of inter-voxel distance (See below). High-resolution anatomical images were aligned with the functional images to be displayed in Figure 2.2.

Eight frequency conditions were taken into account in the GLM analysis. A boxcar model was used to account for hemodynamic responses in a long-TR sparse acquisition. After estimating response amplitude as regression coefficients, F-contrast was applied to detect pure-tone-responsive voxels (F-test, $p<0.05$, uncorrected). A rounded exponential function, which is a Gaussian-like bell-shaped function, was fit as a

frequency tuning function (Rosen and Baker, 1994) to the response amplitudes of each voxel to estimate their preferred frequency. The form of the fitting function was $y = a(1 + k|x - m|)e^{|x-m|}$, where y is the response amplitude for 8 frequencies, x is the vector of log-transformed frequencies and the preferred frequency was parameterized by *m*. Accordingly, the preferred frequency of each voxel was selected at the peak of the function. Note that the 8 linear-scale frequencies (200, 338.8, 573.8, 971.9, 1646.2, 2788.4, 4723.1 and 8000 Hz) were corresponded to integers from 1 to 8 in the log scale and the preferred frequency estimate was bounded at 0.5 and 8.5 in the log scale (correspondingly at 153.7 Hz and 10412 Hz in the linear scale of frequency). The preferred frequency of the voxels that had non-significant level of goodness-of-fit (*F*-test, $p>0.05$; 17.12% [SD=0.01] of voxels) was replaced with the measure of the center of mass of the amplitudes: the amplitude was averaged with the log-transformed frequency values weighted.

2.2.6. Selection of voxels and the definition of the core-fields and the non-core-fields areas

Upon choosing the pure-tone responsive voxels and estimating their preferred frequency, we defined the core-fields and the non-core-fields areas. The border of core-fields area was identified based on tonotopic gradient and multivariate pattern classification under the assumption that the core fields are more sensitive to pure-tone stimuli than the non-core, as determined in a previous study (Schönwiesner et al. 2014 for further details). This method utilizes the support vector machine technique to find the boundaries in the imaging data to classify the frequencies. The eight-class frequency classification problem was solved by partitioning into pair-wise binary classifications. The core-fields area was defined as those voxels in which the classifier predicts the frequencies with statistically significant accuracy. The classification accuracy was significantly correlated with the response magnitude to pure tones and frequency tuning width, which can serve as indicators of response properties of the core-fields area according to previous studies (Morel et al., 1993; Rauschecker et al., 1995; Wessinger et al., 2001; Petkov et al., 2006; Moerel et al., 2012). The delineation of the core area by

this method was generally in agreement with the results of the probabilistic cytoarchitectonic maps (Morosan et al., 2001; Rademacher et al., 2001). Also, this same method identified the core-fields in macaque monkeys that overlap with previous parcellation of AC in the same data (Petkov et al., 2006). Only the voxels that had p-values below 0.05 and reside in the segmented gray matter were included in the present study. The gray matter, the white matter (WM) and the cerebrospinal fluid were segmented using the segmentation tool of SPM2 (Ashburner and Friston, 1997).

The voxels of non-core areas were identified by searching for significantly activated voxels in the gray matter starting from the edge of the core areas: the search algorithm incorporated the surrounding voxels in the 3-dimensional space until it could not find any more significantly activated voxels within the gray matter. This procedure was chosen under the assumption the belt and the parabelt areas surround the core fields, based on the known AC organization in primates (Kaas et al., 1999; Kaas and Hackett, 2000; Hackett, 2011). Figure 2.2A shows a representative subject's voxels of interest marked as core and non-core areas in three selected slices.

2.2.7. Residual functional connectivity and its frequency selectivity in the auditory cortex

Voxel-by-voxel FC was computed as temporal correlation (Pearson's correlation coefficient) of the residual fMRI signal of each voxel after regressing out the model responses predicted by the stimulus (hereafter 'residual' FC). For each pair of voxels, correlation coefficients obtained from two runs were averaged. To ensure linearity, correlation coefficients were transformed to Fisher's z-score, and then averaged and transformed back to correlation coefficients.

FC was analyzed by pairing voxels at two levels: a hemisphere level and an area level. At the hemisphere level, we paired voxels either from one hemisphere (L-L: within the left hemisphere; R-R: within the right hemisphere) or across the hemispheres (L-R: between the left and the right hemispheres, see Figs. 3 to 7). At the area level, voxels were paired within an area or between areas, either within or between hemispheres. In Figure 2.8, 'LC' represents the core area in the left hemisphere; 'RC', the right core; 'LN',

the left non-core; and 'RN', the right non-core area. The label of a pair of the same area such as 'LC-LC' refers to the case where the seed and the target voxels were drawn from the same area. In this way, six pairs of areas were defined within hemispheres (Figure 2.8A) and four pairs of areas were defined between hemispheres (Figure 2.8B).

FC as a function of preferred frequency in Figures 2.3 to 2.5 was obtained by a grid method with respect to preferred frequency of seed and target voxels: FC between a given voxel (seed voxel) and the remaining voxels (target voxels) was sorted by the preferred frequency of target voxels and then the resulting voxel-wise FC data of each seed voxel as function of preferred frequency of target voxels was grouped with respect to preferred frequency of seed voxels. The seed and target voxels were chosen either from the same hemisphere or from different hemispheres, depending on the analysis condition. Note that preferred frequency is expressed on a log-scale that ranged from 0.5 to 8.5 (from 153.7 Hz to 10412 Hz; See the above description in Methods).

In order to examine patterns of FC related to selectivity but irrespective of the preferred frequency of any given voxel, we merged frequency selectivity of FC across multiple seed voxels regardless of their preferred frequencies, by sorting FC data as a function of difference of preferred frequencies on a log-scale (Δ preferred frequency) (Figure 2.2C and 2.2D). The data were binned with bin edges of 0, 0.5, 1, 2, 4 and 8, in order to ensure reliable estimations of average FC even at larger Δ preferred frequencies where we have fewer data points. The binned data were averaged across subjects (Figure 2.3C, 2.5B, 2.6C, 2.7 and 2.8). Page's trend test was applied to test whether frequency selectivity is statistically significant. L-scores were transformed to χ^2 scores to compute p-values (Page, 1963).

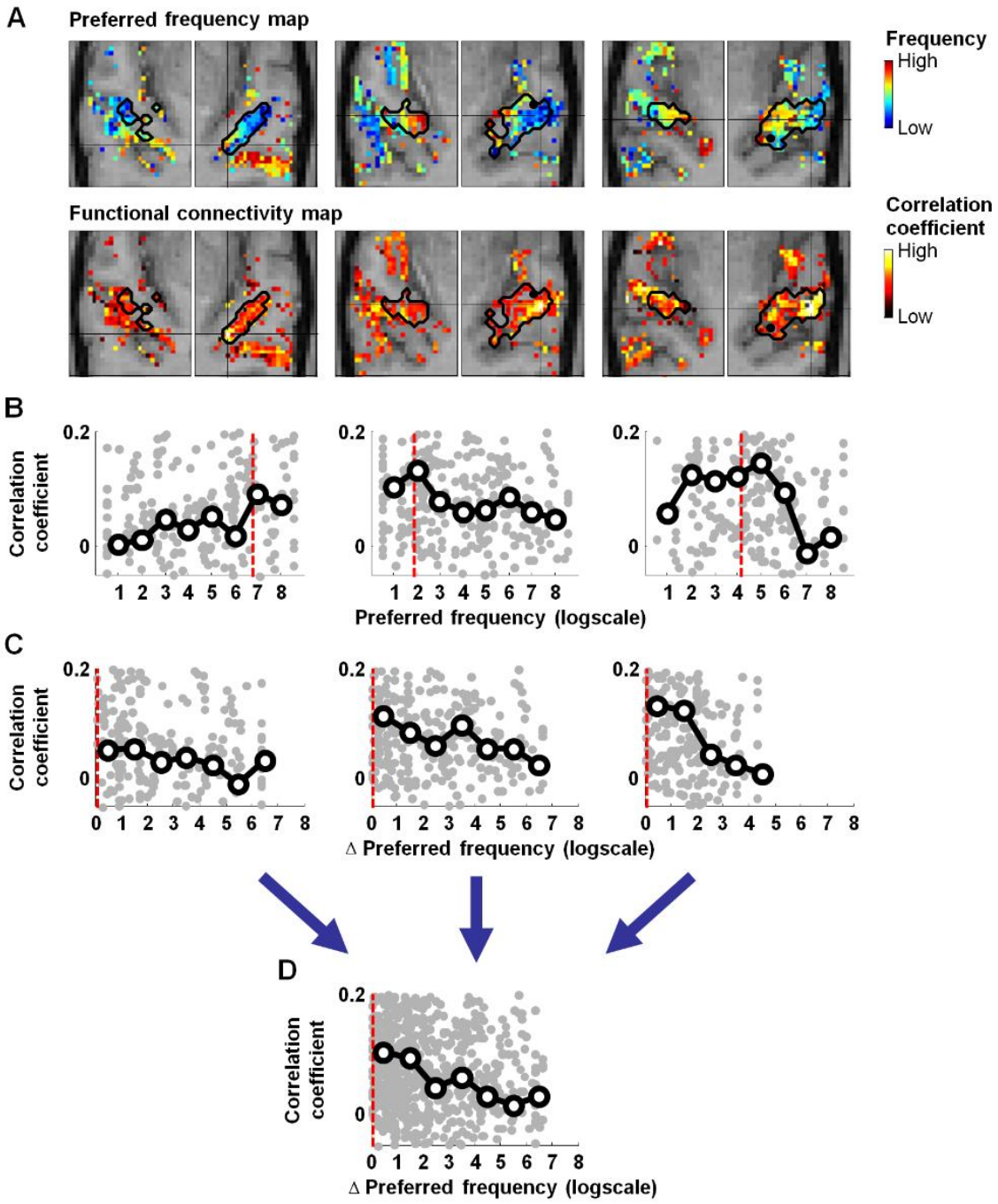

Figure 2.2. Preferred frequency map, FC map, and voxel-by-voxel FC as a function of preferred frequency.

Preferred frequency maps of three slices (in-plane; z=7, 8 and 9) in a representative participant (top) and corresponding FC maps of three seed voxels (bottom). Top: Closed curves indicate the core-fields regions and black crosshairs locate the three seed voxel locations in each slice. Bottom: FC in each panel is computed by correlating the residual

activity of the seed voxel and the remaining (target) voxels. B. Voxel-by-voxel FC as a function of preferred frequency from each slice in the three columns. Gray dots mark FC of every pair of voxels in each slice and black curves are the average of preferred frequency binned with 1-octave width. Red vertical lines indicate the preferred frequency of the seed voxels. C. Voxel-by-voxel FC as a function of difference in preferred frequency (Δ preferred frequency) for each slice in the three columns. The consequence of taking Δ preferred frequency is that the preferred frequency of all seed voxels is aligned to 0 (red vertical lines). Black curves indicate the average of each bin of Δ preferred frequency). D. Pooled data from the three slices. The FC of individual pairs was pooled and binned. Note that this figure shows only the scheme of the method with three exemplary seed voxels.

2.2.8. Correction of inter-voxel distance bias

Possible biases due to the point-spread of fMRI signals (Engel et al., 1997) and the generic FC that extends over large distance in the cortex (Leopold et al., 2003; Bellec et al., 2006; Honey et al., 2009; Schölvinck et al., 2010) were corrected by subtracting FC due to inter-voxel distance in the following way: We first correlated the residual fMRI signals between the voxels in gray matter regions, excluding auditory cortex. We then selected voxels with the lowest 5% F-values in the GLM analysis with the aim to exclude any remaining pure-tone-responsive voxels outside auditory cortex. We then computed voxel-by-voxel correlations between the time courses of these voxels and binned the results along inter-voxel distance with width of 1.5 mm (the in-plane resolution of the functional data). We subtracted this FC estimate from the measured FC in auditory cortex to obtain distance-corrected FC (Figure 2.6).

2.2.9. Resting-epoch FC and testing confounding of stimulus effect

As an alternative measure of intrinsic FC that does not depend on the incoming stimulus, FC was also computed by correlating residual activity that was taken from the 4th TR of every block (every 36 seconds), which is referred to as ‘resting epochs’ (Fair et al., 2007). The acquisition time of 4th TR is relatively far (18 seconds) from the preceding stimulation, and we would expect only minimal effects of the stimulation on the fMRI signal, because hemodynamic response functions are typically close to zero at this point (Hu et al., 2010; Olulade et al., 2011). To rule out any possibility that delayed

hemodynamic responses to the stimulus still affected the signal in resting epochs, we additionally regressed out the stimulus effect from the resting-epoch time series. For this purpose, we applied a GLM that predicts stimulus-induced responses according to the frequency of the sounds given in each block, and subtracted the predicted time course from the resting-epoch time course. The frequency selectivity of resting-epoch FC with and without the stimulus-effect regressed out was tested in the same way as the residual FC (Figure 2.7).

2.2.10. Comparison of frequency selectivity between areas

In order to compare frequency selectivity of FC from one area to another, frequency selectivity of FC was first quantified by computing the slope of a linear function fit to FC as a function of Δ preferred frequency. A higher value thus reflects a steeper slope of the function, indicating higher selectivity. We tested whether frequency selectivity of FC in one area is higher than in another by a permutation test: we re-sampled the frequency selectivity (the negative slope of linear fit) with replacement out of 7 subjects 1000 times for each area and permuted the area membership to obtain the sampling distribution under the null hypothesis. A p-value for the difference in frequency selectivity in the sample mean was then computed.

2.3. Results

2.3.1. Preferred frequency selectivity of functional connectivity in the human auditory cortex

Voxel-by-voxel FC in the human auditory cortex was found to depend on the similarity of the preferred frequencies of voxels (Figure 2.2 and 2.3). Figure 2.2A shows a representative subject's tonotopy maps based on the preferred frequency of the voxels of interest (Figure 2.2A, top), and the maps of FC between a voxel (seed voxel; cross-hair) and the remaining (target) voxels (Figure 2.2A, bottom). The FC of the three exemplary seed voxels is plotted as a function of preferred frequency of the target voxels in Figure 2.2B. This voxel-by-voxel FC is then re-sorted as a function of preferred frequency difference between the seed and the target voxels as shown in Figure 2.2C.

This sorting allows us to pool FC of all pairs of voxels, irrespective of preferred frequency (Figure 2.2D).

Figure 2.3 demonstrates that frequency selectivity of FC is present in the averaged data across participants, both within hemispheres (i.e. when seed and target voxels were chosen within a hemisphere (LL: within the left hemisphere; RR: within the right hemisphere) and across hemispheres (i.e. when seed and target voxels were chosen in different hemispheres, LR). Voxel-by-voxel FC was binned with respect to the preferred frequencies of seed and target voxels to be presented as a matrix (Figure 2.3A) and as a family of curves (Figure 2.3B). High FC is in general observed along the diagonal of the matrices in Figure 2.3A, indicating higher FC between voxels with similar preferred frequencies. This pattern is also reflected in the peaks of FC in Figure 2.3B when seed and target voxels have the same preferred frequency. Note that the roles of seed and target voxels can be exchanged because FC does not contain directionality information. In Figure 2.3C, voxel-by-voxel FC was pooled and binned as a function of difference in preferred frequency (Δ frequency) between the correlated voxels to reveal that FC decreases as Δ frequency increases. Page's trend test indicated that the gradual decrease of FC as a function of Δ frequency is statistically significant for the three conditions of hemisphere pairs (LL: L=383, χ^2=26.42, p<0.0001; RR: L=385, χ^2=28.00, p<0.0001; LR: L=383, χ^2=26.42, p<0.0001). These results hold for each tested individual: FC was found to be frequency-selective in all individual participants (Figure 2.4), and the correlation between voxel-by-voxel FC and Δ frequency was significant in each participant in the within/between hemisphere conditions ($p<10^{-6}$ for all cases).

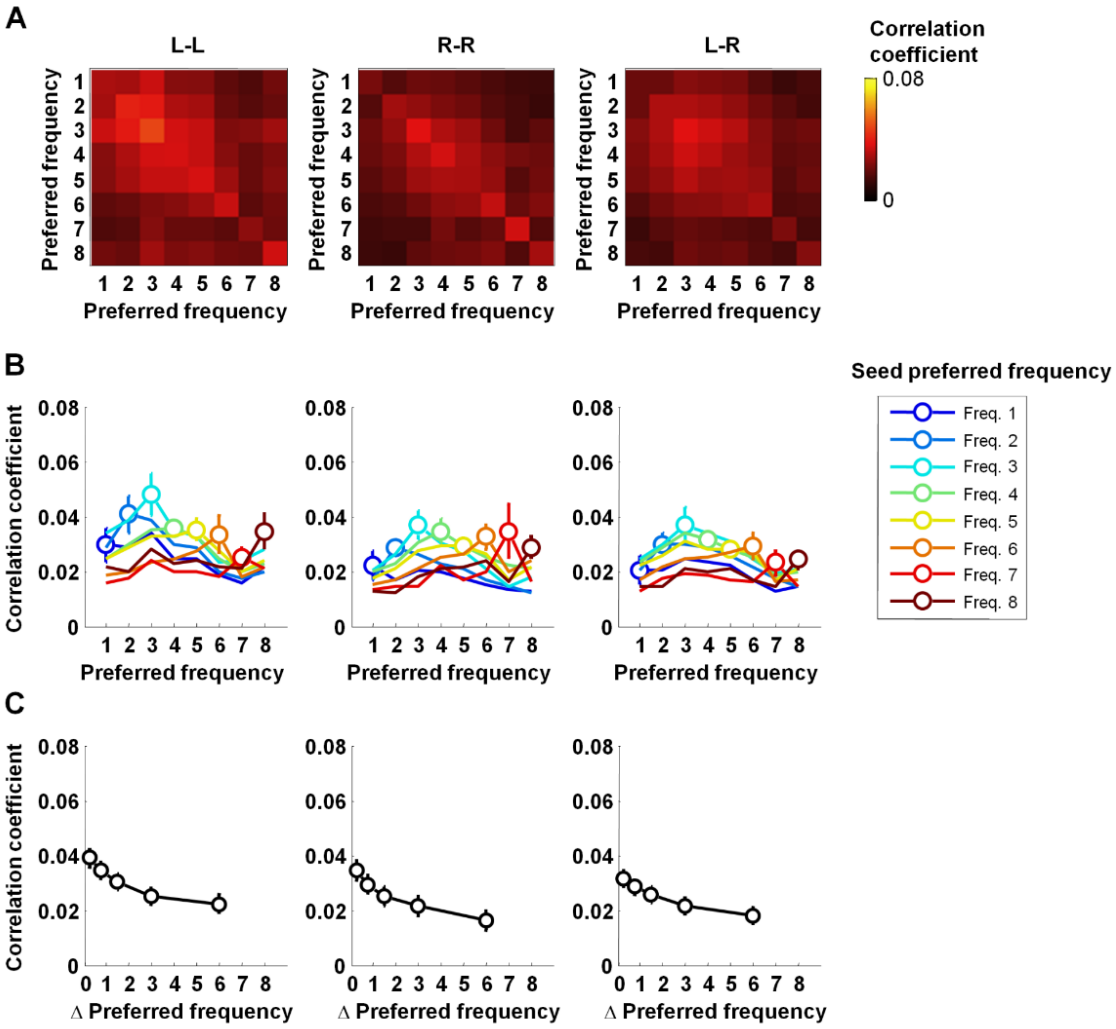

Figure 2.3 Frequency-selective FC within and between hemispheres.
A. FC matrix as a function of preferred frequency of the seed and target voxels. Preferred frequencies were binned in 1 octave steps. Left (L-L): FC of the voxels within the left hemisphere; center (R-R): FC within the right hemisphere; right (L-R): FC between the hemispheres. B. FC as a function of preferred frequency of target voxels. Each of the eight curves corresponds to averaged data across seed voxels that prefer similar frequencies of 1 octave range. Error bars are shown only at the data points of preferred frequency of seed voxels for clarity. Note that each curve in B corresponds to each row of the matrix that is aligned along the column. Error bars represent ±1 STE of the mean across subjects. C. FC as a function of difference in preferred frequency (Δ preferred frequency). In B and C, each column corresponds to the ones in A. These graphs indicate that inter-voxel FC is higher for voxels with more similar frequency tuning.

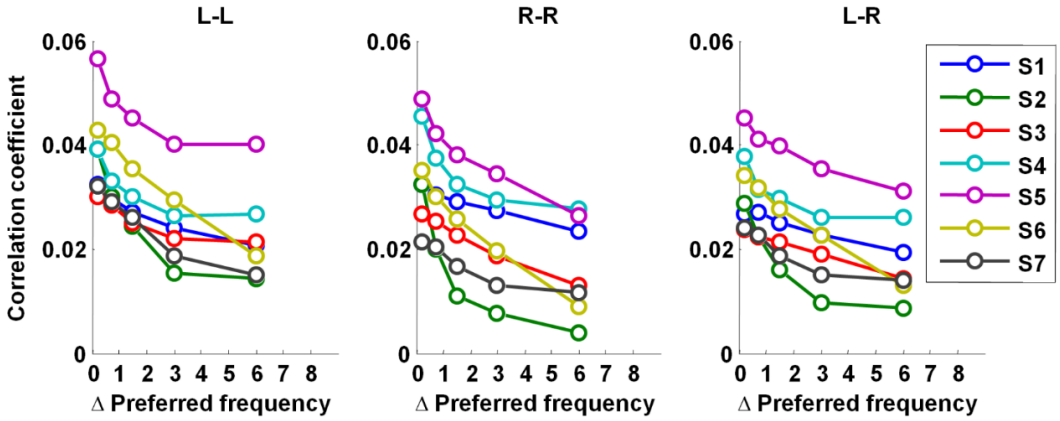

Figure 2.4. FC as a function of difference in preferred frequency within and between hemispheres in individual participants.

Data from the seven individual participants are plotted in the same format as Fig. 3C. All seven individuals clearly show decreasing FC as a function of increasing distance of voxel frequency preference.

2.3.2. Inter-voxel-distance-corrected FC

Because of the tonotopic organization of auditory cortex (i.e., neurons with more similar frequency preference tend to be more closely located to one another), frequency preference of voxels would tend to be correlated with inter-voxel distance. FC is also in general correlated with physical distance between paired areas or voxels (Salvador et al., 2005; Bellec et al., 2006; Honey et al., 2009) due to spatial smoothing of fMRI signals, point spread of fMRI BOLD signal (Engel et al., 1997) and/or the generic FC over the cortex whether local or global (Leopold et al., 2003; Honey et al., 2009; Schölvinck et al., 2010). Therefore, the observed frequency-selective FC could have been only a byproduct of these two correlations (correlation between frequency preference and inter-voxel distance and that between inter-voxel distance and FC). To ascertain that the correlation of FC with preferred frequency was not fully explained by the correlation of FC with distance, we corrected the FC with respect to inter-voxel distance.

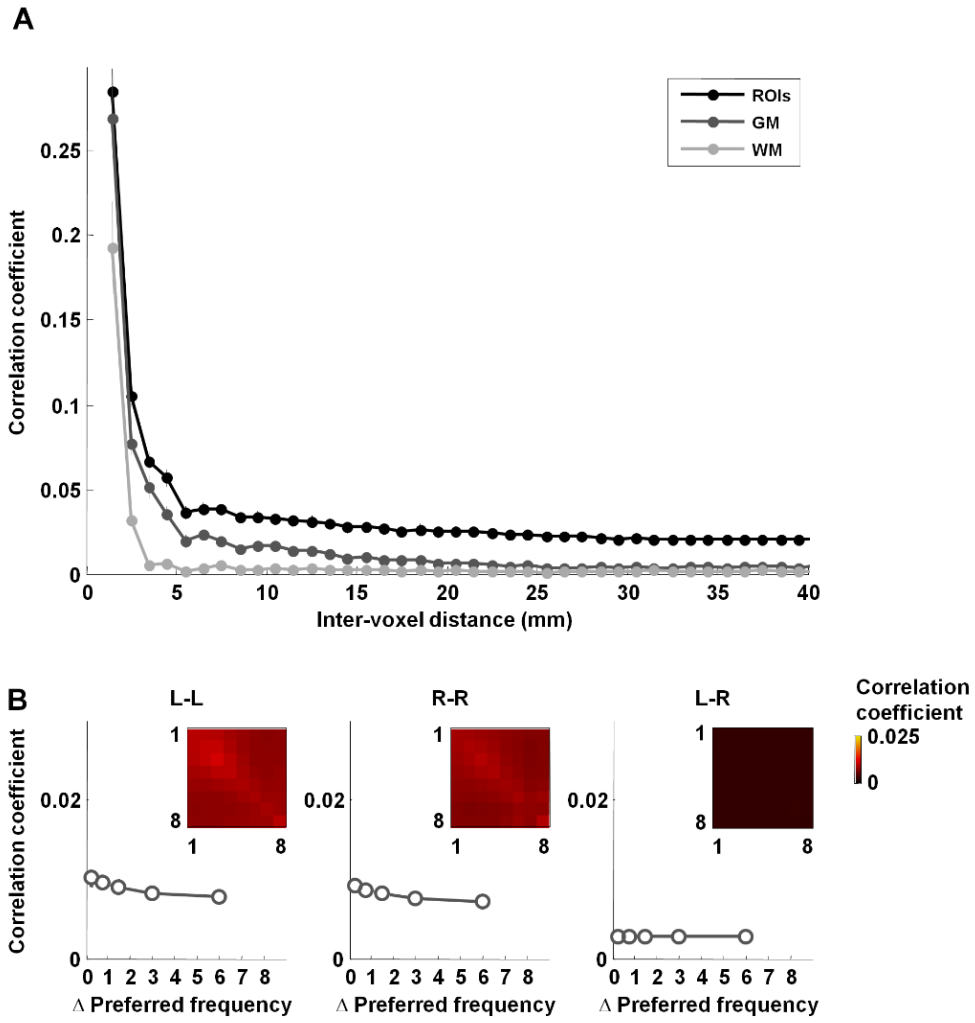

Figure 2.5. Inter-voxel distance effect.

Temporal correlation of residual activity as a function of inter-voxel distance in the pure-tone sensitive ROIs (ROIs; black), the gray matter outside the auditory ROIs (GM; dark gray) and the white matter (WM; light gray). Error bars represent ±1 STE across subjects. B. FC in the ROIs predicted by inter-voxel distance in the GM. The inset shows the FC matrix as in Figure 3A.

We first confirmed that the temporal correlation of fMRI residual signals within the auditory ROI and also outside of the ROI (in the remaining gray and white matter) are dependent on inter-voxel distance (Figure 2.5A). The white matter shows the sharpest decay as a function of distance. The spatial extent (~3 mm) implies that the correlation observed in the white matter is presumably due to spatial smoothing effect in fMRI acquisition and motion correction rather than correlations in neural activity. In contrast,

the gray matter has a less steep decay function, which is consistent with previous interpretations that this function reflects local and global correlation in neural activity (Leopold et al., 2003; Schölvinck et al., 2010). The correlation in non-auditory regions of gray and white matter decayed to zero for distances of less than 30 mm, whereas that in the auditory ROIs reached an asymptote at a non-zero, positive value. This indicates that local FC in the auditory cortex is higher overall than the spatial extent of global FC in the rest of the gray matter, which in turn implies that there is auditory cortex-specific FC in addition to generic correlation in on-going fMRI activity over the entire cortex.

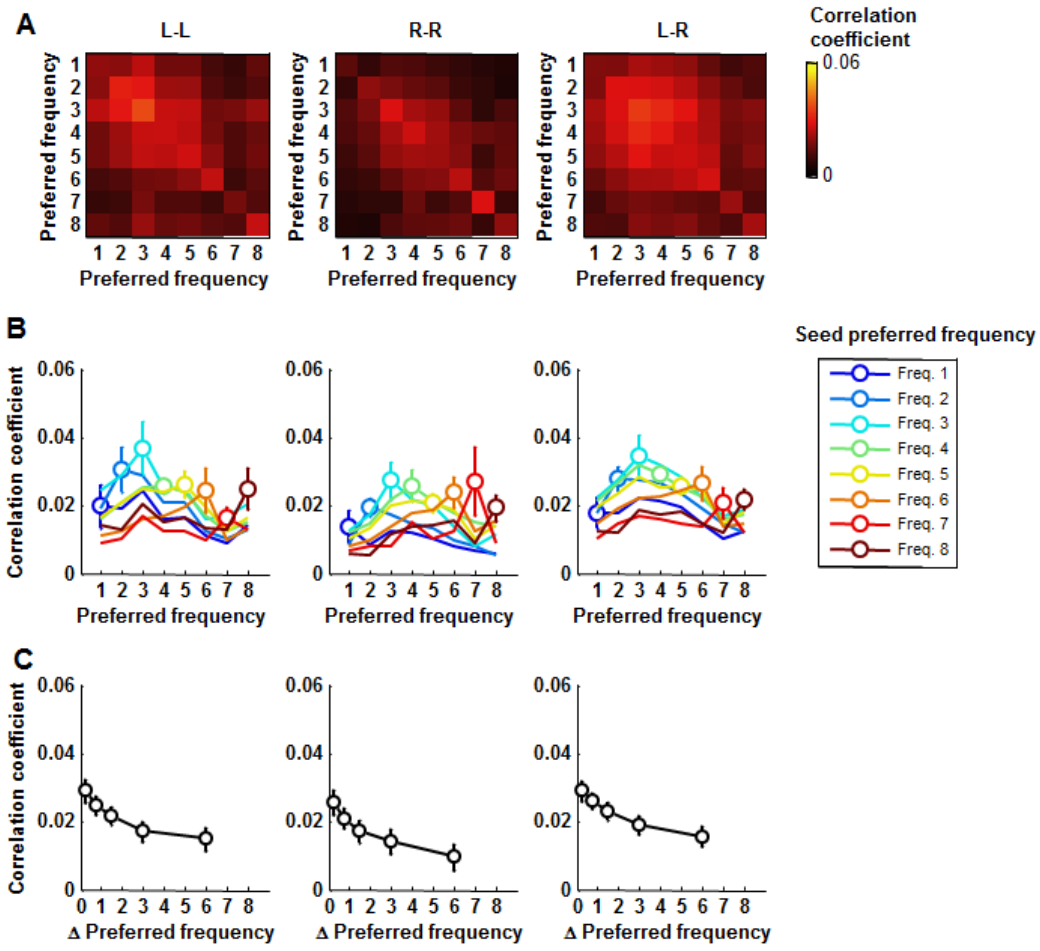

Figure 2.6. Distance-corrected functional connectivity.
Distance-corrected frequency-selective FC within the left hemisphere (L-L), within the right hemisphere (R-R) and between the hemispheres (L-R) is plotted in the same format as in Figure 3. The distance effect is corrected by subtracting the FC predicted by the distance in the gray matter from the original FC. The pattern of corrected results is

similar to the principal effects shown in Fig 3.

As a second verification that distance does not explain the observed FC in auditory cortex, we predicted FC that would have been observed if the generic correlation in the gray matter had completely explained the frequency selectivity of FC in the auditory cortex. We did so by assigning the correlation values in the gray matter to the voxels in the auditory ROIs that have equivalent inter-voxel distance. The FC predicted on this basis showed a weak but significant frequency selectivity within hemispheres, but not between the hemispheres, since inter-hemispheric distances are much larger than 30 mm, where the correlation in the gray matter voxels decays away (Figure 2.5B; LL: L=385, χ^2=28.00, p<0.0001; RR: L=385, χ^2=28.00, p<0.0001; LR: L=334, χ^2=0.50 p=0.096). The small but significant frequency selectivity in the predicted FC within hemispheres could bias our findings, so we corrected this potential problem by subtracting the predicted FC values based solely on distance from the measured FC values. The corrected FC was still frequency-selective within and between hemispheres (Figure 2.6; LL: L=382, χ^2=26.65, p<0.0001; RR: L=385, χ^2=28.00, p<0.0001; LR: L=383, χ^2=26.43, p<0.0001), indicating that the distance effect is not sufficient to account for the frequency selectivity.

2.3.3. Stimulus effect and resting-epoch FC

Although we subtracted the predicted response accounted for by the stimulus from the fMRI response, a stimulus effect might still remain due to incomplete model fit. To control for this possibility, we used only the residual fMRI activity from the 4th TRs of each block. The activity captured in these TRs can be considered as resting or on-going activity rather than stimulus-driven activity since it is collected 18 seconds after the previous stimulus presentation. The frequency selectivity of this ‘resting-epoch FC' was significant for all the within- and between-hemisphere conditions (Figure 2.7A; LL: L=382, χ^2=25.65, p<0.0001; RR: L=384, χ^2=27.21, p<0.0001; LR: L=383, χ^2=26.42, p<0.0001). Furthermore, we regressed out again the model responses to stimulus conditions from the resting-epoch time series in order to remove any remaining effect of the preceding stimulus condition. FC using the baseline activity with the stimulus effect

regressed out was still frequency-selective (Figure 2.7B; LL: L=377, χ^2=21.97, p<0.0001; RR: L=384, χ^2=27.21, p<0.0001; LR: L=382, χ^2=25.65, p<0.0001).

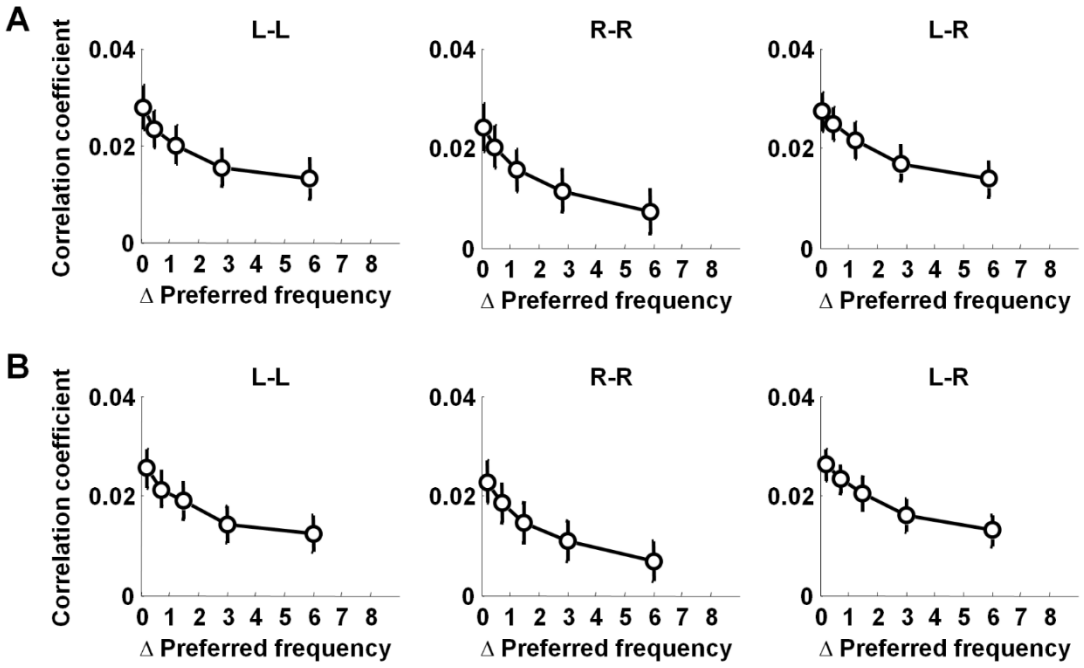

Figure 2.7. Frequency-selective FC in resting epochs.
A. FC in resting epochs as a function of difference in preferred frequency (Δ preferred frequency). B. FC in resting epochs as a function of Δ preferred frequency after regressing out stimulus conditions. Note that only the fourth TRs of the blocks were used to compute FC. The pattern obtained in the resting epochs replicates that observed in the other conditions.

2.3.4. Frequency selectivity of FC in the core and the non-core fields, and hemispheric differences

Upon confirming frequency selectivity of FC in the auditory cortex within and between hemispheres, including with inter-voxel distance and the stimulus effect controlled, we next tested frequency selectivity of FC in the core and the non-core areas separately. We divided these areas to obtain 6 different pairs of areas within the hemispheres (Figure 2.8A) and 4 pairs between the hemispheres (Figure 2.8B). The results show that there is significant frequency selectivity for every pair (LC-LC: L=349,

χ^2=6.61, p<0.05; RC-RC: L=383, χ^2=26.42, p<0.0001; LN-LN: L=381, χ^2=24.89, p<0.0001; RN-RN: L=358, χ^2=28.00, p<0.0001; LC-LN: L=375, χ^2=20.57, p<0.0001; RC-RN: L=382, χ^2=25.65, p<0.0001; LC-RC: L=362, χ^2=12.62, p<0.0005; LN-RN: L=384, χ^2=27.21, p<0.0001; LC-RN: L=371, χ^2=17.92, p<0.0001; RC-LN: L=383, χ^2=26.42, p<0.0001). Therefore, FC in the auditory cortex is frequency selective within and between areas, both within and between the hemispheres.

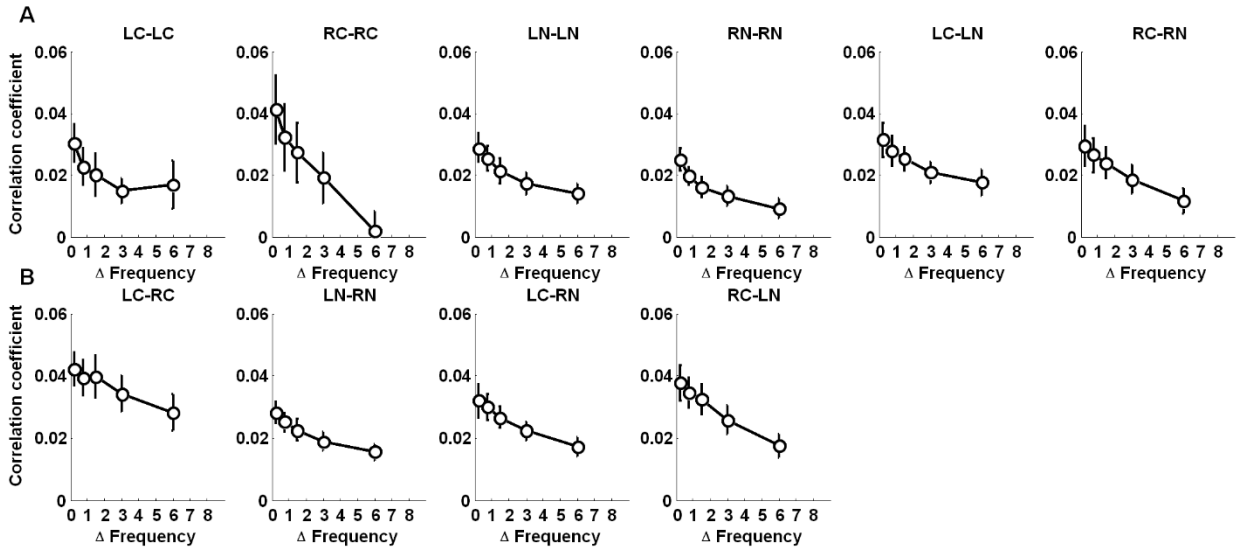

Figure 2.8. Frequency-selective FC in within and between core and non-core fields. FC is plotted as a function of difference in preferred frequency of voxels (Δ frequency) within and between the core and non-core fields within the hemispheres (A) and between the hemispheres (B). Note the steeper slope of the function corresponding to voxels within the right core region, compared to all the rest.

We then investigated whether the degree of frequency selectivity of local FC differs between core vs non-core areas, and whether it differs between left and right hemispheres.We quantified frequency selectivity as the negative slope of a linear function fit to FC data as a function of Δ (preferred) frequency for the four areas (LC, RC, LN and RN), shown in Figure 2.9A. Permutation tests indicated that FC in the right core area had a higher frequency selectivity than the left core (p<0.05; also, Wilcoxon signed-rank test: W=27.0, p<0.05), and than the non-core in the same hemisphere (permutation test: p<0.05; Wilcoxon signed-rank test: W=28.0, p<0.05). There was no difference between the non-core areas of the two hemispheres (permutation test: p=0.29; Wilcoxon signed-

rank test: W=18.0, p=0.29) or between the two areas within the left hemisphere (permutation test: p=0.32; Wilcoxon signed-rank test: W=17.0, p=0.344). The same analysis applied to the resting-epoch FC with the stimulus effect regressed out (corresponding to the data in Figure 2.7B) showed a similar pattern (Figure 2.9B) although the statistical significance was marginal (RC vs. LC: p=0.08; RC vs. RN: p=0.11; RN vs. LN: p=0.24; LC vs. LN: p=0.63). Thus, the right core field has higher frequency selectivity in its within-area FC than the other areas, notably its homologue in the left hemisphere.

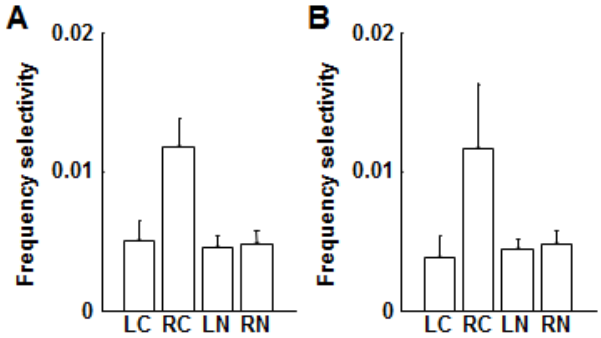

Figure 2.9. Comparison of within-area FC between areas.
Frequency selectivity of residual FC within four ROIs (LC: left core; RC: right core; LN: left non-core; and RN: right non-core). B. Frequency selectivity of resting-epoch FC within four ROIs (LC: left core; RC: right core; LN: left non-core; and RN: right non-core). The frequency selectivity is highest for the right core compared to the other regions.

2.4. Discussion

Our study is, to our best knowledge, the first attempt to link intrinsic FC and frequency selectivity in the human auditory cortex. Our findings demonstrate that intrinsic FC measured with fMRI in human auditory cortex is organized in accordance to frequency preference of voxels. Residual and resting epoch activity in voxels with similar frequency preferences was more strongly correlated than in voxels with dissimilar frequency preferences. This correlation was not explained by generic FC in the activity of the gray matter voxels, or by residual stimulus effects. Furthermore, we observed that the

intrinsic FC is significantly stronger within the core fields of the right hemisphere as compared to the left core, or the right non-core fields.

2.4.1. Frequency-selective FC in the auditory cortex and relation to prior studies

The existence of frequency selectivity of intrinsic FC in the human auditory cortex is in line with findings in other human sensory/motor cortices and non-human auditory cortex. Given the topographic organization of frequency preference (Merzenich and Brugge, 1973; Romani et al., 1982; Morel et al., 1993; Wessinger et al., 2001), frequency-selective FC is the auditory analog of topographically-organized FC previously found in the visual and somatosensory/motor cortices. In the visual cortex, retinotopy-specific FC was observed between early visual areas and ipsilateral and contralateral MT regions in the monkey (Vincent et al., 2007), and between early visual areas (Heinzle et al. 2011; Haak et al. 2012). Somatotopy-specific spatial organization of intrinsic FC was also found in the motor cortex of the human and in the somatosensory cortex of the squirrel monkey (van den Heuvel and Hulshoff Pol, 2010; Cauda et al., 2011; Chen et al., 2011). It is notable that in these studies, resting-state fMRI activity was used for computing FC, and thus the measured FC is intrinsic and not explainable by stimulus input or motor output. Although we used residual activity instead of using resting-state data, previous literature and our own analysis strongly suggest that the FC we measured is intrinsic. There is considerable evidence that residual fMRI activity is highly correlated with spontaneous activity (Fox et al., 2006b, 2007; Saka et al., 2010; Becker et al., 2011). In line with these previous findings, we empirically demonstrated that our residual FC was intrinsic and not accounted for by stimulus-driven activity, and an additional regress-out did not remove frequency-selective pattern of FC (Figure 2.7; See below for further discussion). Therefore, our results supplement evidence for a unifying proposal that intrinsic FC in the cerebral cortex is spatially organized with respect to sensory/motor tuning properties and/or their topographic organization (Jbabdi et al., 2013).

Our findings of frequency-selective FC are also consistent with those in electrophysiological studies in the non-human animal auditory cortex. Brosch and

Schreiner (1999) found that correlation in spontaneous neural activity is strengthened as a function of similarity in receptive field properties in the cat primary auditory cortex. In guinea pigs, spontaneous activity was shown to have similar spatiotemporal patterns with tone-evoked activity (Saitoh et al., 2010). Rothschild et al. (2010) also reported frequency-selective coherence in both residual activity and on-going spontaneous activity in mice, which is closely related to our paradigm: both correlation in residual neural activity during tone-stimulation and correlation in on-going activity taken from pre-stimulation time windows increased when the correlated neurons had similar frequency selectivity. Finally, Fukushima et al. (2012) demonstrated tonotopy-specific FC in spontaneous activity in macaque monkeys in resting-state data. Using micro-electrocorticographic arrays, they were able to find that the spatial pattern of high-gamma-band voltage signals is coherent with the characteristic frequency maps along the supratemporal plane of the lateral sulcus. Considering that fMRI signal is not only correlated with evoked neural activity (Logothetis et al., 2001) but also is related to spontaneous activity, and that very slow fluctuations of gamma-band power in electrophysiological signals are correlated with spontaneous fMRI activity (Leopold et al., 2003; Nir et al., 2008; Shmuel and Leopold, 2008; Schölvinck et al., 2010), our findings of frequency selectivity in residual and ongoing fMRI activity are consistent with those in previous animal studies.

2.4.2. Functional role of functional connectivity in stimulus encoding

While the functional role of frequency-selective FC, or feature-selective FC in general, is yet unclear, the importance of temporal coherence in activity of sensory neurons has been discussed with respect to population coding and decoding of stimulus features (Fries, 2005; Kohn and Smith, 2005; Averbeck and Lee, 2006; Pillow et al., 2008; Stevenson et al., 2012). For example, Stevenson et al. demonstrated that the activity of neurons simultaneously recorded in various cortical areas can be better predicted by a stimulus encoding model that incorporates FC, measured as trial-to-trial correlations (‘noise’ correlations), than a model that accounts only for tuning functions. It is notable that in their study the correlations between neurons increased with tuning

similarity, which is consistent with the present data. Incorporation of FC not only improved prediction accuracy in encoding, but also accuracy in decoding the presented stimuli. In other studies, behavioral performance of animal subjects was also related to trial-to-trial fluctuations and correlations in spiking activity (Bair et al., 2001; Pesaran, 2010). Despite the difference in measurement, trial-to-trial fluctuations or spontaneous fluctuations in fMRI signals seem to have similar functional significance as the aforementioned neurophysiological data for three reasons (See Kohn et al. 2009): Firstly, fast fluctuations observed in spiking activity or field potentials are nested in slow BOLD fluctuations as discussed above; secondly, trial-to-trial fluctuations or spontaneous fluctuations in fMRI signals are also predictive of behavioral performance (e.g., Fox et al. 2007; Monto et al. 2008), and perception (e.g., Boly et al. 2007); and finally, recent successes of using multi-voxel encoding and decoding models in fMRI analysis in predicting neural activity and behaviors indicate the importance of temporal coherence (covariance) information between voxels (Naselaris et al., 2011; Serences and Saproo, 2012). Therefore, correlations in residual activity and resting-epoch activity are likely to have functional significance in encoding and decoding stimulus features. The role of FC in processing of stimulus features is important to interpreting our results with respect to functional hierarchy and asymmetry, as discussed below.

2.4.3. Controlling for inter-voxel distance and stimulus effects

Considering the topographic organization of frequency selectivity in the cortex, the relationship between FC and frequency preference that we observed in our data could have been caused by an artifact due to point spread of fMRI signal (Engel et al., 1997; Parkes et al., 2005), or spatial extent of generic FC that might not be specific to frequency selectivity (Young et al., 1992; Leopold et al., 2003; Bellec et al., 2006; Honey et al., 2009; Schölvinck et al., 2010). The data presented in Figures 2.5 and 2.6, however, do not support this interpretation. Firstly, the spatial extent of correlation in the non-auditory gray matter is still shorter than that in the auditory ROIs, which suggests that the FC in the ROIs has an additional component beyond this generic FC. Secondly, the distance between the hemispheres (Figure 2.5A) is well beyond 25 mm, the point at

which the FC in the non-auditory gray matter reaches zero-asymptote, but we still observed significant interhemispheric FC. Furthermore, we regressed out the portion of FC that could be explained by the spatial function of the generic FC in the non-auditory gray matter to remove any bias in estimation of frequency selectivity in FC, and the corrected FC was still frequency-selective (Figure 2.6). We therefore conclude that the observed frequency-selective FC is not due to artifacts related to spatial smoothness of fMRI or generic FC.

Another possible confounding factor could have arisen from stimulus-driven effects. The residual activity used to compute FC in our study is not supposed to be correlated with stimulus effects if the GLM is a feasible statistical method, since it assumes independence between the explanatory variables and the error. Nevertheless, there might be residual stimulus effect due to non-linearity in hemodynamic response or any systematic error in model fitting. For this reason, we tested frequency selectivity of FC based on the calculation of correlations in the 4th TRs of each block of the residual time-series. The gap between the offset of the preceding stimulus and the 4th TR is 18 seconds so that these time points would reflect on-going spontaneous activity that is lurking under evoked responses (Fox et al. 2006; Saka et al. 2010; Becker et al. 2011; See the discussion above). We found that the FC computed using the data in this time window is still frequency-selective (Figure 2.7). This result is in agreement with Rothschild et al. (2010)'s results where FC in residual activity during stimulus presentation (as our residual FC data) and on-going activity in pre-stimulus time windows (as our resting epoch FC data) are both frequency-selective.

Fair et al. (2007) addressed whether residual fMRI activity and activity taken from inter-leaved resting epochs in evoked response experiments can act as a surrogate for conventional resting-state data. Their analysis showed that FC using residuals of an event-related fMRI dataset has qualitatively similar but quantitatively different topography from resting-state FC, whereas fMRI activity taken from inter-leaved resting epochs between stimulations provides quantitatively similar patterns with FC from continuous resting-state scans. Moreover, the regions that showed significant correlations in the event-related dataset but not in the resting-state dataset overlapped with the regions

that were activated by the task. This might be caused by remnants of task effects or inconsistency in the pattern of intrinsic FC during task performance and at rest. According to Fair et al., our results of frequency selectivity in residual FC might be confounded by the stimulus effects or might reflect a different pattern of FC than that of resting-state FC. However, our analysis of resting epoch data suggests that the FC measures we used in this study would be comparable to that of continuous resting-state scans, and thus intrinsic (Figure 2.7). Furthermore, the additional regress-out procedure indeed removes any bias or error due to poor fitting of the hemodynamic response within a block since only one frame per block was taken (Fig 7B).

2.4.4. Implications of frequency-selective FC for the functional architecture of human auditory cortex

Our findings of frequency selectivity of intrinsic FC are closely related to three important aspects of human auditory cortex in its functional architecture and information processing: frequency-selective connectivity, hierarchical organization, and hemispheric asymmetry. First of all, frequency selectivity of auditory neurons has been thought to be based on tonotopic or frequency-selective projections that are thalamocortical (McMullen and de Venecia, 1993; Hashikawa et al., 1995; Miller et al., 2001; Kimura et al., 2003; Lee et al., 2004a), corticocortical (Read et al., 2001; Lee et al., 2004a) and commissural (Code and Winer, 1985; Rouiller et al., 1991; Lee et al., 2004a). While tonotopic organization in the human auditory cortex has been well documented (Romani et al., 1982; Formisano et al., 2003; Talavage et al., 2004; Humphries et al., 2010; Saenz and Langers, 2014), anatomical connectivity in human brains has rarely been studied due to the methodological limits. Considering that the pattern of intrinsic FC is likely constrained by anatomical connectivity (Fox and Raichle, 2007; Vincent et al., 2007; Van Dijk et al., 2010), frequency-selective FC in our results suggests that anatomical connectivity in the human auditory cortex is also frequency-selectively organized, in accordance with evidence from diffusion imaging (See Upadhyay et al. 2007).

In the framework of hierarchical processing (Rauschecker, 1998; Kaas et al., 1999; Wessinger et al., 2001; Kumar et al., 2007; Rauschecker and Scott, 2009), sensory

features represented in the cortex become more complex and integrative in the later stages of the processing stream. This principle predicts that frequency tuning becomes wider and less selective as the order of hierarchy increases. How do our results relate to the difference in frequency selectivity in terms of response amplitude between cortical processing levels? One simple hypothesis is that the emergence of sharp tuning functions is dependent on local FC within a given area. Conversely, the local FC could be simply a byproduct of response amplitudes. Both predict that the selectivity of FC will follow the selectivity in response amplitude. In other words, the frequency selectivity of FC in the core-fields would be higher than the one in the non-core-fields area. Our results partially support this prediction: Only right core-fields area has particularly high selectivity in its within-area FC compared to the other areas (Figure 2.8 and 2.9). Also, our control analyses in which FC of the resting epochs was used and stimulus effects were regressed out (Figure 2.7) rule out the possibility that FC is a simple reflection or a byproduct of amplitude structures that emerge locally.

Our results may offer an important new conclusion in the context of understanding the functional asymmetry of human auditory cortex. Many prior studies have suggested that there exists a functional asymmetry favoring the right auditory cortex in fine-grained tonal or spectral processing, and the left in temporal processing (Zatorre et al., 2002). For example, Zatorre and Belin (2001) demonstrated that cerebral blood flow in the right superior temporal gyrus and sulcus was more sensitive to differences in spectral separation of a series of pure tones than the left auditory cortex; these findings were subsequently replicated with BOLD signal measures (Jamison et al., 2006). The general conclusion of right auditory cortex advantage for fine-grained spectral processing has been supported by various other studies using related approaches (Patterson et al., 2002; Zatorre et al., 2002; Schönwiesner et al., 2005; Hyde et al., 2008). The finding of greater intrinsic FC in right compared to left core areas adds significantly to this body of literature by suggesting a possible mechanism by which functional asymmetries might emerge. A given voxel in the right auditory cortex is more likely to be connected to another voxel with similar spectral tuning than on the left side; therefore encoding of fine-grained spectral information would tend to be enhanced, since neurons with similar

tuning properties would be more functionally interconnected to one another. Conversely, on the left side, we speculate that the relative lack of such frequency-selective connectivity might reflect integration across frequencies, which could instead enhance temporal resolution.

There is one potential discrepancy, however, between the present data and those obtained earlier: whereas the present lateralized effects were limited to the right core area, prior studies largely reported asymmetries in non-core regions. For example, Schönwiesner et al. (2005) reported that the covariation of spectral complexity and fMRI activity was greatest in the antero-lateral belt on the right superior temporal gyrus; and Hyde et al. (2008) identified the right planum temporale to be sensitive to pitch variation in a tonal sequence. The particularly high frequency selectivity in FC of the right core area rather invites a hypothesis that incorporates both the hierarchical processing model and functional asymmetry: highly frequency-selective FC in the right core area may contribute to asymmetric responses to tonal variations in the later processing stages. In other words, a possible mechanism underlying this effect is that the right core area passes finer frequency information formed by temporal coherence to higher-order auditory areas. This idea is supported by empirical evidence and theoretical considerations. First of all, spectral information processing in the secondary auditory cortex seems to be greatly dependent on the primary auditory cortex in non-human animals. Neurons in the caudomedial area of rhesus monkeys have their responses abolished after deactivation of the primary auditory cortex (Rauschecker et al., 1997). Similarly, deactivation of the cat primary auditory cortex yields reduction in response strength and receptive field bandwidth for pure tone stimuli in the anterior and the posterior auditory fields (Carrasco and Lomber, 2009a, 2009b). Anatomical tracer injection studies in cats and primates also imply frequency-selective inputs in the non-core fields that mostly originate from the core fields: the non-core fields receive most thalamic inputs from the middle and dorsal divisions of medial geniculate complex whose cells are known to be weakly frequency-selective and the topographically organized inputs from the core areas suggest tonotopic organization of the corticocortical inputs (de la Mothe et al., 2006a, 2006b, 2012a, 2012b; Hackett, 2011; Lee and Winer, 2011). Also, it has been reported that most cortical

connections to the posterior auditory field in the cat originate in the primary auditory cortex (Lee and Winer, 2008). These data, taken together suggest that spectral processing in the non-core areas in the right hemisphere is dependent on spectral processing in the ipsilateral core fields. Considering the role of FC as discussed above, this hierarchical organization of auditory cortex and the functional asymmetry of FC in our results support the idea that sharp frequency selectivity of FC in the right core area feeds forward to enable or support the enhanced spectral processing and the emergence of functional asymmetry at the later cortical stages.

2.4.5. Summary/conclusion

Frequency selectivity of auditory neurons in early cortical areas is critical to spectral analysis and perception. We demonstrated that intrinsic FC in the human auditory cortex is frequency-selective, by correlating residual activity on a voxel-by-voxel basis. This pattern is neither explained by generic FC that is correlated with spatial distance nor by stimulus effects. The data in resting epochs maintained the frequency-selective FC even after controlling possible residual stimulus effects. Frequency-selective FC in the auditory cortex is consistent with the previous studies that suggest intrinsic FC is constrained by functional and anatomical organization of the cortex. We also found that frequency selectivity of FC was significantly higher in the right core-fields area than the left and the non-core areas. This finding suggests that frequency-selective temporal fluctuation in the right core-fields has important roles in spectral analysis in higher order areas in the right hemisphere, that are already known to be specialized to process spectrally complex stimuli compared to the counter-parts in the left.

Study 2. Decoding natural sounds in human auditory cortex: joint contribution of spectrotemporal tuning and functional connectivity

The current study is an investigation on functional implications of spectrotemporal tuning-specific functional connectivity. Tuning specificity observed in study 2 is generalized to population spectrotemporal response fields of voxels. Functional significance of functional connectivity is evaluated by means of decoding natural stimuli with the information of resting-state functional connectivity or noise correlations. Study 2 has been prepared as a manuscript for a journal publication, which is here formatted to be included in the thesis.

Abstract

Cortical spontaneous activity in sensory cortices has tuning-specific patterns: neurons with similar tuning show more coherent activity than neurons with dissimilar tuning. This pattern of tuning-specificity can be observed with neuroimaging at the level of voxels. Voxels with similar frequency preference in human auditory cortex show increased functional connectivity (a measure of correlated activity). It is not known whether this result holds for sound features other than frequency, such as spectrotemporal modulation rate. The contribution of tuning-specific functional connectivity to the representation and processing of sound features is also unclear. Here, we show that voxel-wise resting-state functional connectivity is specific to characteristic frequency, spectral density, and modulation rate estimated from responses to natural sounds in single voxels. Tuning-specificity was consistent between functional connectivity from resting-state activity and residual activity, but was higher for residual than resting-state activity. Tuning-specific functional connectivity from residual activity implies correlated noise, which we show is detrimental to decoding when only spectrotemporal tuning functions are used and the correlation is ignored for decoding. However, decoding performance was improved when resting-state functional connectivity was incorporated to the decoder as weight functions to predict trial-to-trial response variations or as covariance estimator for maximum likelihood decoding. Our results suggest that coherent spontaneous activity contributes to stimulus encoding and decoding.

3.1. Introduction:

Studies of resting-state functional connectivity (rsFC) using functional magnetic resonance imaging (fMRI) have exponentially increased in the last two decades because of its implication on understanding large-scale functional integration of the brain (Friston, 2011). Macroscopic analyses of rsFC have established a principle that regions whose functions are similar have correlated activity, even in the absence of a stimulus or task (Lowe et al., 1998; Arfanakis et al., 2000; Cordes et al., 2000; Greicius et al., 2003; Bellec et al., 2006; Smith et al., 2009). This principle has also become evident on a smaller scale within sensory and motor cortex: the pattern of rsFC is correlated with topographic sensory representations. Thus, two voxels that have preference for similar sensory features would have higher rsFC than otherwise. This pattern has been found in retinotopic visual areas (Vincent et al., 2007; Heinzle et al., 2011), somatotopic sensory and motor areas (van den Heuvel and Hulshoff Pol, 2009; Cauda et al., 2011). Our previous study extended this pattern of findings to tonotopic auditory areas in humans by showing voxels that prefer similar frequencies showed temporal coherence in their residual activity and resting-epoch activity (Cha et al., 2014).

The association between topographically organized sensory representation and rsFC is indeed well in line with earlier neurophysiological findings in animals that the spontaneous activity of neurons (or populations of neurons) is more correlated when they have preferences for similar stimulus features than when they have dissimilar preferences (Brosch and Schreiner, 1999; Kenet et al., 2003; Rothschild et al., 2010; Fukushima et al., 2012). This correlation is not limited to tuning properties that are topographically represented on the cortical surface, but has also been found for non-topographic properties, such as orientation selectivity (Kenet et al., 2003).

Despite the consistency of these findings, a major question remains: Is this tuning-specific coherence in spontaneous activity relevant to sensory processing? One possibility is that spontaneous activity influences sensory processing for concurrent sensory inputs either by adding the activity to, or interacting with, the sensory input signals. Previous human brain imaging studies have shown that spontaneous on-going activity preceding a stimulus accounts for trial-to-trial variation in brain responses, i.e.,

residual activity, and behavioral measures (Fox et al., 2006b; Boly et al., 2007; Fox and Raichle, 2007; Hesselmann et al., 2008a, 2008b; Saka et al., 2010; Becker et al., 2011). Some of these studies found an interaction between spontaneous activity and evoked activity measured as variance reduction in evoked activity (Hesselmann et al., 2008b; Sadaghiani et al., 2010). These studies suggest that spontaneous activity contributes to information processing underlying perception and action. However, most previous studies have only addressed the relation of spontaneous activity and residual activity at a regional level, without measuring the detailed patterns of correlations between individual voxels and their relation to voxel-level tuning functions.

Trial-to-trial response variation, in fact, has a similar pattern to that of rsFC: neurons tuned to similar sensory features have more correlated trial-to-trial variability (Lee et al., 1998; Bair et al., 2001; Averbeck and Lee, 2003; Kohn and Smith, 2005). This similarity can be important to discussion of the functional relevance of rsFC because the correlation in response variability, often called 'noise' correlation, has a significant impact on neural encoding and decoding. For instance, correlated variability can possibly be detrimental to coding efficiency especially when assuming the read-out, i.e., decoding, process would try to remove noise by averaging activity across neurons without taking into account the correlated nature of variability (Abbott and Dayan, 1999; Shamir and Sompolinsky, 2004; Averbeck and Lee, 2006). However, information loss can be alleviated if the decoding process takes into account the correlation in response variation (Nirenberg and Latham, 2003; Latham and Nirenberg, 2005; Averbeck et al., 2006; Graf et al., 2011). Therefore, one way to evaluate functional relevance of rsFC might be to assess if rsFC can be utilized in decoding of neural activity.

Here we evaluate the pattern of rsFC in relation to spectrotemporal tuning functions and decoding of fMRI responses to natural sounds in human auditory cortex. We first extend our previous findings of preferred frequency specificity of functional connectivity to the joint spectrotemporal modulation transfer function (MTF) parameters, i.e., characteristic frequency, spectral density and modulation rate. Spectrotemporal MTFs, equivalent to spectrotemporal response fields, compactly describe the linear portion of the relationship between neuronal activity and the spectrotemporal structure of

an acoustic stimulus (Kowalski et al., 1996a, 1996b, Depireux et al., 1998, 2001). MTFs can be estimated for single unit activity (Kowalski et al., 1996a; Klein et al., 2000; Wu et al., 2006; David et al., 2007; Theunissen and Elie, 2014) in animal models, and for single voxels in humans using artificial (Schönwiesner and Zatorre, 2009) and natural sounds (Santoro et al., 2014). Since neural encoding of spectrotemporal response fields are essential to auditory processing not only of simple features but also of complex natural stimuli such as speech (Chi et al., 1999, 2005; Santoro et al., 2014), investigation of the relation between the rsFC and MTF would be essential to understanding the functional contribution of rsFC to spectrotemporal processing.

We estimate single voxel spectrotemporal tuning and rsFC to determine whether rsFC covaries with spectrotemporal tuning similarity between voxels. If this is the case, as we predict, then we could conclude that tuning-specific rsFC might be a generic property of auditory cortical neurons, indicating the relevance of rsFC to auditory processing. We then assess functional importance of correlations in residual activity and spontaneous activity to spectrotemporal encoding and decoding. We demonstrate that correlated noise has a detrimental effect to decoding when the decoder ignores the correlation, but the decoding performance can be improved, or at most recovered, by incorporating rsFC, which indicates functional importance of the pattern of rsFC which is consistent with noise correlations.

3.2. Experimental Procedures

3.2.1. Participants

Thirteen people (8 males, 19–29 years old) with normal hearing participated in the study with informed consent. They received monetary compensation for their time and effort upon the completion of each experiment session. The MR Research Committee and the Ethics Review Board Committee at McGill University approved the experimental procedure.

3.2.2. Stimuli

Seventy-two naturalistic, complex sounds of 6 categories were presented to

participants in the auditory stimulation MRI experiments. The six categories, each of which consisted of 12 sounds, included animal vocalization, human non-speech vocalization, speech, natural environmental sounds, artificial objects, and music. The stimuli were cut to be 1 s long and their initial and last 250 ms segments were ramped using a squared sine function to remove transient onset and offset.

Each sound was then simplified in terms of cortical representation of the sound according to a spectrotemporal response field model (STRF) described in Chi et al. (2005) in order to limit the parameter space of cortical tuning function (See below). To achieve the simplification of the sound, the NSL Tools package (http://www.isr.umd.edu/Labs/NSL/Software.htm) were used. The model first transform an input sound wave function to auditory nerve outputs and then transfers the outputs to the responses of hypothetical cortical neurons according to their STRFs.

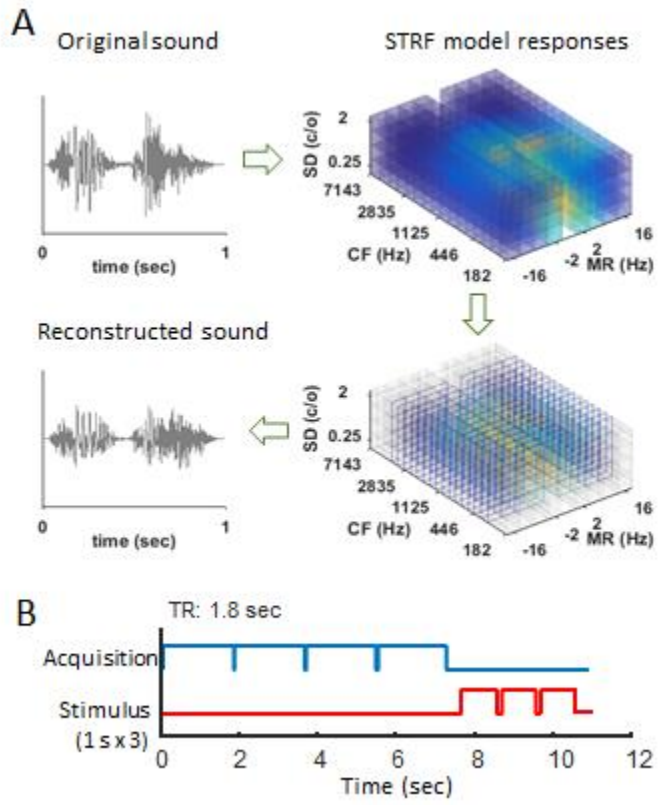

Figure 3.1. Stimulus preparation and presentation in an interleaved silent steady-state (ISSS) fMRI protocol

A. Stimulus preparation. Each of 72 natural sound stimuli (6 categories with 12 sounds

each) were reconstructed from a set of selected MTF parameters in order to minimize the features that will not be included in the MTF encoding model. A stimulus was transformed to cortical spectrotemporal response field model responses in 128 CFs × 4 SDs × 8 MRs and then reduced to 16 CFs × 4 SDs × 8 MRs (512 resulting parameters). The sound was reconstructed using the reduced model responses so to be presented in the experiment. B. Stimulus presentation in fMRI. An epoch of fMRI consisted of 4 TRs of acquisitions followed by a 2 TR-long silent steady state period during which a 1-second long stimulus was presented 3 times.

The cortical representation model specifies the STRF of a neuron with the parameters of characteristic frequency (CF), spectral density (SD) and modulation rate (MR) (Figure 3.1B). The cortical response of the model output for a sound served as a 'linearizing input' to an encoding model of fMRI voxel activity (Figure 3.2A; See Naselaris et al., (2011) and Wu et al., (2006) as to linearizing input). The CFs correspond to a cochlear frequency bank of 128 overlapping bandpass filters that cover 5.3 octaves from 180 to 7040 Hz. The spectral density was set to be 0.25, 0.5, 1 and 2 cyc/oct (cycles per octave) and the modulation rate was set as ± 2, 4, 8, and 16 Hz. This setting leads to the ideal number of parameters of a voxel STRF to be estimated being 4096 (128 × 4 × 8).

To reduce the parameter space, only 16 CFs between 300 to 4000 Hz out of the original 128 CFs were subsampled, and the stimuli were reconstructed by the sound reconstruction algorithm of the NSL tools package (Chi et al., 2005; Figure 3.1A). The resulting number of parameters was 512. The selected CFs ranged from 300 to 4000 Hz, equally spaced in the logarithmic frequency space.

Each sound stimulus was played to the participant through MR-compatible headphones inside the MRI three times in a given trial in the window of a 3.6 s long steady-state silent period between clustered MRI acquisitions (Figure 3.1A). To minimize adaptation effects, the CF was slightly increased by 0.04 oct through the three presentations within a single trial.

3.2.3. MRI experiments

Each participant underwent anatomical and functional magnetic resonance imaging on a 3T scanner (Trio, Siemens) in a single session. For anatomical imaging,

high-resolution MPRAGE protocol with integrated parallel acquisition (1 × 1 × 1 mm^3) was applied in coverage of the whole brain. In the functional MRI runs, interleaved silent steady state (ISSS) protocol was used (repetition time: 1.8 s; echo time: 30 ms, flip angle: 90 °, in-plane resolution: 2 x 2 mm^2, slice thickness: 2 mm, field of view: 224 mm). Six repetition times (TRs) constructed one epoch, where 4 consecutive acquisitions were followed by 2 dummy acquisitions in which there was no volume acquisition for 2 TRs (Figure 3.1B). Twenty two slices were located parallel to the lateral sulcus to cover the auditory cortex including the supratemporal plane and superior temporal gyrus.

Functional MRI started with one resting-state run followed by 10 runs with auditory stimulation. Both type of runs consisted of 46 epochs, which correspond to 184 actual volume acquisitions and 92 dummy acquisitions. In the resting-state run, participants were asked to stay awake with eyes closed. In the auditory stimulation runs, participants passively listened to auditory stimuli played in the silent periods while watching a muted nature documentary movie.

The 72 stimuli were divided into two partitions each of which was assigned to alternating runs to be presented in. The two halves of each sound category (6 out of 12 stimuli) were assigned into the two partitions, so that 36 sounds out of all six categories were presented in each run. In each run, 36 stimulus presentation trials and 10 blank trials were assigned to the 46 epochs. The first epoch and the last three epochs were blank trials where no sound was presented. The remaining 42 epochs were divided into 6 blocks of 7 epochs, in which a blank trial and 6 stimuli out of 6 different categories were randomly assigned. Each stimulus was presented 5 times in total throughout 10 runs in each session.

3.2.4. Processing of anatomical data and selection of atlas-based auditory areas

The segmentation and spatial normalization routine in SPM12 (www.fil.ion.ucl.ac.uk/spm) was used to segment the gray matters and to define the primary auditory cortex (PAC) in individual native image space. For the definition of the PAC, the deformation field of the anatomical images into the MNI space was computed and used to non-linearly transform the regions of Te1.0, Te1.1 and Te1.2 (Morosan et al., 2001) in the Juelich probabilistic cytoarchitectonic atlas (Eickhoff et al., 2005). The

obtained probability maps in the anatomical image space were resampled in the functional image space, in which the values were thresholded at the half of the maximum probability value. The thresholding was necessary since the maps were smoothed by the transformation processes. The PAC was further refined by functional localization of the auditory cortex according to activation statistics (See below).

3.2.5. Preprocessing of fMRI data

Motion correction and high-pass filtering (cut-off: 0.01Hz) were applied to the functional MRI data using SPM12. The high-pass filtering was modified so that the discrete cosine transform to be regressed out were resampled according to the sampling time points of the acquired data. This was to overcome the issue in temporal filtering of time-series obtained from clustered imaging technique. Low-pass filtering was not additionally applied because the sluggish nature of hemodynamic response and the low-frequency (Nyquist frequency: ~0.05 Hz) of the neural events will yield minimal power in the low frequency in the resultant neural activity estimates (see below for neural activity estimation).

3.2.6. Neural activity estimation

The general linear model (GLM) analysis of SPM was used to estimate underlying neural activity of each voxel in a single trial. Each of 5 presentations of 72 stimuli was treated as a single condition (variable) in the GLM, and we thus obtained 360 trials of neural activity parameters from the auditory experiment.

Single-trial activity estimation was applied also to resting-state runs. Excluding the first one and the last three epochs, 42 out of 46 epochs in a given resting-state run were regarded as ‘resting’ trials neural activity was estimated. The resulting estimated neural activity was regarded as spontaneous activity since no evoked activity could be assumed in resting state runs.

The resulting neural activity estimates from both the auditory runs and resting-state runs were divided by the run-specific constant in the GLM for each voxel to normalize scale factors varying across runs and voxels. This procedure is equivalent to normalization by

conversion to percent signal change.

3.2.7. Localization of the auditory cortex

The functionally defined auditory cortex was assumed to be a collection of voxels that are activated by the auditory stimulation and spatially clustered in the temporal cortex. To localize the auditory cortex in both hemispheres, t-statistics were computed for the estimated neural response to all stimuli against the implicit null condition and the spatially smoothed statistical map (Gaussian filter, SD = 4mm) was thresholded ($p<0.001$). Visual inspection confirmed the selected voxels were clustered in the temporal cortex and the selected voxels were further restricted in the gray matter.

3.2.8. Spectrotemporal encoding model (tuning-only model)

The spectrotemporal tuning-only model dictates that the predicted neural activity of an fMRI voxel *i* is postulated in the equation, $\hat{y}_i = \mathrm{X}\hat{h}_i$, where $\hat{y}_i$, X, and $\hat{h}_i$ respectively denote the predicted neural activity, the linearizing input representations of the stimuli, and the estimated MTF (Figure 3.2A). For a given voxel, $\hat{y}_i$ is an n × 1 vector where n is the number of observations, X is an n × p matrix where p is the number of MTF parameters, and $\hat{h}_i$ is a p × 1 vector.

The NSL tools were used to obtain the linearizing input in light of cortical response field model (Chi et al., 2005). The linearizing feature space was the span of 16 characteristic frequencies (CFs), 4 spectral densities (SDs), and 8 modulation rates (MRs), as defined in the stimulus creation (reconstruction) process. By this, each stimulus was represented as a cortical MTF of a 512 × 1 vector space. The neural response representation computed by the NSL is in complex domain to include magnitude and phase responses, and only the magnitude was taken in the linearizing input.

3.2.9. MTF parameter estimation

The dataset was divided into 6 subsets according to the sound categories. Each of 6 training sets was made of trials with 5 sound categories and the corresponding test set was comprised of trials of the remaining sound category. Since each sound was presented

5 times for each session, 300 trials (12 sounds × 5 categories x 5 measurements) were included in each training set while 160 trials in each test set.

To estimate MTFs, principal component regression was used to overcome the problem of multicollinearity of stimulus features and high dimensionality which are common challenges in using natural stimuli to estimate receptive fields (Wu et al., 2006; Theunissen and Elie, 2014). A built-in function 'pca' in MATLAB, which bases on singular vector decomposition, was used to compute principal components (PCs) of the input matrix X for the selected stimuli of the training set. The input had been standardized (z-scored) before the selection of the set. The PCs with the largest corresponding variance explained up to 90% were chosen to estimate PCR coefficients by least squares regression of the voxel activity onto the PCs. Finally the PCR coefficients were projected back to the original tuning parameter space.

The CF-only, SD-only and MR-only encoding models were also trained by using marginalized linearizing inputs and their parameter estimates were used as references to evaluate the reliability of the original full MTF estimates. The full MTF estimates were marginalized into CF, SD and MR functions as well. The peak CFs, SDs and MRs were obtained from the parameters from the both models (full vs. reduced) and the correlation between the parameters of the two models was computed as a measure of reliability.

3.2.10. Computation of resting-state functional connectivity (rsFC) as a function of tuning similarity

In order to investigate the organization of resting-state functional connectivity (rsFC) in relation with tuning similarity between voxels, Pearson's correlation coefficients of every pair of time courses of voxel activity were computed. Note that this measure of FC is descriptive so it is distinct from regression coefficients or covariance for FC that are used to predict and decode voxel activity in this paper (See below). The simple distance effect on FC was estimated in the gray matter voxels outside the auditory cortex and the empirical rsFC function of distance was used to regressed out from rsFC as described in our previous paper (Cha et al., 2014).

Tuning similarity between voxels was measured by correlating the tuning

functions of every pair of voxels with respect to the full MTF, CF, SD and MR. The tuning functions of CF, SD and MR were obtained by marginalizing the full MTF. RsFC was then binned according to tuning similarity. To test whether RsFC increases as a function of tuning similarity, the slope of the binned rsFC as a function of tuning similarity was estimated by linear fitting, and a t-test was performed for the slope estimates.

3.2.11. Residual activity and noise correlations (residFC)

Residual activity, i.e., trial-to-trial variations, in trial *k* where stimulus *j* was presented was obtained by subtracting the mean response the stimulus *j* from the activity of trial *k*. Noise correlations in Figure 3.4 to be compared with rsFC as a descriptive measure were estimated simply by computing Pearson's correlation coefficients of residual activity time course of voxel pairs. To compare tuning-specificity of noise correlations to that rsFC, noise correlations were processed in the same manner as rsFC and the slopes were estimated by linear fitting as well.

3.2.12. RsFC-incorporated activity prediction model

In order to test the hypothesis that rsFC can be used to predict trial-to-trial variations in neural responses to stimuli which in turn benefits decoding of stimuli, we built a model that incorporates rsFC into the spectrotemporal encoding model (Figure 3.5A). In this model, a single trial response is predicted as the sum of evoked activity predicted by the spectrotemporal encoding model and residual activity predicted by the weighted sum of residual activity of other voxels. Importantly, the weighting function is approximated by rsFC. Accordingly, predicted neural activity of voxel *i* in response to stimulus *j* in a trial *k* is formulated as $\hat{y}_{i,j,k} = \hat{y}_{i,j,k}^{evoked} + \hat{u}_{i,j,k}^{residual} = x_j \cdot \hat{h}_i + u_k \cdot \hat{\mathrm{w}}_i$, where x_j and $\hat{h}_i$ are respectively the linearizing input for stimulus *j* and the estimated tuning function (MTF) of voxel *i* as in the spectrotemporal tuning-only model, and u_k and $\hat{\mathrm{w}}_i$are the residual activity of the remaining voxels (i.e., the other voxels than voxel *i* in the auditory cortex) in trial *k* and the estimated FC weights for voxel *i*, respectively. The FC-weights were estimated from two separate sources: resting-state activity in a

separate fMRI run and residual activity in the training dataset. Principal component regression was applied in the estimation of the FC-weight parameters. The PCs of the input resting-state activity of the voxels in the entire ROI were first computed and the best PCs that accounted for 90% of variance of the data were selected for regression on the resting-state activity of each voxel. The PCR coefficients were transformed back to the voxel space.

3.2.13. Model evaluation: single-trial stimulus identification

Prediction accuracy of the tuning-only model and rsFC-incorporated model was evaluated by single-trial stimulus identification performance based on the similarity between predicted and actual patterns of multivoxel activity (Kay et al., 2008; Santoro et al., 2014). Firstly, neural activity of voxels in the test data was predicted by a given model whose parameters were estimated in a separate dataset. Secondly, Euclidean distance in multivoxel activity space between the predicted and the actual activity for each trial was calculated. The Euclidean distance from an observed pattern in trial k, y_k, to predicted patterns for the trial *l* for stimulus *j*, $\hat{y}_{j,l}$, was computed as $\mathrm{d}_{j,k} = \frac{1}{L}\sum_l \sqrt{(y_k - \hat{y}_{j,l}) \cdot (y_k - \hat{y}_{j,l})}$ where L = 5. In the tuning-only model, $\hat{y}_{j,l}$ is the same across trials since it doesn't account for trial-to-trial variation while it varies according to the input spontaneous activity in the rsFC-incorporated model.

The final score for identification performance was computed based on ranking of the distance measure between the predicted pattern of the trial and that of the correct stimulus among those to all the 12 stimulus candidates in test (Figure 3.2B; See Santoro et al. (2014), for the ranking-based scoring). More specifically, let the rank of the distance for trial *k*, g(k), be the number of sounds whose activity distance measure is equal to or smaller than that of the correct sound, and the identification score was defined as $\mathrm{s(k)} = 1 - (\mathrm{g(k)} - 1)/(\mathrm{L} - 1)$ where L is the number of tested sounds. The overall identification score for each subject was obtained by averaging the identification scores across trials and test sets, and used for t-tests for the comparison of the model performance at the group level (N = 13).

The empirical chance level performance was estimated by shuffling stimulus

labels. A hundred repetitions of shuffling were performed for each trial and the score was averaged. For the model with FC-weights shuffled, shuffling the weights in terms of voxel pairs was applied also 100 times and averaged for each trial.

3.2.14. Maximum likelihood decoding

The probability to observe an activity pattern, y, given stimulus s is as follows: $\mathrm{p}(y|s) = (1/C)\exp(-\frac{1}{2}(y-\hat{y}(s))S^{-1}(y-\hat{y}(s))^T$, where C is a normalization factor, $\hat{y}(s)$ is the most probable activity pattern for stimulus s, and S is the covariance matrix. The key of this model is that $\hat{y}(s)$ is predicted by the tuning-only model and the covariance matrix is estimated from resting state activity or residual activity.

The encoding distribution, $\mathrm{p}(y|s)$, leads to the corresponding decoding distribution in light of the maximum a posteriori decoding in which the posterior probability is formulated as $p(s|y) = p(y|s)p(s)/p(y)$. If the prior, $p(s)$, is assumed to be flat, the stimulus that maximizes the posterior probability is equivalent to one that maximizes the likelihood function given the observation y, L(s) = p(y|s). Therefore, the most likely stimulus identity is the one that maximizes L(s).

Finally, maximizing L(s) is equivalent to minimizing the Mahalanobis distance $d^{Mahal}(s) = (y-x(s)H)S^{-1}(y-x(s)H)^T$. The covariance matrix S was estimated by computing the covariance based on either resting-state activity or residual activity. For the estimation of inverse covariance, a matrix shrinkage method (Ledoit and Wolf, 2004) was applied. Once the Mahalanobis distances were computed for the test stimuli, the identification score was calculated based on the rank of the distances in the same way as described above.

3.3. Results:

BOLD fMRI activity was measured in 13 participants with normal hearing while they passively listened to 72 natural sounds drawn from 6 categories (animal vocalization, human non-speech vocalization, speech, natural environmental sounds, artificial objects, and music) with simplified spectrotemporal content (Figure 3.1). Single-trial neural activity in response to the stimuli (5 trials per stimulus) was estimated

with general linear model analysis (fMRI deconvolution: Glover, 1999; Moerel et al., 2012; Mumford et al., 2012) in pre-defined sound-responsive voxels (based on a t-test threshold of $p<0.001$in a sound vs. silence contrast). Resting-state spontaneous activity was estimated from a separate ~9-minute run of fMRI data obtained in the same session before auditory stimulation.

3.3.1. Spectrotemporal tuning-specific rsFC

To assess whether the pattern of rsFC covaries with similarity in spectrotemporal tuning across fMRI voxels, we first characterized the MTF of individual voxels in the auditory cortex using a linearizing encoding model approach (Wu et al., 2006; Kay et al., 2008; Naselaris et al., 2011; Santoro et al., 2014). This 'tuning-only' model predicts activity of a voxel with the MTF of the voxel that serves as a weight for the features in the input stimulus (Figure 3.3A). We presented spectrotemporally simplified natural stimuli, but even these simplified stimuli contained a large number of combinations of acoustic parameters (512) and multicollinearity. Principal component regression was used to overcome this problem (Wu et al., 2006; Theunissen and Elie, 2014).

Figure 3.2A shows an example of the topography of the estimated peak CFs (tonotopy), SDs, and MRs in one participant. The peaks were found after marginalizing the MTFs into each of the three dimensions (Figure 3.2A). RsFC between voxels was computed using Pearson's correlation of estimated resting-state neural activity. As in our previous study, the effect of spatial distance on rsFC was removed by subtracting the FC that is predicted by cortical distance (Cha et al., 2014). RsFC was then binned as a function of tuning similarity, which was measured as Pearson's correlation coefficients between voxel tuning functions. Dependency of rsFC on tuning similarity was apparent when full MTF tuning was considered, as well as when each of the dimensions (CF, SD and MR) was considered separately, both within and between hemispheres (Figure 3.2B). To test the dependency of rsFC on tuning similarity statistically, we fit a linear function to the binned data in individual participants and found that estimated slopes were significantly above zero in all 12 conditions ($p < 0.001$ for all of 3 hemispheric conditions × 4 tuning function types, t-tests). Therefore, rsFC is positively related to

features of spectrotemporal tuning (spectral density and modulation rate), not only to the preferred frequency of voxels.

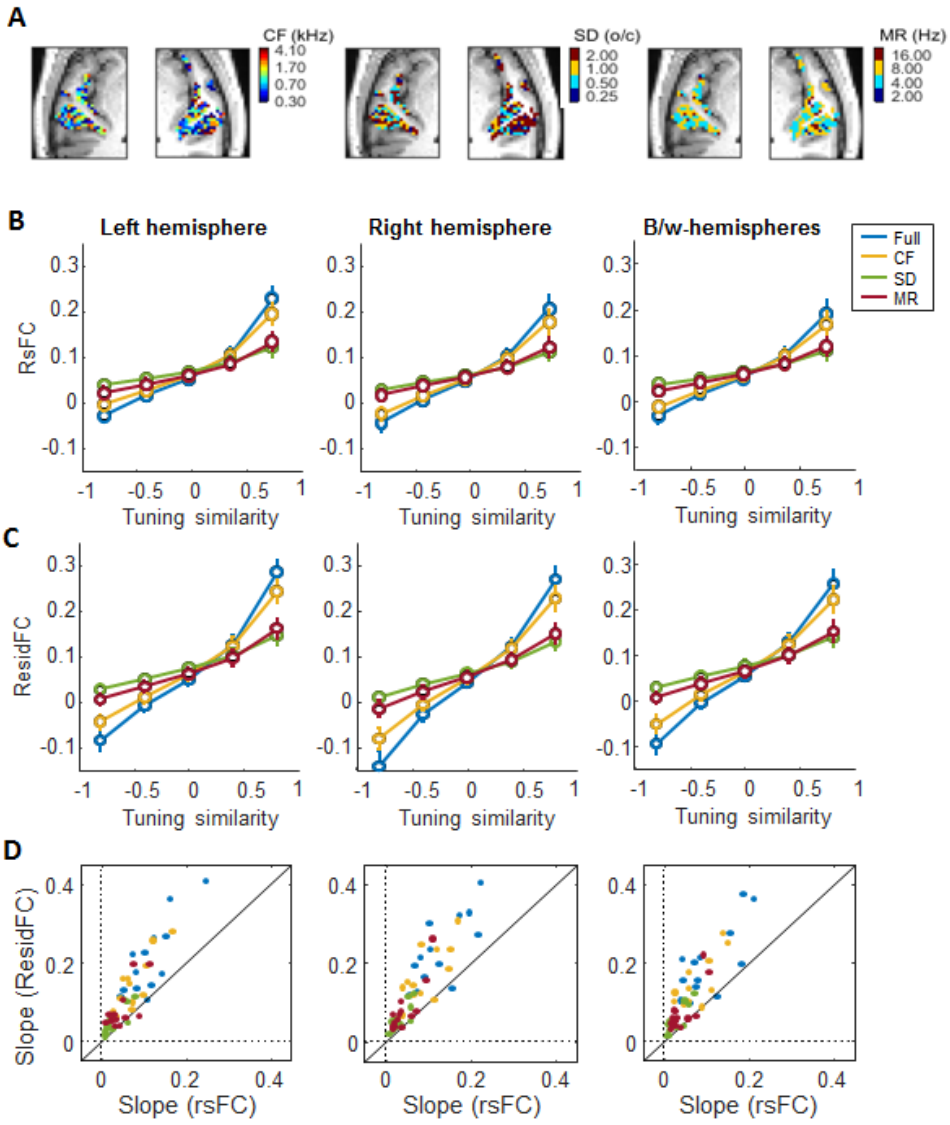

Figure 3.2. Topography of MTF parameter estimates and tuning specificity of rsFC and noise correlation (residFC)

A. Topography of peak characteristic frequency (CF), spectral density (SD) and modulation rate (MR). Only a representative slice of a participant is shown here. The top panels show the topographic maps of best CFs (left), SDs (center) and MRs (right) that were obtained by marginalizing the full MTF estimates of the original MTF encoding model. B. Tuning-specific rsFC. Voxel pairwise resting-state functional connectivity (rsFC) was binned as a function of tuning similarity in terms of full modulation transfer function (MTF), characteristic frequency (CF), spectral density (SD) and modulation rate (MR) within the two hemispheres and across the hemispheres. RsFC increases as tuning

similarity between the voxels increases. C. Noise correlation (residFC) as a function of tuning similarity presented in the same format as B. D. Relation between rsFC and noise correlation with respect to tuning-specificity measured as slopes of a linear function. Each dot represents individual participants. The color scheme is the same as in B and C. It is notable that while both rsFC and residFC have spectrotemopral tuning specificity, residFC has higher specificity than rsFC and the pattern is consistent within subjects.

3.3.2. Tuning specificity of noise correlations

Tuning-specificity is not only observed in rsFC but also in noise correlations. It is reasonable to suppose that noise correlations show a similar pattern of tuning specificity as rsFC, but these patterns have not yet been directly compared. Therefore, we analysed noise correlations in the same way as rsFC and compared the resulting slopes with those obtained from the rsFC analysis (Figur 3C). Here we refer to noise correlations as 'residual' functional connectivity (residFC) because the functional connectivity is obtained by correlating residual activity after subtracting the average response to a stimulus from original single trial responses. The slopes of residFC were significantly higher than zero in all 7 conditions ($p < 0.001$ for each of the 7 conditions, one-tailed t-tests). The slopes of residFC were highly consistent with rsFC across subjects, that is, a participant who had high residFC had high rsFC (Figure 3.2D; $p<0.01$ for each of the 12 conditions, Pearson correlation). However, when the slopes of residFC were compared to rsFC within a participant, residFC had larger slopes than rsFC in all conditions ($p<0.01$, one-tailed paired t-tests).

3.3.3. Decoding multivoxel activity by the MTF model and the effect of decorrelating noise

Multivoxel activity in response to novel sounds was decoded using the MTF (tuning-only) model in various configurations including trial-averaged, single-trial, MTF estimates-shuffled, and noise-decorrelated conditions. Single voxel activity was predicted as the MTF-weighted sum of STRF model responses of an input sound (Figure 3.3A). The input was drawn from sound category sets that had not been used in the MTF parameter estimation. Stimulus identification was performed based on prediction error, which is similar to the methods that have been described in the previous studies (Kay et

al., 2008; Santoro et al., 2014). The MTF model predicts multivoxel activity patterns for the 12 input sounds from one of the 6 test datasets. These predicted patterns are compared to the actual pattern of activity for a given stimulus, and the identification score was determined based on the ranking of the distance between the observed pattern and the predicted pattern of the correct stimulus (Figure 3.3B).

The identification performance significantly exceeded chance level when averaging activity patterns across trials ($p < 0.001$, one-tailed t-test), and for single trial activity ($p < 0.01$, one-tailed t-test, Figure 3.3C). However, the decoding performance was significantly degraded when the MTF parameters were shuffled across voxels ($p < 0.02$, one-tailed t-test, Figure 3.3C). This indicates that the specific spatial organization of MTF parameters has a significant role in encoding and decoding. Note that we computed an empirical chance level by permuting stimulus labels 100 times for each of the tested observation in order to avoid bias.

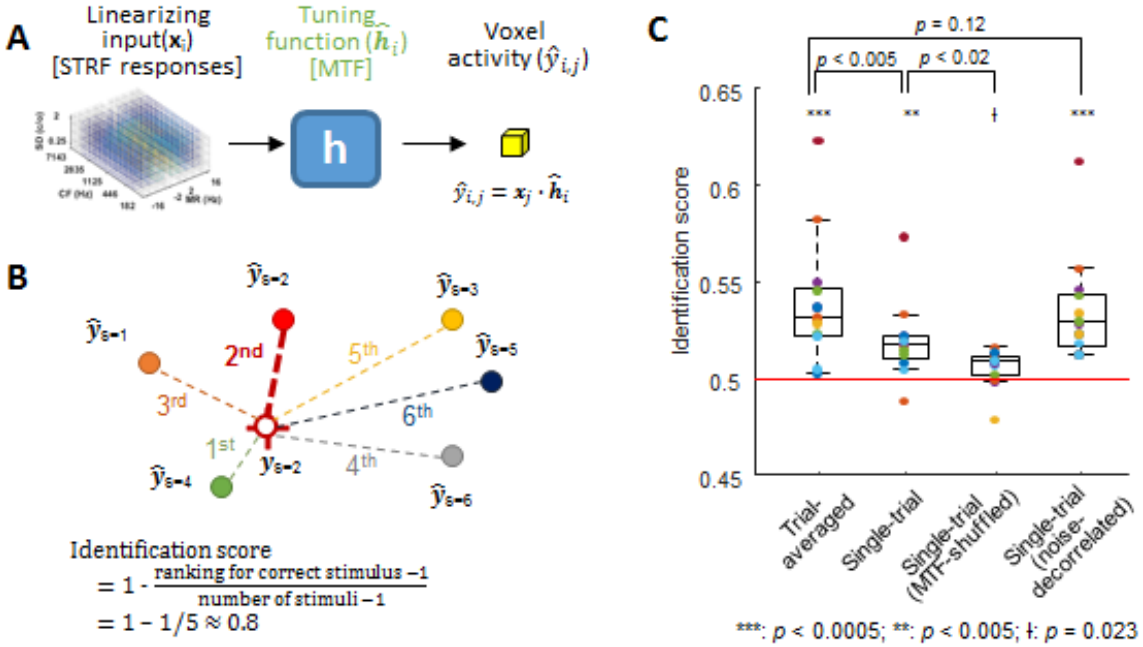

Figure 3.3. Stimulus identification using the tuning-only model and the effect of noise correlation

A. Scheme of activity prediction by the tuning-only model. Activity of a voxel i for a stimulus j, which has not been presented in the training dataset, is predicted as an inner product of the STRF model responses for stimulus j (a 512 × 1 vector) and the tuning

function of voxel i (a 512 × 1 vector) estimated in the training stage. B. Scheme of computation of identification performance based on rankings of Euclidean distances in case of 5 stimuli. Predictions are made for 5 stimuli $\hat{\boldsymbol{y}}_{s=1,2,\ldots,5}$ (filled circles) and the Euclidean distances between the predicted patterns and the actual response pattern for stimulus 2, $\boldsymbol{y}_{s=2}$, (open circle) is evaluated and the ranking for the correct stimulus (in this case, s=2) is used to determine the identification score ranged from 0 (the worst prediction) to 1 (the best prediction). In the single-trial identification the observed activity is taken from a single trial whereas the activity is averaged across trials in the trial-averaged case. C. Stimulus identification performance of the MTF tuning-only model. The performance is significantly higher than the chance level (red line) both in single-trial ($p < 0.005$) and trial-averaged ($p < 0.0005$) activity decoding (red line: an empirical chance level estimated by label permutations). When MTF estimates are shuffled across voxels, the decoding performance was degraded compared to decoding without shuffling ($p < 0.02$). When noise (residual activity) is decorrelated, single trial performance was enhanced ($p < 0.001$) so to be incomparable to identification with trial-averaged data ($p = 0.12$). Boxes and whiskers indicate the 75 and 95 percentiles, respectively, and colored dots show the performance in each of 13 individual participants.

The performance difference between trial-averaged and single-trial decoding ($p<0.005$) indicates the impact of trial-to-trial variability in neural decoding. What would be then the contribution of correlation in trial-to-trial variability? Since this question has long been of theoretical interest to sensory neuroscientists particularly in regard to population coding (Abbott and Dayan, 1999), we evaluated the decoding performance with the residual activity, i.e., noise, decorrelated. The decorrelation was performed by permuting the residual activity across trials for each voxel. The decoder performed better with noise decorrelated than with it intact ($p < 0.001$, one-tailed paired t-test, Figure 3.3) and it was comparable to decoding for averaged data ($p = 0.12$, two-tailed paired t-test). Therefore, consistent with previous studies, when activity is decoded only by predicting the mean activity pattern, the performance is degraded due to the correlated trial-to-trial variability.

3.3.4. Improvement in single-trial decoding performance when rsFC is incorporated

Would it be beneficial to decode activity if noise correlation was considered? Previous theoretical and neurophysiological studies indicate that this is the case (Nirenberg and Latham, 2003; Latham and Nirenberg, 2005; Graf et al., 2011): when a

decoder takes into account activity co-variability, the accuracy is improved. However, would it be also the case when rsFC is incorporated into a decoder? To test whether that is the case, we built an activity prediction model that uses the patterns in rsFC to predict trial-to-trial variations of responses to stimuli. These variations are then added to the prediction of stimulus-evoked activity based only on tuning functions (Figure 3.4A). In other words, the predicted activity of a voxel *i* in response to stimulus *j* in a given trial *k* is the sum of the stimulus-evoked activity predicted by the tuning-only model for stimulus *j* and the residual activity predicted by rsFC-weighted residual activity of other voxels in trial *k*. Since it is a high dimensional regression model with multi-collinearity, principal component regression was used to estimate the weight coefficients.

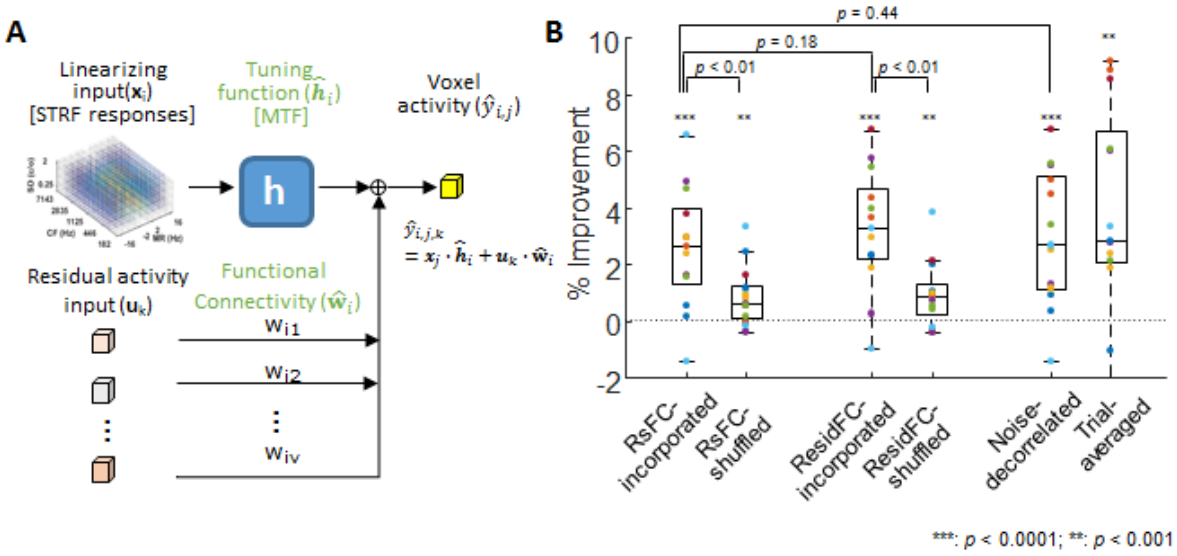

Figure 3.4. RsFC-incorporated activity prediction model and its decoding performance

The scheme of rsFc-incorporated activity prediction model. The model predicts trial-to-trial variation of single-voxel activity based on the residual activity of other voxels based on functional connectivity estimated in resting-state activity. The predicted residual activity is added to the evoked activity predicted by the spectrotemporal encoding model. In contrast to the tuning model, the prediction is made for each trial. Subscipts i, j, and k denote voxel, stimulus and trial number. B. Improved stimulus identification performance of the rsFC-incorporated model compared to the tuning-only model. The performance improvement is presented as percent improvement with respect to the tuning-only model. RsFc-incorporated model outperformed the tuning only model ($p < 0.001$). When rsFC was shuffled, the performance was degraded compared to the original rsFC-incorporated model ($p < 0.01$; rsFC-shuffled). When FC weights were estimated from residual activity

in the training datasets (ResidFC-incorporated), the performance was also improved compared to the tuning-only model ($p < 0.001$) and the improvement did not differ from the rsFC-incorporated model ($p = 0.18$). Shuffling residual-based FC (ResidFc-shuffled) had a similar effect as shuffling resting-state FC. Also the performance improvement of rsFC-incorporated model did not differ from that of the tuning-only model with noise decorrelated (Noise-decorrelated; $p = 0.44$). Boxes and whiskers indicate the 75 and 95 percentiles, respectively, and colored dots show the performance in each of 13 individual participants. It is remarkable that providing functional connectivity information, whether rsFC or residFC, to the model improves decoding performance, which becomes comparable to the case with noise decorrelated.

Stimulus identification performance of the rsFC-incorporated model was evaluated by the same measure as the tuning-only model, based on which percentage improvement in comparison to the tuning-only model was computed (Figure 3.4B). We found the rsFC-incorporated model significantly outperformed the tuning-only model ($p < 0.001$, one-tailed t-test, $n = 13$). However, the improvement was degraded when rsFC was shuffled in terms of voxel pairs (rsFC-intact vs. rsFC-shuffled: $p<0.01$, one-tailed paired t-test, $n = 13$), indicating the specific structure of correlation is necessary for the improvement. In fact, the model with shuffled rsFC also significantly outperformed the tuning-only model ($p<0.001$, one-tailed t-test, $n = 13$), presumably due to the effect of overall correlations.

We then compared the improvement in decoding performance by the rsFC-incorporated model to a model where FC coefficients were estimated based on residual activity instead of resting-state activity (See Methods). Note that the coefficients estimated from residual activity correspond to residFC and noise correlation. The model with residFC-based coefficients (residFC-incorporated model in Figure 3.4B) showed the same pattern as the rsFC-incorporated model: improved performance compared to the tuning-only model ($p < 0.001$, one-tailed t-test, $n = 13$), and shuffling the pattern degraded the improvement ($p < 0.01$, one-tailed paired t-test, $n = 13$). We found that the percentage improvement did not significantly differ between the two sources of FC coefficients ($p = 0.18$, two-tailed paired t-test, $n = 13$). These results suggest that specifically organized rsFC provides information for predicting and decoding single-trial responses to auditory stimuli to an extent comparable to what informing residFC, or noise

correlations, can provide to decoding cortical responses in the auditory cortex.

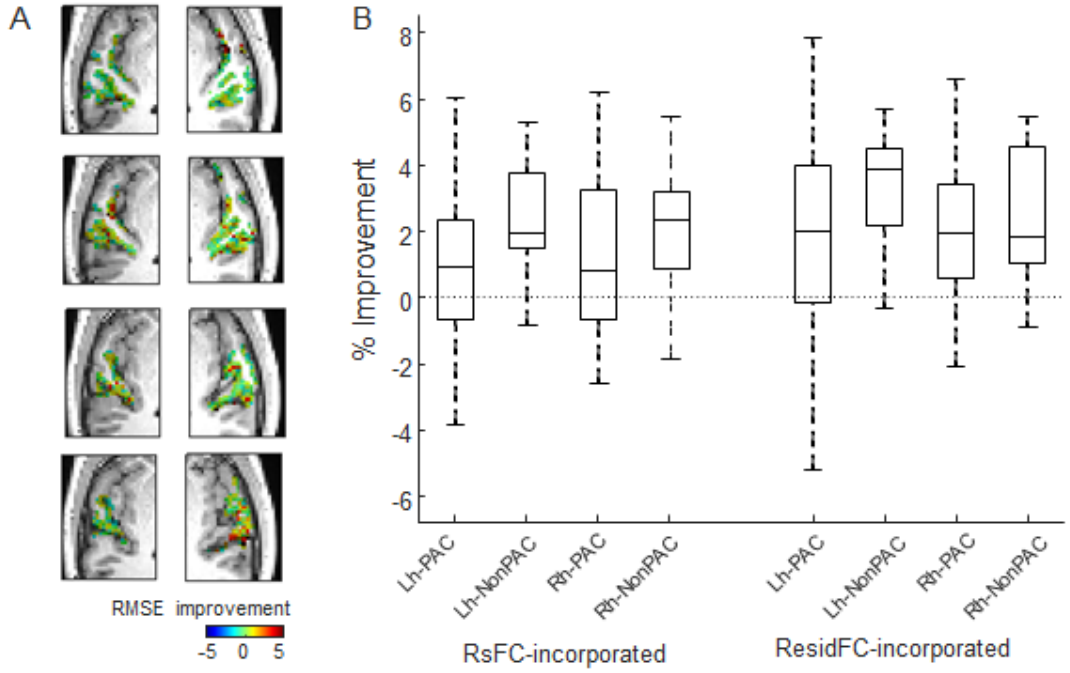

Figure 3.5. No regional bias in the improvement by FC-incorporated activity prediction

A. Topography of the improvement in voxel activity prediction with rsFC incorporated compared to the tuning-only model. Four slices from one representative participant are shown. The improvement was measured by root mean squared error (RMSE). B. Percent improvement of decoding performance in four auditory regions. There is no difference between the regions in both cases of the rsFc-incorporated (RsFC-incorporated) and the residual-based FC-incorporated (ResidFC-incorporated) model ($p > 0.05$; one-way ANOVA). Boxes and whiskers indicate the 75 and 95 percentiles, respectively.

3.3.5. No regional bias in decoding improvement by the rsFC-incorporated model

We also tested whether the improvement in decoding performance by incorporation of rsFC varies across sub-regions of the auditory cortex, specifically primary and non-primary auditory cortex. The topography of voxelwise prediction errors of the tuning-only model and the rsFC-incorporated model did not exhibit immediately obvious regional differences in the improvement in prediction accuracy (Fig. 6A, data from a representative participant). In order to statistically test regional biases, we computed the percentage improvement of stimulus identification performance in four separate auditory regions that included the primary and non-primary auditory cortices in

both hemispheres. There was no significant difference among the regions whichever correlation information (rsFC or residFC) was used ($p>0.05$, one-way ANOVA for each of the two models).

3.3.6. RsFC as covariance in maximum likelihood decoding

The improved performance by the incorporation of rsFC or noise correlations may be in part due to the particular architecture of our model, in which trial-to-trial variation is predicted based on the concurrent residual activity in the test datasets. To rule out this potential problem, we replicated the results using a maximum likelihood decoder. A virtue of maximum likelihood decoding, a specific case of Bayesian decoding, is that it directly links encoding and decoding models and takes into account the probabilistic nature of neural activity (Latham and Nirenberg, 2005; Naselaris et al., 2011). The maximum likelihood decoder assumes that a stimulus is probabilistically encoded in multi-voxel activity space and, under a Gaussian noise assumption, the likelihood that an activity pattern y is observed given a stimulus s is formulated as follows:

$$\mathrm{p}(y|s) = (1/C)\exp(-\frac{1}{2}(y-\hat{y}(s))S^{-1}(y-\hat{y}(s))^{T},$$

where C is a normalization factor, $\hat{y}(s)$ is the mean activity pattern for stimulus s, and S is the covariance matrix that describes the joint distribution of the activity across voxels. The mean activity $\hat{y}(s)$ is predicted by the tuning model and the covariance S can be estimated either from resting-state or residual activity. The tuning-only model would be the particular case where the distribution is assumed to be independent and identical across voxels (Figure 3.6.A). While most encoding models assume independent noise between recording units (Wu et al., 2006; Naselaris et al., 2011), supplying the covariance of noise of neural activity to a decoder provides a measure of the importance of the information in the correlations (Latham and Nirenberg, 2005; Averbeck et al., 2006; Graf et al., 2011).

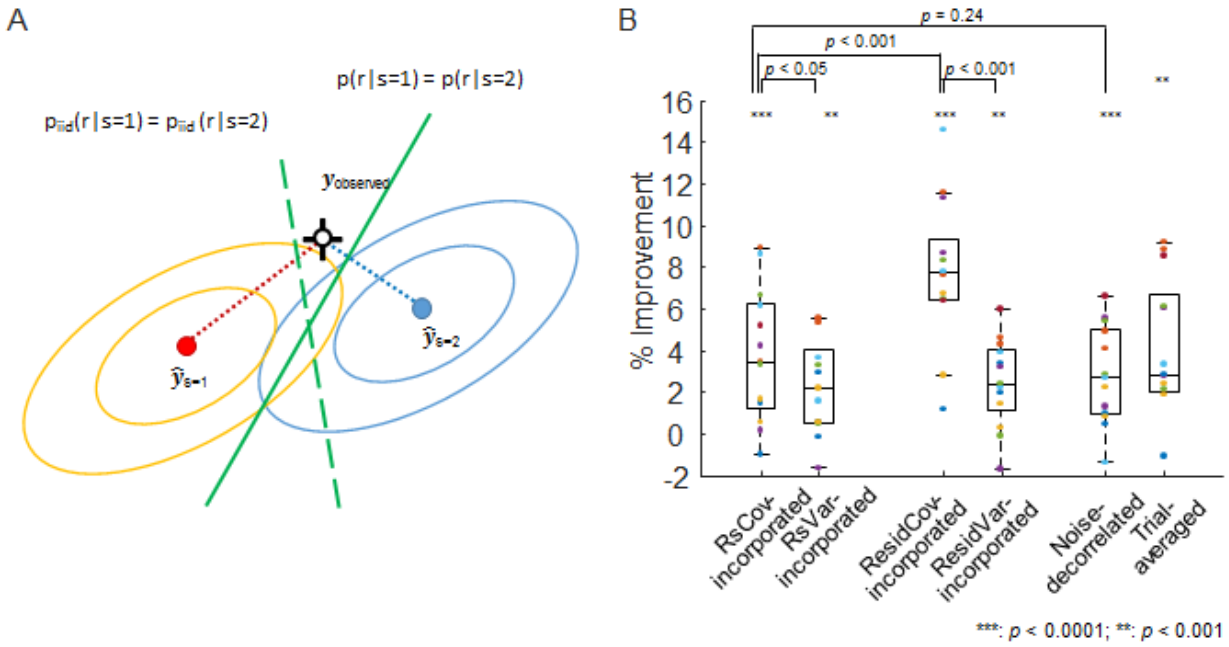

Figure 3.6. Maximum likelihood decoding with and without correlation information from resting-state activity and residual activity

A. How information of activity covariance improves maximum likelihood decoding. The two dots (red and blue) represent maximally probable activity patterns given two stimuli (s = 1 and s = 2) in the 2-dimensional space (i.e., the joint activity of 2 voxels). The ellipsoids around the two dots are iso-probability lines of the activity patterns for the two stimuli. The correlated variability is indicated by the oriented geometry of the ellipsoids, which makes the green solid line the optimal boundary to decide which stimulus an observed activity is closer to than the other. In this case, $\boldsymbol{y}_{\text{observed}}$ (black cross-haired circle) belongs to the area closer to $\hat{\boldsymbol{y}}_{s=2}$ (i.e., p(r|s=2) > p(r|s=1). When the correlation ignored and the activity distribution is assumed to be identical and independent between the 2 voxels as in the tuning-only model, the decision boundary lies along the green dashed line and $\boldsymbol{y}_{\text{observed}}$ is classified as s = 1. B. Percent improvement in stimulus identification by maximum likelihood decoding compared to the tuning only model. Decoding with full covariance estimated from resting-state activity (RsCov-incorporated) outperforms the tuning only model ($p < 0.001$). Informing only variances from resting-state data to the decoder (RsVar-incorporated) performs significantly worse than decoding with full covariance ($p < 0.05$). This pattern is replicated in the case where residual activity was used to estimate covariance and variances (ResidCov-incorporated and ResidVar-incorporated). It is also notable that decoding with covariance from residual activity gives a better performance than that using resting-state activity ($p < 0.001$). The performance improvement by incorporating the covariance from resting-state data did not differ from that of the tuning only model with noise decorrelated. Boxes and whiskers indicate the 75 and 95 percentiles, respectively, and colored dots show the performance in each of 13 individual participants.

We again computed percentage improvement in single-trial stimulus identification performance of the maximum likelihood decoder with full covariance information to the tuning-only model (Figure 3.6B). The decoders with full covariance based on either source outperformed the decoder with identity covariance, i.e., the tuning-only model (Figure 3.6B, $p < 0.05$ for resting-state-based covariance and $p < 0.001$ for residual-based covariance, one-sided paired t-test, $n = 13$), although the decoder with covariance based on residual activity had a better performance than the one based on resting-state activity ($p<0.001$). We also performed decoding with only variances included in the model by setting the off-diagonal elements of S to zero. Although the variance-only decoders performed better than the tuning-only (identity-covariance) decoder ($p < 0.001$, one-sided paired t-test, $n = 13$), it was not sufficient to perform as well as the decoder with full covariance ($p < 0.001$ for resting-state-based covariance, $p < 0.05$ for residual-based covariance, one-tailed paired t-test, $n = 13$).

3.4. Discussion

Our results indicate that rsFC between voxels has a positive relation with similarity in spectrotemporal tuning functions, or MTFs, of fMRI voxels, and that incorporating the information of rsFC into a spectrotemporal encoding model improves predicting and decoding noisy single-trial activity patterns. The positive relation between rsFC and tuning similarity was found not only in frequency tuning, as shown previously (Fukushima et al., 2012; Cha et al., 2014; Striem-Amit et al., 2016), but also spectral density and modulation rate tuning. We also found that noise correlations, i.e. correlations in trial-to-trial response variation, have a consistent pattern with rsFC. As previously proposed (Shamir and Sompolinsky, 2004; Averbeck and Lee, 2006; Mitchell et al., 2009), decorrelating noise, i.e., trial-to-trial response variation, improved single-trial decoding compared to decoding the data with correlated noise intact, when only MTFs were taken into account to predict activity. However, when incorporation of rsFC to predict trial-to-trial variations to the encoding model improved decoding performance. Similar effects were found when noise correlation was taken into account, which is consistent with previous studies (Nirenberg and Latham, 2003; Latham and Nirenberg,

2005; Averbeck et al., 2006; Graf et al., 2011). The results were consistent when using maximum likelihood decoding where covariance was estimated from resting-state or residual activity. There were no regional biases across left and right, primary and non-primary auditory areas. The consistency between rsFC and noise correlations and the improved decoding performance by including rsFC in the model suggests that correlated fluctuations in spontaneous activity have a tight functional relation with correlated variability in neural responses.

3.4.1. Spectrotemporal tuning-specificity of rsFC

In our previous work, we found increased voxelwise residual FC between voxels with similar preferred frequencies (Cha et al., 2014). We also demonstrated that frequency-specificity of FC was preserved when activity was taken from silent resting epochs. Our current findings with a full run of resting state activity confirm that rsFC is frequency tuning-specific, in accordance with other studies in humans or non-human animals (Brosch and Schreiner, 1999; Fukushima et al., 2012; Striem-Amit et al., 2016). We extended these findings to the two other feature domains in spectrotemporal tuning functions, that is, spectral density (SD) and modulation rate (MR). To our best knowledge, SD- or MR- specific functional connectivity has never been reported previously either in humans nor animals.

In our results, the positive relation between rsFC and sensory tuning similarity does not appear to be restricted to sensory feature domains that are topographically organized. There has been little evidence in single-unit electrophysiological studies to prove that the cortical representation of SD and MR has topographical organizations at a macroscopic level, and human imaging studies have reported inconsistent results (Schönwiesner and Zatorre, 2009; Santoro et al., 2014). Although a limited number of studies have shown topographical organization of other tuning properties such as spectral asymmetry (Shamma et al., 1993) and periodicity (Langner et al., 2009), CF is the only auditory tuning property, especially among the ones with respect to spectrotemporal tuning, that has been widely agreed to have macroscopic topography consistently across species and individual subjects.

Given that functional connectivity measured in resting-state fMRI reflects anatomical connectivity whether monosynaptic or polysynaptic (Vincent et al., 2007; Honey et al., 2009), our findings are in line with CF-specific anatomical connectivity that has been repeatedly reported (Code and Winer, 1985; Rouiller et al., 1991; McMullen and de Venecia, 1993; Miller et al., 2001; Read et al., 2001; Kimura et al., 2003; Lee et al., 2004a). Since the origin of correlated spontaneous activity is elusive (Leopold and Maier, 2012), both thalamocortical and corticorticocortical projections can be the underlying substrate of the functional connectivity. However, anatomical connectivity with respect to similarity in SD and MR has little been known. Our findings suggest that neurons with similar SD or MD tuning functions could have denser anatomical projections or higher synaptic efficacy, whether directly or indirectly, than ones with dissimilar tuning functions.

3.4.2. Comparison of tuning specificity between rsFC and noise correlations

Trial-to-trial response variations, or noise correlations, are dependent on tuning similarities (Bair et al., 2001; Kohn and Smith, 2005; Smith and Kohn, 2008; Rothschild et al., 2010), which suggests that they may also depend on spectrotemporal tuning. However, this has never been demonstrated with experimental data. Our results indicate that trial-to-trial response variations, which is herein referred to as residFC, depend on similarity of full MTF functions and the three components of the MTF separately. It is not only consistent with the pattern of rsFC we observed on average, but there were also significant subject-to-subject correlations between noise correlations and rsFC. This suggests that a common mechanism is involved to yield correlated fluctuations in trial-to-trial responses and spontaneous activity (Jermakowicz et al., 2009; Luczak et al., 2009) or that evoked activity is constrained by spontaneous activity (Luczak et al., 2013).

In our data, noise correlations had higher tuning specificity than rsFC. This appears to be discrepant with previous studies. For instance, Kohn and Smith (2005) reported that stimulus presentation decreased noise correlations between two neurons when compared to correlations in spontaneous activity. Also, in our previous study (Cha et al., 2014), there was no significant difference in frequency tuning specificity between

noise correlations and rsFC. This discrepancy might be due to the difference in the temporal scale and the stimulus configuration. The decorrelation in Kohn and Smith (2005) occurs only transiently at stimulus onset or offset and the decorrelation effect decays in sustained period of stimulus presentation. The length of our stimuli and the temporal resolution of fMRI do not allow us to detect such transient effects. Also, overall reduction of correlation across the whole neuronal population would not necessarily change the tuning specificity of noise correlations. In Cha et al. (2014), we used residual activity that included a whole run which included resting-epochs. In contrast, we obtained single-trial responses from which residual activity was obtained without including any blank trials. Such difference in the methods could have reduced the effect we observed in the current study.

Most importantly, we used naturalistic sounds, which contained many features preferred by heterogeneous groups of neurons. Most studies on noise correlations used simple stimuli such as oriented bars and pure tones whose effects cannot necessarily be extrapolated to complex stimuli (Klein et al., 2000; Machens et al., 2004; Theunissen and Elie, 2014). Also, noise correlations show some stimulus specificity: a stimulus preferred by two neurons causes higher noise correlations than one that is not preferred (Kohn and Smith, 2005; Jermakowicz et al., 2009; Lin et al., 2015; Franke et al., 2016; Zylberberg et al., 2016). This interaction between stimuli and tuning functions in determining noise correlations could cause higher tuning-specificity in residFC than rsFC.

3.4.3. Effect of decorrelating noise in decoding

The impact of correlated trial-to-trial variability, i.e., noise correlation, on neural coding and decoding has been rigorously studied especially in theoretical neuroscience (Abbott and Dayan, 1999; Nirenberg and Latham, 2003; Schneidman et al., 2003; Shamir and Sompolinsky, 2004; Averbeck and Lee, 2006; Averbeck et al., 2006; Moreno-Bote et al., 2014). While coding efficiency is often measured by information-theoretic measures, decoding noise-shuffled data has also been suggested to provide a measure of coding efficiency (Nirenberg and Latham, 2003; Latham and Nirenberg, 2005; Averbeck et al., 2006). If decoding noise-shuffled data provides higher accuracy than the original data,

correlated noise is detrimental; and if it leads to lower accuracy, correlated noise is beneficial, under the assumption that the system would try to remove the noise by averaging responses across neurons (Averbeck et al., 2006). Studies have also suggested that coding efficiency can be lower than otherwise if noise correlation is tuning-specific (Shamir and Sompolinsky, 2004; Averbeck and Lee, 2006). Although the theoretical considerations and simulations are supported by some experimental data, testing these hypotheses is challenging because the number of neurons to be recorded is limited in electrophysiological recordings. Thus, previous studies only extrapolated their empirical results to a larger population or used simulated data (Shamir and Sompolinsky, 2004; Averbeck and Lee, 2006; Graf et al., 2011; Moreno-Bote et al., 2014). Our results that decoding with noise decorrelated performs better than that with noise correlation intact supports the hypothesis that tuning-specific noise correlation is detrimental to coding efficiency when an entire auditory cortex is included in the analysis.

3.4.4. Role of rsFC in predicting and decoding neural activity

In both of our decoding frameworks, incorporating rsFC or noise correlations improved stimulus identification performances. The importance of knowing noise correlations in decoding has been demonstrated in a number of studies (Nirenberg and Latham, 2003; Latham and Nirenberg, 2005; Averbeck et al., 2006; Graf et al., 2011). For instance, a decoding model performs sub-optimally if response distributions are correlated between two neuron and the decoder assumes identically independently distributed responses (Nirenberg and Latham, 2003; Latham and Nirenberg, 2005). Graf and colleagues (2011) provided empirical evidence that neural decoding with taking into account noise correlations in neural responses improves the performance compared to when independent noise is assumed. We confirmed the previous proposals and findings when incorporating residFC, i.e., noise correlations, into prediction and decoding of voxel-level fMRI responses from human auditory cortex. We furthermore showed that rsFC instead of residFC can be used to improve decoding performance.

Why do spontaneous activity and trial-to-trial variations have similar patterns of correlations across voxels even to the extent of providing information for decoding neural

responses? Recent studies have suggested that structured spontaneous activity can contribute to sensory encoding. For instance, (Luczak et al., 2009) demonstrated that the regime of evoked responses of a neural population is bounded by that of its coherent spontaneous activity. Also, a later study showed that spiking activity is temporally coordinated with population activity measured by multiunit recording activity or local field potential, suggesting that coherent spontaneous activity gates sensory input signals (Luczak et al., 2013). These studies suggest that coherent spontaneous activity regulated can induce a similar pattern in noise correlations and thereby contribute to regulating neural encoding (Luczak et al., 2009; Schneidman, 2016). This does not mean that rsFC should be identical to noise correlations. Differences between rsFC and noise correlations are evident in our data, and previous results indicate a stimulus-dependency of noise correlations (Shamir and Sompolinsky, 2004; Kohn and Smith, 2005; Franke et al., 2016; Zylberberg et al., 2016). Therefore, it is likely that rsFC rather provides a common structure of coherent activity to which more information can be added by stimulation, which would then yield stimulus-specific noise correlations.

Another hypothesis is that spontaneous activity encodes a prior probability distribution associated with internal models of the environment (Fiser et al., 2004). Namely, spontaneous activity samples probable activity patterns based on prior experiences of stimuli to which external inputs are incorporated so to update the internal model as a posterior distribution. This idea is supported by demonstrations that neural responses represent probability or its associated quantities (Koechlin et al., 1999; Anastasio et al., 2000; Graf et al., 2011; Pouget et al., 2013). This framework of Bayesian learning and inference presumes the involvement of neuronal connectivity in its implementation of representations (Harris, 2005; Fiser et al., 2010; Pouget et al., 2013), which is also understood as the basis of the organization of spontaneous activity (Vincent et al., 2007). Although our results do not directly address this particular hypothesis of rsFC representing prior probability for internal models, it is consistent with the idea of the pattern of rsFC as the representation of stimulus-independent coherence or joint distribution of population activity, which can evolve to be more specific by stimulation. Considering that the brain has to decode an uncountable, or virtually infinite, number of

stimuli, maintaining rsFC as a generalized or versatile patterns of neural code that can be adapted to new stimuli may be an economic strategy for neural encoding (Fiser et al., 2010; Jeanne et al., 2013; Miller et al., 2014; Schneidman, 2016).

General discussion

4.1. Tuning specific functional connectivity: what, how and why

In the studies of the current thesis, three main questions were addressed: (1) whether coherent spontaneous activity in human auditory cortex is specific to spectrotemporal tuning, (2) whether tuning specificity of functional connectivity reflects functional architecture of auditory cortex such as functional asymmetry, and (3) whether coherent spontaneous activity in auditory cortex is associated with spectrotemporal processing. In study 1, it was demonstrated that functional connectivity depends on similarity in frequency preference between voxels within and between sub-regions and hemispheres; and that the dependency of functional connectivity on frequency preference was high particularly in the right core area. The patterns were consistent whether functional connectivity was computed from residual activity or resting-epoch activity. In study 2, the dependency of functional connectivity on tuning similarity was generalized to spectrotemporal tuning properties, including spectral density and modulation rate. When predicting and decoding fMRI responses to natural sounds using a voxelwise spectrotemporal receptive field model, decorrelating noise (residual) improved the performance, indicating the detrimental effect of correlated noise. However, incorporating resting-state functional connectivity to the decoders helped to overcome the effect of correlated noise, indicating the functional significance of coherent spontaneous activity. The results were qualitatively similar whether resting-state activity or residual activity was used to estimate functional connectivity; and there the improvement of decoding performance was observed throughout the auditory cortex without regional preference.

4.1.1. What and where: tuning-specific functional connectivity and its relation to functional organization of human auditory cortex

The findings of tuning specificity of intrinsic functional connectivity provide evidence that human auditory cortex follows the organizational principles such as tonotopic projection patterns or functional asymmetry that have been implied in the previous studies on sensory cortices in various species including humans (Zatorre et al.,

2002; Hackett, 2011). However, the findings have more implications than replicating previous studies to other species or sensory modalities.

First, preferred frequency-specific functional connectivity may provide important clues to infer the organization of anatomical connectivity in the human auditory brain. As indicated in chapter 2, the pattern of functional connectivity associated with frequency tuning is largely in agreement with the tonotopic or frequency-selective projections that are thalamocortical (McMullen and de Venecia, 1993; Hashikawa et al., 1995; Miller et al., 2001; Kimura et al., 2003; Lee et al., 2004a), corticocortical (Read et al., 2001; Lee et al., 2004a), and commissural (Code and Winer, 1985; Rouiller et al., 1991; Lee et al., 2004a). Note that the corticocortical projections are inclusive of local projections along iso-frequency strips as long as those across different areas or tonotopic fields (Read et al., 2001; Lee et al., 2004a). While these patterns in anatomical projection are found in non-human mammals, neuroanatomical data in humans are sparse.

The findings of tonotopic functional connectivity between the core and belt areas in study 1 can imply two possibilities of anatomical connectivity in humans: (1) tonotopic functional connectivity between the two areas is mediated by thalamocortical connections that diverge to core and non-core fields; and (2) it arises through corticocortical projections. In non-human primates, tonotopic thalamocortical projections terminate mostly in the core fields (Hackett, 2011). If the human auditory system has the same pattern, the tonotopic pattern of functional connectivity is likely due to tonotopic projections between the human core and belt areas rather than direct projections from the thalamus to the belt area although a definitive answer requires more evidence from anatomical data.

Tonotopic functional connectivity between the two hemispheres (Figure 2.7, for instance) can be also taken as evidence of tonotopically organized commissural projections (Code and Winer, 1985; Rouiller et al., 1991; Lee et al., 2004b). It is indeed possible that interhemispheric functional connectivity is mediated by contralateral projections from the subcortical structures instead of direct callosal connections. However, anatomical connectivity in mammalians indicates that the closest contralateral origin of axonal projections to the cortex is the inferior colliculus, which is already two

stations away from the core because of the lack of direct inputs from the inferior colliculus to the cortex (Calford and Aitkin, 1983; Hackett, 2011; Pickles, 2015). Also, callosotomy leads to loss of interhemispheric functional connectivity between homotopic regions (Johnston et al., 2008). These suggest that preferred frequency specific functional connectivity between hemispheres is likely mediated by correspondingly organized callosal connections. In the absence of direct examinations of anatomical connections, these issues could be better addressed if one analyzes tonotopic functional connectivity or effective connectivity between the cortical and subcortical regions including the inferior colliculus using ultra-high resolution fMRI (De Martino et al., 2013; Moerel et al., 2015).

Second, tuning-specific functional connectivity with respect to spectral density and modulation rate (study 2) suggests that there is a similar pattern of anatomical connectivity, whether direct or indirect, between neurons that have similar tuning functions for spectral density and modulation rate. Such a pattern of anatomical connectivity has never been reported. It remains an open question whether the underlying anatomical projections has a form of topographic connectivity similar to tonotopy. One neurophysiological study demonstrated that spectral bandwidth has columnar representations in the cat primary auditory cortex, and that the columns have modular anatomical projections for similar bandwidths (Read et al., 2001). Connectivity for bandwidth could be a proxy of connectivity for spectral density since bandwidth and spectral density have been reported to be highly correlated in neurophysiological data (Connor et al., 2006), and the cortical response model used in study 2 assumes complete association of both features (Chi et al., 2005). High field fMRI can also contribute to resolving the issue on whether the representation of spectral density and modulation rate is topographically organized (Schönwiesner and Zatorre, 2009; Santoro et al., 2014). Nonetheless, the existence of anatomical modular projection patterns can be ultimately tested using anatomical tracer studies with neurophysiological characterization of auditory neurons.

Third, study 1 showed that the degree of tuning specificity of functional connectivity can be reflective of functional specialization at a regional or hemispheric level. The particularly high specificity to frequency preference found in study 1, for

example, indicates that the high selectivity in connectivity may provide relevant information to higher-order areas in the right hemisphere known to process spectral features on a finer scale (Zatorre and Belin, 2001; Zatorre et al., 2002; Schönwiesner et al., 2005; Hyde et al., 2008). However, this finding was not replicated in study 2. The discrepancy might be due to differences in the methods between the two studies including the range of frequency used for tuning function (200 to 8000 Hz in study 1 vs. 300 to 4000 Hz in study 2) and the definition of the primary auditory cortex (functional localization in study 1 vs. anatomical localization in study 2). Also, pure tone and natural sounds could lead to difference in estimated tuning functions (Laudanski et al., 2012). The hypothesis of transferring functional connectivity information to a higher area can be tested by more sophisticated computational modeling or analysis methods such as causality analysis (Upadhyay et al., 2008), or by invasive experiments that might involve disturbing functional connectivity in the core area to examine whether the spectral processing is impaired in higher-order areas.

Fourth, the two studies showed strong similarity in tuning specificity between the data from resting-state activity and residual activity, which is possibly relevant to the origin of neural response variability. A number of studies addressed the possibility that spontaneous activity might be the source of neural response variability, following the results that either pre-stimulus activity within the region of interest (Arieli et al., 1996; Saka et al., 2010) or activity in a functionally connected area (Fox et al., 2006b; Schölvinck et al., 2012) can be predictive of variability of evoked activity. The studies in this thesis elaborated this notion with respect to tuning-specific organization of functional connectivity. The finding in study 2 that single-trial prediction and the resulting decoding performance were improved when resting-state functional connectivity was incorporated (Figure 3.4 and 3.6) suggests that resting-state functional connectivity is predictive of variability in evoked activity. This implies that if the neural response variability originated from spontaneous activity, it would involve tuning-specific integration of the activity. Alternatively, the similarity between the resting-state and residual activity could be caused by a common origin instead of one being caused by the other. The similarity between spontaneous activity and residual activity can be evidence for functional

significance of coherent spontaneous activity (Luczak et al., 2009, 2013), which will be discussed later.

Last, the findings in the two studies support both functional specialization and distributed processing in the auditory cortex. Both mechanisms in fact seem to be intertwined. For example, the very notion of tuning specificity of functional connectivity indicates functional specialization. However, functional connectivity over voxels that are tuned to different features, despite the specificity, substantiates functional integration and thus distributed processing in a large sense. Moreover, the impact of functional connectivity on neural decoding implies that interaction between inhomogeneous units can play an important role in neural information processing. The high preferred frequency specificity of functional connectivity within the right core area observed in study 1 (Figure 2.8 and 2.9) also supports functional specification, and at the same time, functional interaction between distributed units underlies this specificity. Also, the contribution of functional connectivity to decoding was not limited to a certain region or hemisphere (Figure 3.5). Therefore, the auditory cortex seems to process information both in terms of modular and distributed processing, although theorizing on how they interplay together would require more detailed data.

4.2.1. How: the origin and mechanism of tuning-specific functional connectivity

What underlying mechanisms give rise to tuning-specific functional connectivity? This question must be addressed in terms of two regimes: spontaneous activity and variability in evoked activity. The first has also been referred to as resting-state (or resting-epoch) functional connectivity in this thesis according to the specific experimental settings, while the latter was designated as residual functional connectivity in the sense that it is computed from activity after removing stimulus-evoked activity. Residual functional connectivity can be also regarded as a measure of noise correlation.

The origin of spontaneous activity is attributed to be thalamocortical or corticocortical recurrent circuitry (Sakata and Harris, 2009; Leopold and Maier, 2012; Hartmann et al., 2015). A number of studies support the importance of thalamocortical network as being important in generating spontaneous activity. For instance, high

spontaneous firing rate in the primate visual cortex has been observed in layers 4A, 4C and 6 which receive thalamic inputs while other layers, especially those receiving corticocortical inputs, have scarce spontaneous activity (Snodderly and Gur, 1995). The significant contribution of corticothalamocortical circuits to drive information transmission to cortical activity (Theyel et al., 2010) also emphasizes the importance of thalamocortical recurrent circuits. However, these studies do not directly address how recurrent circuits can generate spontaneous activity.

Other studies stress the role of corticocortical circuits in driving spontaneous activity. Sanchez-Vives and McCormick (2000) found that spontaneous recurrent activity is generated among pyramidal cells in layer 5 of the ferret neocortex in vitro, followed by activity in other layers. The generation of spontaneous activity in their experiments was intrinsic because there was no thalamocortical input. Sakata and Harris also reported similar findings that both spontaneous activity and evoked activity are prominent in layer 2/3 and 5, but the former propagates from layer 5 while the latter spreads from layer 2/3 (Sakata and Harris, 2009). These results support that spontaneous activity arises within the cortex. However, it is still possible that activity in layer 5 can also involve the corticothalamocortical loops as in Theyel et al. (2010).

Other researchers attribute coherent spontaneous activity to neuromodulatory effects in consideration of global functional connectivity over the almost entire cortex (Schölvinck et al., 2010). This account concerns neurochemical or neuromodulatory innervations from the brain stem or other subcortical structures to affect neuronal activity or neurovascular coupling over the cortex (Schölvinck et al., 2010; Leopold and Maier, 2012).

How are these accounts related to tuning-specific resting-state functional connectivity? There are at least two possibilities. One is that functional connectivity arises directly from the generative mechanisms of spontaneous activity from recurrent circuits or neuromodulatory inputs. This assumption immediately rejects the neuromodulatory account for tuning-specific functional connectivity since neuromodulatory inputs in this account are non-specific. Then, direct recurrent circuits can be the substrate for tuning-specific functional connectivity if these circuits are tuning-

specifically organized within and between the hemispheres. The other possibility is that functional connectivity arises from propagation of activity to a region that is spatially distant from the origin of spontaneous activity. In this case, localized recurrent circuits or globally spread neuromodulatory inputs can equally likely generate the tuning-specific correlations in spontaneous activity: even if the generation of spontaneous activity is non-specific, the correlation can be refined through specific local projections to become tuning-specific. This is supported by previous reports of spatiotemporal propagation of spontaneous activity in the cortex in a tuning-specific fashion (Song et al., 2006; Nauhaus et al., 2009, 2012; Saitoh et al., 2010).

What is, then, the origin of trial-to-trial response variability? A simple and old hypothesis is that trial-to-trial variability arises from spontaneous activity that is simply linearly superimposed on evoked activity (Arieli et al., 1996; Fox et al., 2006b; Saka et al., 2010). Arieli and colleagues, for instance, demonstrated that single-trial responses to a visual stimulus can be better predicted by simply adding pre-stimulus spontaneous activity to the average response to the stimulus. Other studies also support linear superposition between spontaneous activity and neural variability using various techniques and paradigms in different species (Fox et al., 2006b; Saka et al., 2010, 2012; Becker et al., 2011; Schölvinck et al., 2012).

There is, however, evidence that functional connectivity or neural correlation varies depending on stimuli or cognitive states. For example, variance in stimulus-evoked cortical activity is smaller than that of ongoing baseline activity (Hesselmann et al., 2008b; He, 2013); and attention allocation quenches correlations in trial-to-trial variability (Cohen and Maunsell, 2009; Mitchell et al., 2009). Recent studies have also shown that trial-to-trial variability in retinal ganglion cells varies with stimulus orientation according to the geometric mean of orientation tuning functions of paired neurons, which suggests tuning-specific noise correlations is affected by stimuli (Franke et al., 2016; Zylberberg et al., 2016). These findings support the possibility that correlations in spontaneous activity and trial-to-trial variability interact with one another rather than the latter simply reflects the former (Fiser et al., 2010; Hesselmann et al., 2010; He, 2013). Thus, there might be other sources of variability and correlation, such as

stimulus effects, in neural responses in addition to spontaneous fluctuations in baseline activity.

Other researchers propose that evoked activity is constrained by a mechanism that generates spontaneous activity (Harris and Mrsic-Flogel, 2013; Luczak et al., 2015). Proponents of this view specifically put stress on cortically-originated recurrent activity that plays a role as building blocks of correlated activity (Harris, 2005; Sakata and Harris, 2009). From this view, one can hypothesize that while spontaneous activity in the cortex maintains the building blocks of ensemble activity, the brain system can engage such internally generated activity to a more specific code for an incoming stimulus (Miller et al., 2014). It is also possible, and possibly consistent with the above hypothesis, that correlated spontaneous activity serves as a gating function for evoked activity (Luczak et al., 2013).

The similar patterns between resting-state and residual functional connectivity found in both studies in this thesis partly support linear superposition of spontaneous activity (Figure 2.7, 2.9 and 3.2); however, the higher tuning specificity in residual functional connectivity found in study 2 (Figure 3.2) is consistent with the previous findings that stimulus can modulate tuning-specific noise correlations (Franke et al., 2016; Zylberberg et al., 2016). Therefore, the results support that noise correlations are driven by both stimulus effects and a common mechanism that it shares with the generation of spontaneous activity.

4.2.2. Why: Functional implications of tuning-specific functional connectivity

Possible functional benefits or disadvantages of having tuning-specific functional connectivity both in spontaneous activity and residual activity (noise correlation) have already been introduced and discussed throughout the thesis. As to tuning-specific coherent spontaneous activity, the replay hypothesis (Ji and Wilson, 2007), the sensory gating hypothesis (Luczak et al., 2013) and the internal model hypothesis (Fiser et al., 2010) were addressed; and it was pointed out that if the spontaneous activity is only an epiphenomenon of random noise shared in the network without any functional benefit, it would be wasteful to consume high metabolic demands at rest. For correlated variability,

the presence of stimulus-independent noise correlation that increases with tuning similarity has been known to be detrimental to neural coding efficiency especially when it is presumed that a neural decoder, or a signal receiver, in the brain tries to extract the information by averaging (Abbott and Dayan, 1999; Shamir and Sompolinsky, 2004; Averbeck et al., 2006). However, the effect can vary depending on the characteristics of noise correlation (Shamir and Sompolinsky, 2004; Moreno-Bote et al., 2014) and in particular, stimulus-dependent noise correlation in the retina has recently been reported to increase the amount of coded information compared to the case of independent noise (Shamir and Sompolinsky, 2004; Franke et al., 2016; Zylberberg et al., 2016). On the other hand, to the decoding point of view, incorporating information about actual noise correlation to decoding can be beneficial compared to decoding under the assumption of independent noise (Latham and Nirenberg, 2005; Averbeck et al., 2006). In the previous section, it was discussed that correlated spontaneous activity can be the origin of correlated response variability. Therefore, it might be possible for these accounts to come to a unified framework to understand both types of functional connectivity (Fiser et al., 2010; Schneidman, 2016).

The studies in this thesis have addressed the functional implications of tuning-specific functional connectivity with respect to auditory information processing. In study 1, high preferred frequency specificity of functional connectivity of the right core area was suggested to be related to functional specialization for high-resolution spectral processing. Study 2 was an attempt to address the functional significance of tuning-specific functional connectivity more directly by comparing the resting-state functional connectivity and noise correlations as well as showing that both can be useful to improve neural decoding performance. The maximum likelihood decoding analysis indicated that decoding with residual functional connectivity (noise correlations), which showed higher tuning-specificity, outperforms decoding with resting-state functional connectivity. This result might be related to the interpretation of high specificity in the right core in study 1: high tuning-specificity in functional connectivity can lead to better resolution of sensory processing in the higher cortical areas that might extract information from functional connectivity in the earlier stations.

As to the impact of noise correlations, study 2 demonstrated that when residual activity, i.e. noise, is decorrelated across voxels by shuffling trials independently for individual voxels, the decoder that takes into account only the spectrotemporal tuning model identified the stimulus better than when noise is intact (Figure 3.3C). This result is consistent with numerous theoretical and experimental studies that have suggested detrimental effects of correlated noise on coding efficiency in the neural systems especially when it has a positive relation with tuning similarity (Abbott and Dayan, 1999; Shamir and Sompolinsky, 2004; Averbeck et al., 2006). These, including the result in study 2, suggest that if the decoder only extracts the information in terms of tuning functions and predicts mean activity patterns for a particular stimulus, it would be better for the encoding system to have uncorrelated noise (Mitchell et al., 2009). However, this is not the case in real neural systems: noise correlations are usually positively correlated with tuning similarity (Lee et al., 1998; Averbeck et al., 2006; Luczak et al., 2009).

One possible solution to this problem is to provide noise correlation information to a neural decoder: studies on neural decoding have shown that adding information to a decoder about noise correlation that exists in neural responses can improve decoding performance (Averbeck et al., 2006; Graf et al., 2011). The results that the incorporation of correlation information from functional connectivity improved decoding performance (Figure 3.4B and 3.6B) are consistent with the previous studies. However, it still remains unclear whether decoding with correlation information can recover all information loss in encoding if any; whether the brain actually uses implements a decoding strategy to use noise correlation; and why the coding system would allow inefficiency in the first place even if it can decode the information after all.

A number of researchers propose that coding efficiency might not be the only measure to evaluate the neural coding system; rather, reliability or learnability should also be considered (Barlow, 2001; Luczak et al., 2009; Fiser et al., 2010; Harris et al., 2011; Schneidman, 2016). As to reliability, redundant coding by correlated activity can increase reliability in the sense that if one neuron fails to respond faithfully to a stimulus at a given time, other neurons with similar response patterns can still make a reliable contribution to the neural code (Schneidman et al., 2006; Luczak et al., 2009; Ganmor et

al., 2015). Also, it has been suggested that correlations in neural activity can help the neural system increase the capability of learning from activity samples (Fiser et al., 2004; Ganmor et al., 2011, 2015), for instance by flexibly engaging stimulus-evoked activity of single neurons to ensemble spontaneous activity (Miller et al., 2014).

This view is also consistent with the sensory gating hypothesis of spontaneous activity (Luczak et al., 2009, 2013) and the internal model account (Fiser et al., 2010; Berkes et al., 2011; Peyrache et al., 2015). Luczak and colleagues (Luczak et al., 2009, 2013, 2015) point out that the similarity between spontaneous activity and evoked activity suggests that common regulatory mechanisms might lead spontaneous activity to serve as a gating function, which in turn restricts possible codes that evoked activity can choose for encoding. On the other hand, Fiser and colleagues propose that the neural system can use spontaneous activity to learn the prior probability for the model of the environment, and evoked activity is combined with spontaneous activity to infer the incoming stimuli and to update the prior (Fiser et al., 2004). Importantly, the above accounts commonly predict that correlated patterns in spontaneous activity would be similar to noise correlations (Figure 2.8, 2.9 and 3.2D) and that a stimulus input could alter the correlations (Figure 3.2D and 3.6B) as shown in the current thesis. Therefore, the results currently presented are consistent with the notion of utilization of coherent spontaneous activity in sensory encoding and decoding.

4.3. Methodological implications

The two studies in the thesis are suggestive of computational linking between fMRI and electrophysiological studies in terms of encoding and decoding models. On the encoding model side, fMRI activity was fit by neurophysiologically plausible encoding models. In addition to that, functional connectivity was computed for each voxel pair and associated with tuning functions. On the decoding side, study 2 introduced neurophysiologically plausible multivoxel decoding rather than only finding decoding model parameters in an abstract space, as done in most fMRI decoding studies. The following section discusses these two points briefly.

4.3.1. Neural encoding in fMRI: linking voxels to neurons

Since the beginning of human fMRI studies, the methods have been heavily used to link mental representations (whether it is of incoming stimuli, outward actions or cognitive processes in between) and brain activity in a linear fashion. For this reason, the general linear model has been the essential procedure in fMRI analysis. In this approach, an activated voxel or region is assumed to encode some relevant aspect of the mental representation. In many fMRI studies, researchers seek associations between voxels (or regions) and a single type of category, or for relative preferences between a few types of mental representations. While the former is merely functional localization or brain mapping, the latter can be called 'cognitive encoding tuning' or 'cognitive preference' function in the sense that it describes what cognitive process a voxel prefers although it is still a type of functional localization (Haxby et al., 2001).

The concept of tuning or preference functions has been used in sensory neurophysiology for decades. The traditional approach is in fact very similar to the practices in fMRI research: a set of simple stimuli are presented and a neuron is characterized with respect to its response magnitude to each of the stimuli. The stimuli are parameterized by only one feature dimension, e.g., bar orientation, and thus the tuning function of a neuron can be described by one variable. Sensory neuroscientists have adopted this approach to characterize sensory tuning functions of single voxels in fMRI, for instance, for frequency tuning function or orientation selectivity (Freeman et al., 2011; Park et al., 2013; Schönwiesner et al., 2014). Once tuning functions are established, one can fit a model to it in order to express it as a functional form which leads to estimation of biologically meaningful parameters such as best frequency, tuning width or periodicity (Moerel et al., 2012; Schönwiesner et al., 2014). Study 1 used this approach to characterize frequency tuning functions of single voxels and estimate best frequencies as a continuous variable. These parameters are often comparable to neuronal tuning properties: for instance, the width of frequency tuning functions is larger in the non-core areas than the core (Moerel et al., 2012; Schönwiesner et al., 2014) which is in agreement with neurophysiological findings in animals (Rauschecker, 1998; Kaas and Hackett, 2000).

Another approach to estimate sensory encoding functions using fMRI is to model the responses of hypothetical neurons in terms of their tuning properties and associate fMRI voxel responses to the responses of multiple hypothetical neurons to a stimulus (Kay et al., 2008; Brouwer and Heeger, 2009; Naselaris et al., 2011; Santoro et al., 2014). In other words, tuning functions or receptive fields of hypothetical neurons yields filter responses to various features in a stimulus and the outputs of the filters are linearly combined to produce an fMRI response. Individual voxels have characteristic weights in this linear mapping that serve as tuning function in terms of particular stimulus feature variables (e.g., spatial frequency, orientation, and spectral density), and the weights indicate how much each of the hypothetical neurons (or corresponding filters) contribute to the fMRI response. In this approach, it is important to have biologically plausible assumptions about the receptive fields and response properties of neurons. The advantages of this approach include the capability of using complex or natural stimuli as input for model estimation and as output to be decoded, characterizing multiple feature variables at once, and testing neurophysiological models of receptive fields without direct electrophysiological recordings. Study 2 took this approach to identify spectrotemporal encoding functions of individual voxels of human auditory cortex (Figure 3.1). It opened the possibility to characterize tuning functions for the three variables of spectrotemporal receptive field (characteristic frequency, spectral density, and modulation rate) and to test models that can account for natural sound processing.

Furthermore, voxelwise functional connectivity was computed in both studies and related to the tuning properties of the voxels. This approach allowed not only to quantify the relation between tuning functions and functional connectivity (studies 1 and 2) but to evaluate the effect of functional connectivity on encoding and decoding (study 2). Quantification of the relation of tuning functions and functional connectivity led to comparison between different areas (study 1: Figure 2.9) or between two different types of functional connectivity (study 2: Figure 3.2D). Testing prediction or decoding models based on functional connectivity in study 2 brought out discussions on the importance of noise correlations using human fMRI data that cover an entire sensory cortex. Quantification of tuning-specific functional connectivity (Jermakowicz et al., 2009; Goris

et al., 2014; Moreno-Bote et al., 2014) and research on noise correlations (Averbeck and Lee, 2006; Kohn et al., 2016) have mostly concerned animal electrophysiological and theoretical studies. The commonly addressed limitation in those studies is that the data to fit the models are limited to small populations of neurons (Abbott and Dayan, 1999; Shamir and Sompolinsky, 2004; Franke et al., 2016). The current thesis takes the discourse in the classical neurophysiological community into the regime of fMRI to replicate the findings and test the hypotheses on a larger scale, and in humans.

4.3.2. Neural decoding in fMRI: modeling information to be decoded

After decades of practice of univariate analysis in fMRI to associate a certain mental representation or state to specific voxels, Haxby and colleagues (2001) first applied fMRI multivoxel pattern analysis to decode the stimulus identity out of activity patterns in the human ventral visual cortex. In fact, their methods were similar to the tuning model-based decoder in study 2: the stimulus category preference function is estimated in a dataset and used to predict multivoxel patterns to identify the stimulus by comparing the predicted patterns. Although these two approaches are multivoxel pattern analysis, they do not take into account the interaction of voxels or trial-to-trial variability (i.e., only mean activity is predicted).

Subsequent fMRI studies, however, soon adopted various existing machine learning methods including the support vector machine (Kamitani and Tong, 2005) and linear discriminant analysis (Haynes and Rees, 2005). These machine learning methods take into account variability and correlations between voxels partially (support vector machine) or fully (linear discriminant analysis). Since then, various decoding methods derived from machine learning that incorporate trial-to-trial variability in the data have been introduced to the field. However, only a few methods, such as linear discriminant analysis fully incorporates the co-variability; but the biological underpinnings of co-variability between voxels have been ignored. This is due to the computational challenge in estimating covariance from limited samples (Ledoit and Wolf, 2004) and to the limitation that the decoding approach in general cannot explicitly track down the encoding process (Kriegeskorte, 2011; Serences and Saproo, 2012).

Representational similarity analysis is another multi-voxel pattern analysis method that is believed to model the brain's information processing (Kriegeskorte, 2011), but it does not necessarily concern the co-variability across voxels. In general, it is sufficient to compute similarity between the patterns of average activity for distinct representations. Receptive field modeling-based analysis, which is the kind of tuning-only model used in study 2 is in a similar position. Namely, it models the encoding process of the brain but it does not necessarily take into account co-variability between voxels in most cases (Kay et al., 2008; Naselaris et al., 2009, 2011; Santoro et al., 2014).

As discussed in many studies, correlation in neuronal response variability may lead to information loss (Shadlen and Newsome, 1994; Abbott and Dayan, 1999; Shamir and Sompolinsky, 2004; Averbeck and Lee, 2006). This was the case in the data in study 2. When the inter-voxel correlation is intact in the original data, the decoding performance was worse than the case where the correlation in trial-to-trial variability was disturbed in single trial decoding. The decoding performance with trial-averaged test data used was equivalent to the single-trial decoding with the co-variability disturbed (Figure 3.3). This is probably due to the fact that averaging across trials decreases the effect of co-variability (by removing noise). However, there is no means by which a brain system can actually remove noise in this way because it needs to be able to decode the activity in a single trial. Even for engineering, for instance when developing a neural prosthetic device, the real problem lies in a single trial situation. Therefore, taking into account co-variability across neurons or voxels is critical to studying neural decoding.

Study 2 stresses how important knowing co-variability in the data is in decoding brain activity, and how it can be combined with a biologically-based tuning model. Moreover, the study explicitly and fully incorporated the co-variability factor into decoding rather than implicitly or abstractly as in other methods. Therefore, this approach brings encoding models and co-variability, both of which are biologically tractable, together into neural decoding. Furthermore, the findings demonstrated that the co-variability can be estimated from resting-state data, which not only has the aforementioned biological implications but also has the practical implication that researchers can run resting-state fMRI runs to obtain data for a reliable covariance

estimation, which usually requires much more amount of data than for estimation of mean activity.

4.4. Limitations and suggestions for future research

The present thesis has addressed the three main hypotheses: (1) functional connectivity in human auditory cortex has spectrotemporal tuning-specific organization; (2) tuning-specific functional connectivity reflects known functional architecture of human auditory cortex such as tonotopic organization of anatomical connectivity and functional asymmetry; and (3) coherent spontaneous activity has a functional implication related to trial-to-trial co-variability (noise correlations), such that including the information of resting-state functional connectivity can improve activity prediction and decoding. The results from this thesis supporting these hypotheses will contribute to discussions in the field to elucidate the organization of neuronal interactions and the nature of coordinated spontaneous activity that form the basis of human cognition and behavior, as Hebb foresaw.

It is, however, necessary to address the inevitable limitations of the studies. First, despite the application of neurophysiologically-motivated receptive field models and voxelwise analysis, the results cannot provide sufficient evidence for any strong inference about behaviors of individual neurons. Rather, voxel activity must be understood as population activity of a mixture of homogeneous and inhomogeneous neurons (Heeger and Ress, 2002; Boynton, 2005; Dumoulin and Wandell, 2008; Brouwer and Heeger, 2009). For topographically organized features such as visual receptive field locations (retinotopy) or auditory characteristic frequency (tonotopy), activity in response to the stimuli of interest could be regarded as arising from a relatively homogeneous group of neurons; however, other tuning properties such as orientation preference of a voxel cannot be attributed to responses from a homogeneous group of neurons since the spatial distribution of the feature representation such as orientation columns cannot be resolved by conventional fMRI voxel size (Boynton, 2005; Chaimow et al., 2010; Freeman et al., 2011). The spatial organization of spectral density or modulation rate has not been documented in previous studies although it’s been indicated that there might be

bandwidth columns that run across iso-frequency maps (Read et al., 2001). Previous fMRI studies have presented inconsistent results on the spatial organization of spectrotemporal modulation transfer function on a macroscopic scale (Langers et al., 2003; Schönwiesner and Zatorre, 2009; Santoro et al., 2014) and Schönwiesner and Zatorre (2009) reported cross-subject variability on a smaller scale. These considerations, taken together, suggest that the common resolution of fMRI might not be able to precisely delineate the topography of these two feature parameters. It does not, however, mean that the estimated modulation transfer function derived from our results is flawed, or that the tuning-specific functional connectivity is irrelevant to the underlying neuronal organization: it only means that the signal reflects biases in the neural population in a voxel which is still highly relevant to neurophysiological underpinnings (Haynes and Rees, 2005; Kamitani and Tong, 2005; Chaimow et al., 2010; Freeman et al., 2011). This point, together with the lack of anatomical data on the relation between spectrotemporal tuning parameters (except characteristic frequency) and projection patterns, makes it difficult to infer about the underyling anatomical and functional substrates of the functional connectivity results. To resolve this issue, more advanced fMRI techniques such as high field MRI (> 7T) or non-conventional sequences in a lower field strength can be used (Olman et al., 2003; Yacoub et al., 2008; De Martino et al., 2013).

Second, the high tuning-specificity of functional connectivity in the right core fields observed in study 1 (Figure 2.8 and 2.9) was not replicated in study 2. There are, in fact, multiple methodological differences that could cause the inconsistency, as briefly mentioned above. Study 1 used pure tone sounds whereas natural sounds were presented in study 2. Discrepancies between receptive fields estimated from artificial sounds and those from natural sounds have been documented in animal neurophysiological studies (Theunissen et al., 2001; Machens et al., 2004; Laudanski et al., 2012; Theunissen and Elie, 2014). Considering that voxel activity may be a mixture of inhomogeneous neuronal groups, as described above, natural sounds can drive more complex pattern of tuning functions such as more robust multi-peaks (Moerel et al., 2013). The inconsistent results might have also been caused by compromised reliability in the estimation of parameters in study 2 due to the large number of parameters. Another possibility is that the

discrepancy was caused by the smaller range of characteristic frequency parameter in study 2. The range of frequency was 1.5 times smaller in study 2, and the high specificity in the core in study 1 appears to be more strongly related to the highest frequency difference bin (Figure 2.8). To resolve this issue, it is suggested to present both types of stimuli to the same participants and use a wider range of frequency for the spectrotemporal response field model. Studying the differences in tuning properties between the responses to artificial stimuli and to natural stimuli in humans would, in fact, be of great interest to human auditory neuroscientists by itself, as would the study of the modulation of functional connectivity caused by the different characteristics of stimuli.

Third, the results in studies 1 and 2 support both hierarchical and distributed processing particularly with respect to functional interactions between neural units, but the detailed computational mechanism to integrate the two schemes is elusive. To study hierarchical processing, it might be necessary to implement causal modeling approaches (Kumar et al., 2007). Computational modelling using effective connectivity, i.e., estimation of directed influences between voxels, can be also useful to investigate how both processing strategies are combined throughout the processing stages in the cortex. Moreover, including analysis of subcortical activity simultaneously imaged in the model will help to understand how interactions between neural populations in voxels influence information processing in progression of neural stations.

Fourth, although functional implications of coherent spontaneous activity are indicated by the results that both resting-state functional connectivity and noise correlations have tuning-specific patterns, and that incorporating resting-state functional connectivity into a spectrotemporal encoding model improves activity prediction and stimulus decoding, understanding of the exact mechanism would need to depend on electrophysiological data to decide among options such as sensory-gating mechanism or Bayesian inference/learning. The sensory-gating hypothesis is challenging to test using fMRI data since the mechanism is essentially described in terms of temporal coherence between spiking activity and multi-unit activity (or local field potential) (Luczak et al., 2013) which requires data at a sufficient temporal resolution. However, under the assumption that sensory gating plays a role for a perceptually ambiguous stimulus to

reach awareness (Kiefer et al., 2011), the hypothesis can be tested by decoding the percept of an ambiguous stimulus with functional connectivity from pre-stimulus activity. If the sensory gating mechanism holds, the decoding performance or decoded stimulus with pre-stimulus connectivity would be correlated with the percept. The hypothesis of Bayesian inference and learning can be also tested using fMRI. For instance, an investigator can give participants a learning task related to artificial or natural stimuli with certain subsets of features altered so to develop an altered internal model (or mental representation) about the stimulus statistics. Then measure changes in functional connectivity to test whether it reflects the statistics of the learnt stimuli. It would be also interesting to use the functional connectivity information to decode the stimuli and assess whether it improves decoding of the learnt stimuli better than the stimuli that have not been learnt.

Lastly, it is suggested that researchers in the fields of neurophysiology and human brain imaging collaborate to integrate the understanding of functional connectivity or population dynamics at different scales. The studies in this thesis demonstrated that the combination of voxel-wise fMRI analysis and neurophysiologically-based computational modelling can bridge the two streams of research. These two regimes of neurophysiological studies are complementary: electrophysiology provides more precise temporal information in neural activity despite the lack of spatial extension (in unit recording) or spatial precision (in such techniques as electroencephalography) whereas fMRI provides data on a spatially large scale up to the entire brain. Therefore, unifying the models of neural encoding and decoding that widely fit to different types of datasets will benefit not only understanding of the brain but also developing applications such as neural prostheses and diagnostic tools.

4.5. Towards a bigger picture: unifying two views of brain function

Raichle, one of the pioneers in studying spontaneous activity of the brain, articulated in his review (Raichle, 2010) that there have been two views on brain function in the history of neuroscience. One is to assume the brain as a reflexive system to be momentarily driven by external demands from the environment while the other view is

that the brain rather builds up intrinsic operations to interpret, respond and predict environmental demands. The first view is mostly interested in characterizing the representation of the features in environmental stimuli or demands that has been already established in the system. In this view, the representation of cognitive operations and motor outcome can be regarded as the end product of processing sensory inputs (Cisek and Kalaska, 2010). Therefore, deterministic associations between neural activity and stimuli or movement control are key for brain function.

In contrast, the second view emphasizes the necessity to generate intrinsic activity which is not immediately reflexive to external demands. While it is certain that the brain maintains intrinsic activity without receiving any stimulation or executing motor outcome, the key of this view is to assign functional utility to intrinsic activity as evidenced by the existence of central pattern generators in the spinal cord, intrinsic oscillations in cortical circuits and coordinated spontaneous activity (Buzsáki and Draguhn, 2004; Yuste et al., 2005; Ji and Wilson, 2007; Fiser et al., 2010; Schneidman, 2016). Cortex has been also found to sustain dynamic state changes such as up/down or synchronized/desynchronized states (Cossart et al., 2003; Harris et al., 2011; Luczak et al., 2013) and spontaneously vary its functional connectivity over time (Hutchison et al., 2013)). As discussed earlier, emerging thoughts interpret these data as evidences that the brain actively might constantly make predictions (Friston et al., 2009) or regularizations (Fiser et al., 2010; Luczak et al., 2015) to infer what stimulus it is given or what outcome is optimal.

While the first view has motivated researchers to characterize the tuning function or response preference that link sensory inputs or cognitive processes to the magnitude of average response of neural units after removing the variability, the second view would promote investigations on spontaneous activity and response variabilities, i.e., how brain activity changes independently of cognitive representations. These two approaches are complementary to one another rather than conflicting – at least in the methodological sense, and yet studies on the intrinsic activity of the brain are far sparser than those on sensory/cognitive representations. Therefore, the emerging studies to understand the

intrinsic operations will continue to make a significant impact on systems and cognitive neuroscience.

Bibliography

Abbott LF, Dayan P (1999) The effect of correlated variability on the accuracy of a population code. Neural Comput 11:91–101 Available at: http://www.mitpressjournals.org/doi/abs/10.1162/089976699300016827.

Anastasio TJ, Patton PE, Belkacem-Boussaid K (2000) Using Bayes' rule to model multisensory enhancement in the superior colliculus. Neural Comput 12:1165–1187 Available at: http://www.ncbi.nlm.nih.gov/pubmed/10905812.

Anderson B, Southern BD, Powers RE (1999) Anatomic asymmetries of the posterior superior temporal lobes: A postmortem study. NEUROPSYCHIATRY Neuropsychol Behav Neurol 12:247–254.

Angelucci A, Levitt JB, Walton EJS, Hupe J-M, Bullier J, Lund JS (2002) Circuits for local and global signal integration in primary visual cortex. J Neurosci 22:8633–8646.

Arfanakis K, Cordes D, Haughton VM, Moritz CH, Quigley M a, Meyerand ME (2000) Combining independent component analysis and correlation analysis to probe interregional connectivity in fMRI task activation datasets. Magn Reson Imaging 18:921–930 Available at: http://www.ncbi.nlm.nih.gov/pubmed/11121694.

Arieli a, Shoham D, Hildesheim R, Grinvald a (1995) Coherent spatiotemporal patterns of ongoing activity revealed by real-time optical imaging coupled with single-unit recording in the cat visual cortex. J Neurophysiol 73:2072–2093 Available at: http://www.ncbi.nlm.nih.gov/pubmed/7623099.

Arieli A, Sterkin A, Grinvald A, Aertsen A (1996) Dynamics of ongoing activity: explanation of the large variability in evoked cortical responses. Science 273:1868–1871 Available at: http://www.ncbi.nlm.nih.gov/pubmed/8791593.

Ashburner J, Friston K (1997) Multimodal image coregistration and partitioning--a unified framework. Neuroimage 6:209–217 Available at: http://www.ncbi.nlm.nih.gov/pubmed/9344825 [Accessed June 29, 2013].

Atlas L, Shamma S a. (2003) Joint Acoustic and Modulation Frequency. EURASIP J Adv Signal Process 2003:668–675 Available at: http://asp.eurasipjournals.com/content/2003/7/310290.

Averbeck BB, Latham PE, Pouget A (2006) Neural correlations, population coding and computation. Nat Rev Neurosci 7:358–366 Available at: http://www.ncbi.nlm.nih.gov/pubmed/16760916 [Accessed February 28, 2013].

Averbeck BB, Lee D (2003) Neural noise and movement-related codes in the macaque supplementary motor area. J Neurosci 23:7630–7641 Available at: http://www.ncbi.nlm.nih.gov/entrez/query.fcgi?cmd=Retrieve&db=PubMed&dopt=Citation&list_uids=12930802.

Averbeck BB, Lee D (2006) Effects of noise correlations on information encoding and decoding. J Neurophysiol 95:3633–3644 Available at:

http://www.ncbi.nlm.nih.gov/pubmed/16554512 [Accessed October 23, 2013].

Bair W, Zohary E, Newsome WT (2001) Correlated firing in macaque visual area MT: time scales and relationship to behavior. J Neurosci 21:1676–1697 Available at: http://www.ncbi.nlm.nih.gov/pubmed/11222658 [Accessed December 1, 2013].

Barlow H (2001) Redundancy reduction revisited. Network 12:241–253 Available at: http://www.ncbi.nlm.nih.gov/pubmed/11563528.

Barlow H (2009) Grandmother Cells, Symmetry, and Invariance: How the Term Arose and What the Facts Suggest. Cogn Neurosci:309–320.

Baumann S, Petkov CI, Griffiths TD (2013) A unified framework for the organization of the primate auditory cortex. Front Syst Neurosci 7:11 Available at: http://www.pubmedcentral.nih.gov/articlerender.fcgi?artid=3639404&tool=pmcentrez&rendertype=abstract [Accessed May 26, 2014].

Becker R, Reinacher M, Freyer F, Villringer A, Ritter P (2011) How ongoing neuronal oscillations account for evoked fMRI variability. J Neurosci 31:11016–11027 Available at: http://www.ncbi.nlm.nih.gov/pubmed/21795550 [Accessed December 2, 2013].

Beckmann CF, DeLuca M, Devlin JT, Smith SM (2005) Investigations into resting-state connectivity using independent component analysis. Philos Trans R Soc London Ser B Biol Sci 360:1001–1013 Available at: http://www.ncbi.nlm.nih.gov/pubmed/16087444.

Behrens TEJ, Sporns O (2012) Human connectomics. Curr Opin Neurobiol 22:144–153 Available at: http://www.pubmedcentral.nih.gov/articlerender.fcgi?artid=3294015&tool=pmcentrez&rendertype=abstract [Accessed April 5, 2013].

Belin P, Zatorre RJ, Hoge R, Evans AC, Pike B (1999) Event-related fMRI of the auditory cortex. Neuroimage 10:417–429 Available at: http://www.ncbi.nlm.nih.gov/pubmed/10493900 [Accessed June 14, 2014].

Bellec P, Perlbarg V, Jbabdi S, Pélégrini-Issac M, Anton J-L, Doyon J, Benali H (2006) Identification of large-scale networks in the brain using fMRI. Neuroimage 29:1231–1243 Available at: http://www.ncbi.nlm.nih.gov/pubmed/16246590.

Berkes P, Orbán G, Lengyel M, Fiser J (2011) Spontaneous cortical activity reveals hallmarks of an optimal internal model of the environment. Science 331:83–87 Available at: http://www.ncbi.nlm.nih.gov/pubmed/21212356.

Bharmauria V, Bachatene L, Cattan S, Brodeur S, Chanauria N, Rouat J, Molotchnikoff S (2016) Network-selectivity and stimulus-discrimination in the primary visual cortex: Cell-assembly dynamics. Eur J Neurosci 43:204–219.

Bharmauria V, Bachatene L, Cattan S, Rouat J, Molotchnikoff S (2014) Synergistic activity between primary visual neurons. Neuroscience 268:255–264 Available at: http://dx.doi.org/10.1016/j.neuroscience.2014.03.027.

Biswal B, Yetkin FZ, Haughton VM, Hyde JS (1995) Functional connectivity in the motor cortex of resting human brain using echo-planar MRI. Magn Reson Med 34:537–541 Available at: http://www.ncbi.nlm.nih.gov/pubmed/8524021.

Boly M, Balteau E, Schnakers C, Degueldre C, Moonen G, Luxen A, Phillips C, Peigneux P, Maquet P, Laureys S (2007) Baseline brain activity fluctuations predict somatosensory perception in humans. Proc Natl Acad Sci U S A 104:12187–12192 Available at: http://www.pubmedcentral.nih.gov/articlerender.fcgi?artid=1924544&tool=pmcentrez&rendertype=abstract [Accessed December 2, 2013].

Boynton GM (2005) Imaging orientation selectivity: decoding conscious perception in V1. Nat Neurosci 8:541–542.

Brosch M, Schreiner CE (1999) Correlations between neural discharges are related to receptive field properties in cat primary auditory cortex. Eur J Neurosci 11:3517–3530 Available at: http://www.ncbi.nlm.nih.gov/pubmed/10564360 [Accessed December 2, 2013].

Brouwer GJ, Heeger DJ (2009) Decoding and reconstructing color from responses in human visual cortex. J Neurosci 29:13992–14003 Available at: http://www.pubmedcentral.nih.gov/articlerender.fcgi?artid=2799419&tool=pmcentrez&rendertype=abstract [Accessed October 1, 2013].

Buzsáki G, Draguhn A (2004) Neuronal oscillations in cortical networks. Science 304:1926–1929 Available at: http://www.ncbi.nlm.nih.gov/pubmed/15218136 [Accessed March 1, 2013].

Calford MB, Aitkin LM (1983) Ascending projections to the medial geniculate body of the cat: evidence for multiple, parallel auditory pathways through thalamus. J Neurosci 3:2365–2380.

Carr MF, Jadhav SP, Frank LM (2011) Hippocampal replay in the awake state: a potential substrate for memory consolidation and retrieval. Nat Neurosci 14:147–153 Available at: http://dx.doi.org/10.1038/nn.2732.

Carrasco A, Lomber SG (2009a) Evidence for hierarchical processing in cat auditory cortex: nonreciprocal influence of primary auditory cortex on the posterior auditory field. J Neurosci 29:14323–14333 Available at: http://www.ncbi.nlm.nih.gov/pubmed/19906979 [Accessed December 3, 2013].

Carrasco A, Lomber SG (2009b) Differential modulatory influences between primary auditory cortex and the anterior auditory field. J Neurosci 29:8350–8362 Available at: http://www.ncbi.nlm.nih.gov/pubmed/19571126 [Accessed February 7, 2014].

Cauda F, Giuliano G, Federico D, Sergio D, Katiuscia S (2011) Discovering the somatotopic organization of the motor areas of the medial wall using low-frequency BOLD fluctuations. Hum Brain Mapp 32:1566–1579 Available at: http://www.ncbi.nlm.nih.gov/pubmed/20814959 [Accessed May 15, 2013].

Cha K, Zatorre RJ, Schönwiesner M (2014) Frequency Selectivity of Voxel-by-Voxel

Functional Connectivity in Human Auditory Cortex. Cereb Cortex:1–14 Available at: http://www.ncbi.nlm.nih.gov/pubmed/25183885 [Accessed November 10, 2014].

Chaimow D, Yacoub E, Ugurbil K, Shmuel A (2010) Modeling and analysis of mechanisms underlying fMRI-based decoding of information conveyed in cortical columns. Neuroimage Available at: http://www.ncbi.nlm.nih.gov/pubmed/20868757 [Accessed March 24, 2011].

Chen L, Mishra A, Newton AT, Morgan VL, Stringer EA, Rogers BP, Gore JC (2011) Fine-scale functional connectivity in somatosensory cortex revealed by high-resolution fMRI. Magn Reson Imaging 29:1330–1337 Available at: http://www.ncbi.nlm.nih.gov/pubmed/3285506 [Accessed May 15, 2013].

Chi T, Gao Y, Guyton MC, Ru P, Shamma S (1999) Spectro-temporal modulation transfer functions and speech intelligibility. J Acoust Soc Am 106:2719–2732 Available at: http://www.ncbi.nlm.nih.gov/pubmed/10573888.

Chi T, Ru P, Shamma SA (2005) Multiresolution spectrotemporal analysis of complex sounds. J Acoust Soc Am 118:887–906.

Cisek P, Kalaska JF (2010) Neural mechanisms for interacting with a world full of action choices. Annu Rev Neurosci 33:269–298 Available at: http://www.ncbi.nlm.nih.gov/pubmed/20345247 [Accessed July 5, 2011].

Code RA, Winer JA (1985) Commissural neurons in layer III of cat primary auditory cortex (AI): pyramidal and non-pyramidal cell input. J Comp Neurol 242:485–510 Available at: http://www.ncbi.nlm.nih.gov/pubmed/2418078 [Accessed May 15, 2013].

Cohen MR, Kohn A (2011) Measuring and interpreting neuronal correlations. Nat Neurosci 14:811–819 Available at: http://dx.doi.org/10.1038/nn.2842.

Cohen MR, Maunsell JHR (2009) Attention improves performance primarily by reducing interneuronal correlations. Nat Neurosci 12:1594–1600 Available at: http://www.pubmedcentral.nih.gov/articlerender.fcgi?artid=2820564&tool=pmcentrez&rendertype=abstract [Accessed February 28, 2013].

Cordes D, Haughton VM, Arfanakis K, Wendt GJ, Turski PA, Moritz CH, Quigley MA, Meyerand ME (2000) Mapping functionally related regions of brain with functional connectivity MR imaging. AJNR Am J Neuroradiol 21:1636–1644 Available at: http://www.ncbi.nlm.nih.gov/pubmed/11039342 [Accessed November 7, 2013].

Cossart R, Aronov D, Yuste R (2003) Attractor dynamics of network UP states in the neocortex. Nature 423:283–288.

Da Costa S, van der Zwaag W, Marques JP, Frackowiak RSJ, Clarke S, Saenz M (2011) Human primary auditory cortex follows the shape of Heschl's gyrus. J Neurosci 31:14067–14075 Available at: http://www.ncbi.nlm.nih.gov/pubmed/21976491 [Accessed March 29, 2012].

Damoiseaux JS, Rombouts SARB, Barkhof F, Scheltens P, Stam CJ, Smith SM,

Beckmann CF (2006) Consistent resting-state networks across healthy subjects. Proc Natl Acad Sci U S A 103:13848–13853 Available at: http://www.ncbi.nlm.nih.gov/pubmed/16945915.

David S V, Mesgarani N, Shamma S a (2007) Estimating sparse spectro-temporal receptive fields with natural stimuli. Network 18:191–212.

de la Mothe LA, Blumell S, Kajikawa Y, Hackett TA (2006a) Thalamic connections of the auditory cortex in marmoset monkeys: core and medial belt regions. J Comp Neurol 496:27–71 Available at: http://www.ncbi.nlm.nih.gov/pubmed/16528722 [Accessed November 26, 2013].

de la Mothe LA, Blumell S, Kajikawa Y, Hackett TA (2006b) Cortical connections of the auditory cortex in marmoset monkeys: core and medial belt regions. J Comp Neurol 496:27–71 Available at: http://www.ncbi.nlm.nih.gov/pubmed/16528722 [Accessed December 3, 2013].

de la Mothe LA, Blumell S, Kajikawa Y, Hackett TA (2012a) Cortical connections of auditory cortex in marmoset monkeys: lateral belt and parabelt regions. Anat Rec (Hoboken) 295:800–821 Available at: http://www.pubmedcentral.nih.gov/articlerender.fcgi?artid=3379817&tool=pmcentrez&rendertype=abstract [Accessed December 3, 2013].

de la Mothe LA, Blumell S, Kajikawa Y, Hackett TA (2012b) Thalamic connections of auditory cortex in marmoset monkeys: Lateral belt and parabelt regions. Anat Rec 295:822–836 Available at: http://www.ncbi.nlm.nih.gov/pubmed/22467603 [Accessed November 26, 2013].

De Martino F, Moerel M, van de Moortele P-F, Ugurbil K, Goebel R, Yacoub E, Formisano E (2013) Spatial organization of frequency preference and selectivity in the human inferior colliculus. Nat Commun 4:1386 Available at: http://www.nature.com/ncomms/journal/v4/n1/full/ncomms2379.html#methods.

Depireux DA, Simon JZ, Klein DJ, Shamma SA (2001) Spectro-temporal response field characterization with dynamic ripples in ferret primary auditory cortex. J Neurophysiol 85:1220–1234 Available at: http://www.ncbi.nlm.nih.gov/pubmed/11247991.

Depireux DA, Simon JZ, Shamma SA (1998) Measuring the dynamics of neural responses in primary auditory cortex. arXiv Prepr q-bio/0309027 Available at: http://arxiv.org/abs/q-bio/0309027 [Accessed October 11, 2014].

Dumoulin SO, Wandell B a (2008) Population receptive field estimates in human visual cortex. Neuroimage 39:647–660 Available at: http://www.pubmedcentral.nih.gov/articlerender.fcgi?artid=3073038&tool=pmcentrez&rendertype=abstract [Accessed July 18, 2011].

Eickhoff SB, Stephan KE, Mohlberg H, Grefkes C, Fink GR, Amunts K, Zilles K (2005) A new SPM toolbox for combining probabilistic cytoarchitectonic maps and functional imaging data. Neuroimage 25:1325–1335.

Engel S a, Glover GH, Wandell B a (1997) Retinotopic organization in human visual cortex and the spatial precision of functional MRI. Cereb Cortex 7:181–192 Available at: http://www.ncbi.nlm.nih.gov/pubmed/9087826 [Accessed May 6, 2013].

Fair DA, Schlaggar BL, Cohen AL, Miezin FM, Dosenbach NUF, Wenger KK, Fox MD, Snyder AZ, Raichle ME, Petersen SE (2007) A method for using blocked and event-related fMRI data to study "resting state" functional connectivity. Neuroimage 35:396–405 Available at: http://www.pubmedcentral.nih.gov/articlerender.fcgi?artid=2563954&tool=pmcentrez&rendertype=abstract [Accessed February 28, 2013].

Farley BJ, Noreña AJ (2013) Spatiotemporal coordination of slow-wave ongoing activity across auditory cortical areas. J Neurosci 33:3299–3310 Available at: http://www.ncbi.nlm.nih.gov/pubmed/23426658 [Accessed December 16, 2014].

Fiser J, Berkes P, Orbán G, Lengyel M (2010) Statistically optimal perception and learning: from behavior to neural representations. Trends Cogn Sci 14:119–130 Available at: http://linkinghub.elsevier.com/retrieve/pii/S1364661310000045.

Fiser J, Chiu C, Weliky M (2004) Small modulation of ongoing cortical dynamics by sensory input during natural vision. Nature 431:573–578 Available at: http://www.nature.com/nature/journal/v431/n7008/full/nature02907.html.

Formisano E, Kim DS, Di Salle F, van de Moortele PF, Ugurbil K, Goebel R (2003) Mirror-symmetric tonotopic maps in human primary auditory cortex. Neuron 40:859–869 Available at: http://www.ncbi.nlm.nih.gov/pubmed/14622588 [Accessed February 7, 2014].

Fox MD, Corbetta M, Snyder AZ, Vincent JL, Raichle ME (2006a) Spontaneous neuronal activity distinguishes human dorsal and ventral attention systems. Proc Natl Acad Sci U S A 103:10046–10051 Available at: http://www.ncbi.nlm.nih.gov/pubmed/11058227.

Fox MD, Raichle ME (2007) Spontaneous fluctuations in brain activity observed with functional magnetic resonance imaging. Nat Rev Neurosci 8:700–711 Available at: http://www.ncbi.nlm.nih.gov/pubmed/17704812.

Fox MD, Snyder AZ, Vincent JL, Raichle ME (2007) Intrinsic fluctuations within cortical systems account for intertrial variability in human behavior. Neuron 56:171–184 Available at: http://www.ncbi.nlm.nih.gov/pubmed/17920023 [Accessed February 28, 2013].

Fox MD, Snyder AZ, Zacks JM, Raichle ME (2006b) Coherent spontaneous activity accounts for trial-to-trial variability in human evoked brain responses. Nat Neurosci 9:23–25 Available at: http://www.ncbi.nlm.nih.gov/pubmed/16341210 [Accessed February 28, 2013].

Franke F, Fiscella M, Sevelev M, Roska B, Hierlemann A, da Silveira RA (2016) Structures of Neural Correlation and How They Favor Coding. Neuron 89:409–422

Available at: http://dx.doi.org/10.1016/j.neuron.2015.12.037.

Freeman J, Brouwer GJ, Heeger DJ, Merriam EP (2011) Orientation decoding depends on maps, not columns. J Neurosci 31:4792–4804 Available at: http://www.ncbi.nlm.nih.gov/pubmed/21451017.

Fries P (2005) A mechanism for cognitive dynamics: neuronal communication through neuronal coherence. Trends Cogn Sci 9:474–480 Available at: http://www.ncbi.nlm.nih.gov/pubmed/16150631 [Accessed April 12, 2013].

Friston K, Kiebel S, Barlow HB, Feynman RP, Neal RM, Hinton GE, Neisser U (2009) Predictive coding under the free-energy principle. Philos Trans R Soc Lond B Biol Sci 364:1211–1221 Available at: http://www.ncbi.nlm.nih.gov/pubmed/19528002%5Cnhttp://www.pubmedcentral.nih.gov/articlerender.fcgi?artid=PMC2666703.

Friston KJ (1994) Functional and effective connectivity in neuroimaging: A synthesis. Hum Brain Mapp 2:56–78 Available at: http://doi.wiley.com/10.1002/hbm.460020107 [Accessed November 11, 2013].

Friston KJ (2011) Functional and effective connectivity: a review. Brain Connect 1:13–36 Available at: http://www.ncbi.nlm.nih.gov/pubmed/22432952 [Accessed March 13, 2013].

Friston KJ, Buechel C, Fink GR, Morris J, Rolls E, Dolan RJ (1997) Psychophysiological and modulatory interactions in neuroimaging. Neuroimage 6:218–229 Available at: http://www.ncbi.nlm.nih.gov/entrez/query.fcgi?cmd=Retrieve&db=PubMed&dopt=Citation&list_uids=9344826.

Friston KJ, Frith CD, Liddle PF, Frackowiak RS (1993) Functional connectivity: the principal-component analysis of large (PET) data sets. J Cereb Blood Flow Metab 13:5–14 Available at: http://www.ncbi.nlm.nih.gov/pubmed/8417010 [Accessed November 29, 2013].

Fukunaga M, Horovitz SG, de Zwart J a, van Gelderen P, Balkin TJ, Braun AR, Duyn JH (2008) Metabolic origin of BOLD signal fluctuations in the absence of stimuli. J Cereb Blood Flow Metab 28:1377–1387.

Fukushima M, Saunders RC, Leopold DA, Mishkin M, Averbeck BB (2012) Spontaneous high-gamma band activity reflects functional organization of auditory cortex in the awake macaque. Neuron 74:899–910 Available at: http://www.ncbi.nlm.nih.gov/pubmed/22681693 [Accessed March 27, 2013].

Galuske RAW, Schlote W, Bratzke H, Singer W (2000) Interhemispheric asymmetries of the modular structure in human temporal cortex. 289:1946–1949.

Ganmor E, Segev R, Schneidman E (2011) Sparse low-order interaction network underlies a highly correlated and learnable neural population code. Proc Natl Acad Sci U S A 108:9679–9684 Available at: http://www.pubmedcentral.nih.gov/articlerender.fcgi?artid=3111274&tool=pmcentrez&rendertype=abstract.

Ganmor E, Segev R, Schneidman E (2015) A thesaurus for a neural population code. Elife 4:1–19.

Gawne TJ, Richmond BJ (1993) How independent are the messages carried by adjacent inferior temporal cortical neurons? J Neurosci 13:2758–2771 Available at: http://www.ncbi.nlm.nih.gov/pubmed/8331371 [Accessed December 4, 2013].

Gerstein GL, Perkel DH (1969) Simultaneously recorded trains of action potentials: analysis and functional interpretation. Science (80-) 164:828–830.

Giraud A, Lorenzi C, Ashburner J, Wable J, Johnsrude I, Frackowiak R, Kleinschmidt A, Wolfgang J, Lorenzi C, Ashburner J, Johnsrude I, Frackowiak R (2000) Representation of the temporal envelope of sounds in the human brain. J Neurophysiol 84:1588–1598 Available at: http://www.ncbi.nlm.nih.gov/pubmed/10980029 [Accessed July 26, 2014].

Glover GH (1999) Deconvolution of impulse response in event-related BOLD fMRI. Neuroimage 9:416–429 Available at: http://www.ncbi.nlm.nih.gov/pubmed/10191170.

Goris RLT, Movshon JA, Simoncelli EP (2014) Partitioning neuronal variability. Nat Neurosci 17:858–865 Available at: http://dx.doi.org/10.1038/nn.3711.

Graf ABA, Kohn A, Jazayeri M, Movshon JA (2011) Decoding the activity of neuronal populations in macaque primary visual cortex. Nat Neurosci 14:239–245 Available at: http://www.pubmedcentral.nih.gov/articlerender.fcgi?artid=3081541&tool=pmcentrez&rendertype=abstract [Accessed November 6, 2013].

Greicius MD, Krasnow B, Reiss AL, Menon V (2003) Functional connectivity in the resting brain: a network analysis of the default mode hypothesis. Proc Natl Acad Sci U S A 100:253–258 Available at: http://www.pnas.org/content/100/1/253.short.

Haak K V, Cornelissen FW, Morland AB (2012a) Population receptive field dynamics in human visual cortex. PLoS One 7:e37686 Available at: http://www.pubmedcentral.nih.gov/articlerender.fcgi?artid=3359387&tool=pmcentrez&rendertype=abstract [Accessed May 15, 2013].

Haak K V, Winawer J, Harvey BM, Renken R, Dumoulin SO, Wandell BA, Cornelissen FW (2012b) Connective field modeling. Neuroimage 66C:376–384 Available at: http://www.ncbi.nlm.nih.gov/pubmed/23110879 [Accessed June 1, 2014].

Hackett TA (2011) Information flow in the auditory cortical network. Hear Res 271:133–146 Available at: http://www.pubmedcentral.nih.gov/articlerender.fcgi?artid=3022347&tool=pmcentrez&rendertype=abstract [Accessed November 15, 2013].

Hall D a, Johnsrude IS, Haggard MP, Palmer AR, Akeroyd M a, Summerfield a Q (2002) Spectral and temporal processing in human auditory cortex. Cereb Cortex 12:140–149 Available at: http://www.ncbi.nlm.nih.gov/pubmed/11739262.

Hall DA, Haggard MP, Akeroyd MA, Palmer AR, Summerfield AQ, Elliott MR, Gurney EM, Bowtell RW (1999) “Sparse” temporal sampling in auditory fMRI. Hum Brain Mapp 7:213–223 Available at: http://www.ncbi.nlm.nih.gov/pubmed/10194620 [Accessed June 14, 2014].

Han F, Caporale N, Dan Y (2008) Reverberation of Recent Visual Experience in Spontaneous Cortical Waves. Neuron 60:321–327 Available at: http://dx.doi.org/10.1016/j.neuron.2008.08.026.

Harris KD (2005) Neural signatures of cell assembly organization. Nat Rev Neurosci 6:399–407.

Harris KD, Bartho P, Chadderton P, Curto C, de la Rocha J, Hollender L, Itskov V, Luczak A, Marguet SL, Renart A, Sakata S (2011) How do neurons work together? Lessons from auditory cortex. Hear Res 271:37–53 Available at: http://dx.doi.org/10.1016/j.heares.2010.06.006.

Harris KD, Mrsic-Flogel TD (2013) Cortical connectivity and sensory coding. Nature 503:51–58 Available at: http://dx.doi.org/10.1038/nature12654.

Hart HC, Palmer AR, Hall DA (2003) Amplitude and frequency-modulated stimuli activate common regions of human auditory cortex. Cereb Cortex 13:773–781.

Hartmann C, Lazar A, Nessler B, Triesch J (2015) Where’s the Noise? Key Features of Spontaneous Activity and Neural Variability Arise through Learning in a Deterministic Network. PLoS Comput Biol 11:1–35.

Harvey BM, Dumoulin SO (2011) The relationship between cortical magnification factor and population receptive field size in human visual cortex: constancies in cortical architecture. J Neurosci 31:13604–13612 Available at: http://www.ncbi.nlm.nih.gov/pubmed/21940451 [Accessed November 14, 2013].

Hashikawa T, Molinari M, Rausell E, Jones EG (1995) Patchy and laminar terminations of medial geniculate axons in monkey auditory cortex. J Comp Neurol 362:195–208 Available at: http://www.ncbi.nlm.nih.gov/pubmed/8576433 [Accessed May 15, 2013].

Haxby J V, Gobbini MI, Furey ML, Ishai A, Schouten JL, Pietrini P (2001) Distributed and overlapping representations of faces and objects in ventral temporal cortex. Science (80-) 293:2425–2430.

Haynes J-D, Rees G (2005) Predicting the orientation of invisible stimuli from activity in human primary visual cortex. Nat Neurosci 8:686–691 Available at: http://www.nature.com/neuro/journal/v8/n5/full/nn1445.html%5Cnfiles/850/NatNeurosci-Haynes-Rees-2005-Predicting_the_orientation_of_invisible_stimuli_from_activity_in_human_primary_visual_cortex.pdf.

He BJ (2013) Spontaneous and task-evoked brain activity negatively interact. J Neurosci 33:4672–4682 Available at: http://www.pubmedcentral.nih.gov/articlerender.fcgi?artid=3637953&tool=pmcentr

ez&rendertype=abstract [Accessed October 22, 2013].

Hebb DO (1949) The Organization of Behavior. Organ Behav 911:335.

Heeger DJ, Ress D (2002) What does fMRI tell us about neuronal activity? Nat Rev Neurosci 3:142–151 Available at: http://www.ncbi.nlm.nih.gov/pubmed/11836522 [Accessed April 11, 2011].

Heinzle J, Kahnt T, Haynes J-D (2011) Topographically specific functional connectivity between visual field maps in the human brain. Neuroimage 56:1426–1436 Available at: http://www.ncbi.nlm.nih.gov/pubmed/21376818 [Accessed August 25, 2014].

Hesselmann G, Kell CA, Eger E, Kleinschmidt A (2008a) Spontaneous local variations in ongoing neural activity bias perceptual decisions. Proc Natl Acad Sci U S A 105:10984–10989 Available at: http://www.pnas.org/content/105/31/10984.abstract?ijkey=d12ef1f42d4837cf836ac5296af8e529802af0f4&keytype2=tf_ipsecsha.

Hesselmann G, Kell CA, Kleinschmidt A (2008b) Ongoing activity fluctuations in hMT+ bias the perception of coherent visual motion. J Neurosci 28:14481–14485.

Hesselmann G, Sadaghiani S, Friston KJ, Kleinschmidt A (2010) Predictive coding or evidence accumulation? False inference and neuronal fluctuations. PLoS One 5:1–5.

Honey CJ, Sporns O, Cammoun L, Gigandet X, Thiran JP, Meuli R, Hagmann P (2009) Predicting human resting-state functional connectivity from structural connectivity. Proc Natl Acad Sci U S A 106:2035–2040 Available at: http://www.pubmedcentral.nih.gov/articlerender.fcgi?artid=2634800&tool=pmcentrez&rendertype=abstract [Accessed July 13, 2010].

Howard MA, Volkov IO, Abbas PJ, Damasio H, Ollendieck MC, Granner MA (1996) A chronic microelectrode investigation of the tonotopic organization of human auditory cortex. Brain Res 724:260–264 Available at: http://www.ncbi.nlm.nih.gov/pubmed/8828578 [Accessed December 2, 2013].

Hu S, Olulade O, Castillo JG, Santos J, Kim S, Tamer GG, Luh W-M, Talavage TM (2010) Modeling hemodynamic responses in auditory cortex at 1.5 T using variable duration imaging acoustic noise. Neuroimage 49:3027–3038 Available at: http://www.pubmedcentral.nih.gov/articlerender.fcgi?artid=2818577&tool=pmcentrez&rendertype=abstract [Accessed June 14, 2014].

Hubel DH, Wiesel TN (1974) Uniformity of monkey striate cortex: a parallel relationship between field size, scatter, and magnification factor. J Comp Neurol 158:295–305 Available at: http://www.ncbi.nlm.nih.gov/pubmed/4436457 [Accessed November 30, 2013].

Humphries C, Liebenthal E, Binder JR (2010) Tonotopic organization of human auditory cortex. Neuroimage 50:1202–1211 Available at: http://www.pubmedcentral.nih.gov/articlerender.fcgi?artid=2830355&tool=pmcentrez&rendertype=abstract [Accessed March 20, 2012].

Hutchison RM, Womelsdorf T, Allen EA, Bandettini PA, Calhoun VD, Corbetta M, Della S, Duyn JH, Glover GH, Gonzalez-castillo J, Handwerker DA, Keilholz S, Kiviniemi V, Leopold DA, Pasquale F De, Sporns O, Walter M, Chang C (2013) NeuroImage Dynamic functional connectivity : Promise , issues , and interpretations. 80:360–378.

Hyde KL, Peretz I, Zatorre RJ (2008) Evidence for the role of the right auditory cortex in fine pitch resolution. Neuropsychologia 46:632–639 Available at: http://www.ncbi.nlm.nih.gov/pubmed/17959204 [Accessed December 1, 2013].

Jamison HL, Watkins KE, Bishop DVM, Matthews PM (2006) Hemispheric specialization for processing auditory nonspeech stimuli. Cereb Cortex 16:1266–1275 Available at: http://www.ncbi.nlm.nih.gov/pubmed/16280465 [Accessed November 11, 2013].

Jbabdi S, Sotiropoulos SN, Behrens TE (2013) The topographic connectome. Curr Opin Neurobiol 23:207–215 Available at: http://www.ncbi.nlm.nih.gov/pubmed/23298689 [Accessed March 3, 2013].

Jeanne JM, Sharpee TO, Gentner TQ (2013) Associative learning enhances population coding by inverting interneuronal correlation patterns. Neuron 78:352–363 Available at: http://dx.doi.org/10.1016/j.neuron.2013.02.023.

Jermakowicz WJ, Chen X, Khaytin I, Bonds AB, Casagrande VA (2009) Relationship Between Spontaneous and Evoked Spike-Time Correlations in Primate Visual Cortex. J Neurophysiol 101:2279–2289.

Ji D, Wilson MA (2007) Coordinated memory replay in the visual cortex and hippocampus during sleep. Nat Neurosci 10:100–107 Available at: http://www.ncbi.nlm.nih.gov/pubmed/17173043 [Accessed March 18, 2013].

Jo HJ, Saad ZS, Simmons WK, Milbury LA, Cox RW (2010) Mapping sources of correlation in resting state FMRI, with artifact detection and removal. Neuroimage 52:571–582.

Johnston JM, Vaishnavi SN, Smyth MD, Zhang D, He BJ, Zempel JM, Shimony JS, Snyder AZ, Raichle ME (2008) Loss of resting interhemispheric functional connectivity after complete section of the corpus callosum. J Neurosci 28:6453–6458 Available at: http://www.ncbi.nlm.nih.gov/pubmed/18562616.

Kaas JH, Hackett TA (2000) Subdivisions of auditory cortex and processing streams in primates. Proc Natl Acad Sci U S A 97:11793–11799 Available at: http://www.pubmedcentral.nih.gov/articlerender.fcgi?artid=34351&tool=pmcentrez&rendertype=abstract [Accessed October 20, 2013].

Kaas JH, Hackett TA, Tramo MJ (1999) Auditory processing in primate cerebral cortex. Curr Opin Neurobiol 9:164–170 Available at: http://www.ncbi.nlm.nih.gov/pubmed/10322185 [Accessed December 1, 2013].

Kahnt T, Chang LJ, Park SQ, Heinzle J, Haynes J-D (2012) Connectivity-based parcellation of the human orbitofrontal cortex. J Neurosci 32:6240–6250 Available

at: http://www.ncbi.nlm.nih.gov/pubmed/22553030 [Accessed May 7, 2014].

Kamitani Y, Tong F (2005) Decoding the visual and subjective contents of the human brain. Nat Neurosci 8:679–685 Available at: http://www.nature.com/neuro/journal/v8/n5/full/nn1444.html%5Cnfiles/849/NatNeurosci-Kamitani-Tong-2005-Decoding_the_visual_and_subjective_contents_of_the_human_brain.pdf.

Kay KN, Naselaris T, Prenger RJ, Gallant JL (2008) Identifying natural images from human brain activity. Supplementary information. Nature 452:1–40 Available at: http://www.nature.com/nature/journal/v452/n7185/full/nature06713.html [Accessed September 19, 2013].

Kenet T, Bibitchkov D, Tsodyks M, Grinvald A, Arieli A (2003) Spontaneously emerging cortical representations of visual attributes. Nature 425:954–956 Available at: http://www.ncbi.nlm.nih.gov/pubmed/14586468 [Accessed May 10, 2013].

Kennedy H, Dehay C, Bullier J (1986) Organization of the callosal connections of visual areas V1 and V2 in the macaque monkey. J Comp Neurol 247:398–415 Available at: http://www.ncbi.nlm.nih.gov/pubmed/3088065.

Kiefer M, Ansorge U, Haynes JD, Hamker F, Mattler U, Verleger R, Niedeggen M (2011) Neuro-cognitive mechanisms of conscious and unconscious visual perception: From a plethora of phenomena to general principles. Adv Cogn Psychol 7:55–67.

Kim J-H, Lee J-M, Jo HJ, Kim SH, Lee JH, Kim ST, Seo SW, Cox RW, Na DL, Kim SI, Saad ZS (2010) Defining functional SMA and pre-SMA subregions in human MFC using resting state fMRI: functional connectivity-based parcellation method. Neuroimage 49:2375–2386 Available at: http://www.pubmedcentral.nih.gov/articlerender.fcgi?artid=2819173&tool=pmcentrez&rendertype=abstract [Accessed July 4, 2011].

Kimura A, Donishi T, Sakoda T, Hazama M, Tamai Y (2003) Auditory thalamic nuclei projections to the temporal cortex in the rat. Neuroscience 117:1003–1016 Available at: http://www.ncbi.nlm.nih.gov/pubmed/12654352 [Accessed May 15, 2013].

Klein DJ, Depireux D a, Simon JZ, Shamma S a (2000) Robust spectrotemporal reverse correlation for the auditory system: optimizing stimulus design. J Comput Neurosci 9:85–111 Available at: http://www.ncbi.nlm.nih.gov/pubmed/10946994.

Koechlin E, Anton JL, Burnod Y (1999) Bayesian inference in populations of cortical neurons: a model of motion integration and segmentation in area MT [In Process Citation]. Biol Cybern 80:25–44.

Kohn A, Coen-cagli R, Kanitscheider I, Pouget A (2016) Correlations and Neuronal Population Information. Annu Rev Neurosci 39:237–256.

Kohn A, Smith MA (2005) Stimulus dependence of neuronal correlation in primary visual cortex of the macaque. J Neurosci 25:3661–3673 Available at: http://www.ncbi.nlm.nih.gov/pubmed/15814797 [Accessed July 4, 2014].

Kohn A, Zandvakili A, Smith MA (2009) Correlations and brain states: from electrophysiology to functional imaging. Curr Opin Neurobiol 19:434–438 Available at: http://www.pubmedcentral.nih.gov/articlerender.fcgi?artid=2889912&tool=pmcentrez&rendertype=abstract [Accessed March 7, 2013].

Kowalski N, Depireux DA, Shamma SA (1996a) Analysis of dynamic spectra in ferret primary auditory cortex. I. Characteristics of single-unit responses to moving ripple spectra. J Neurophysiol 76:3503–3523 Available at: http://www.ncbi.nlm.nih.gov/pubmed/8930289 [Accessed December 16, 2012].

Kowalski N, Depireux DA, Shamma SA (1996b) Analysis of dynamic spectra in ferret primary auditory cortex. II. Prediction of unit responses to arbitrary dynamic spectra. J Neurophysiol 76:3524–3534 Available at: http://jn.physiology.org/content/jn/76/5/3524.full.pdf [Accessed November 3, 2014].

Kriegeskorte N (2011) Pattern-information analysis: from stimulus decoding to computational-model testing. Neuroimage 56:411–421 Available at: http://www.ncbi.nlm.nih.gov/pubmed/21281719 [Accessed October 4, 2013].

Kriegeskorte N, Bandettini P (2007) Analyzing for information, not activation, to exploit high-resolution fMRI. Neuroimage 38:649–662 Available at: http://www.pubmedcentral.nih.gov/articlerender.fcgi?artid=2099257&tool=pmcentrez&rendertype=abstract [Accessed September 19, 2013].

Kumano H, Uka T (2010) The spatial profile of macaque MT neurons is consistent with Gaussian sampling of logarithmically coordinated visual representation. J Neurophysiol 104:61–75 Available at: http://www.ncbi.nlm.nih.gov/pubmed/20445031 [Accessed November 30, 2013].

Kumar S, Stephan KE, Warren JD, Friston KJ, Griffiths TD (2007) Hierarchical processing of auditory objects in humans. PLoS Comput Biol 3:e100 Available at: http://www.pubmedcentral.nih.gov/articlerender.fcgi?artid=1885275&tool=pmcentrez&rendertype=abstract [Accessed December 1, 2013].

Langers DRM, Backes WH, van Dijk P (2007) Representation of lateralization and tonotopy in primary versus secondary human auditory cortex. Neuroimage 34:264–273 Available at: http://www.ncbi.nlm.nih.gov/pubmed/17049275 [Accessed October 6, 2012].

Langers DRM, Backes WH, Van Dijk P (2003) Spectrotemporal features of the auditory cortex: The activation in response to dynamic ripples. Neuroimage 20:265–275.

Langers DRM, van Dijk P (2012) Mapping the tonotopic organization in human auditory cortex with minimally salient acoustic stimulation. Cereb Cortex 22:2024–2038 Available at: http://www.pubmedcentral.nih.gov/articlerender.fcgi?artid=3412441&tool=pmcentrez&rendertype=abstract [Accessed February 13, 2013].

Langner G, Dinse HR, Godde B (2009) A map of periodicity orthogonal to frequency

representation in the cat auditory cortex. Front Integr Neurosci 3:27.

Latham PE, Nirenberg S (2005) Synergy, redundancy, and independence in population codes, revisited. J Neurosci 25:5195–5206 Available at: http://www.ncbi.nlm.nih.gov/pubmed/15917459 [Accessed September 19, 2013].

Laudanski J, Edeline J-M, Huetz C (2012) Differences between spectro-temporal receptive fields derived from artificial and natural stimuli in the auditory cortex. PLoS One 7:e50539 Available at: http://www.pubmedcentral.nih.gov/articlerender.fcgi?artid=3507792&tool=pmcentrez&rendertype=abstract [Accessed September 17, 2014].

Laufs H, Krakow K, Sterzer P, Eger E, Beyerle A, Salek-Haddadi A, Kleinschmidt A (2003) Electroencephalographic signatures of attentional and cognitive default modes in spontaneous brain activity fluctuations at rest. Proc Natl Acad Sci 100:11053–11058 Available at: http://www.ncbi.nlm.nih.gov/pubmed/12958209.

Lauter JL, Herscovitch P, Formby C, Raichle ME (1985) Tonotopic organization in human auditory cortex revealed by positron emission tomography. Hear Res 20:199–205 Available at: http://www.ncbi.nlm.nih.gov/pubmed/3878839 [Accessed December 2, 2013].

Ledoit O, Wolf M (2004) Honey, I Shrunk the Sample Covariance Matrix. J Portf Manag 30:110–119 Available at: http://www.iijournals.com/doi/abs/10.3905/jpm.2004.110.

Lee CC, Imaizumi K, Schreiner CE, Winer JA (2004a) Concurrent tonotopic processing streams in auditory cortex. Cereb Cortex 14:441–451 Available at: http://www.cercor.oupjournals.org/cgi/doi/10.1093/cercor/bhh006 [Accessed April 3, 2012].

Lee CC, Schreiner CE, Imaizumi K, Winer JA (2004b) Tonotopic and heterotopic projection systems in physiologically defined auditory cortex. Neuroscience 128:871–887 Available at: http://www.ncbi.nlm.nih.gov/pubmed/15464293 [Accessed May 15, 2013].

Lee CC, Winer JA (2008) Connections of cat auditory cortex: III. Corticocortical system. J Comp Neurol 507:1920–1943 Available at: http://www.pubmedcentral.nih.gov/articlerender.fcgi?artid=2678022&tool=pmcentrez&rendertype=abstract [Accessed March 21, 2014].

Lee CC, Winer JA (2011) Convergence of thalamic and cortical pathways in cat auditory cortex. Hear Res 274:85–94 Available at: http://www.pubmedcentral.nih.gov/articlerender.fcgi?artid=2965817&tool=pmcentrez&rendertype=abstract [Accessed November 13, 2013].

Lee D, Port NL, Kruse W, Georgopoulos AP (1998) Variability and correlated noise in the discharge of neurons in motor and parietal areas of the primate cortex. J Neurosci 18:1161–1170 Available at: http://www.ncbi.nlm.nih.gov/pubmed/9437036 [Accessed May 15, 2013].

Lehky SR, Sejnowski TJ (1988) Network model of shape-from-shading: neural function

arises from both receptive and projective fields. Nature 333:452–454.

Leopold DA, Maier A (2012) Ongoing physiological processes in the cerebral cortex. Neuroimage 62:2190–2200 Available at: http://www.ncbi.nlm.nih.gov/pubmed/22040739 [Accessed May 30, 2014].

Leopold DA, Murayama Y, Logothetis NK (2003) Very slow activity fluctuations in monkey visual cortex: implications for functional brain imaging. Cereb Cortex 13:422–433 Available at: http://www.ncbi.nlm.nih.gov/pubmed/12631571.

Lin IC, Okun M, Carandini M, Harris KD (2015) The Nature of Shared Cortical Variability. Neuron 87:645–657 Available at: http://dx.doi.org/10.1016/j.neuron.2015.06.035.

Liu X, Duyn JH (2013) Time-varying functional network information extracted from brief instances of spontaneous brain activity. Proc Natl Acad Sci U S A 110:4392–4397 Available at: http://www.pubmedcentral.nih.gov/articlerender.fcgi?artid=3600481&tool=pmcentrez&rendertype=abstract.

Logothetis NK, Pauls J, Augath M, Trinath T, Oeltermann A (2001) Neurophysiological investigation of the basis of the fMRI signal. Nature 412:150–157 Available at: http://www.ncbi.nlm.nih.gov/pubmed/11449264.

Lowe MJ, Mock BJ, Sorenson JA (1998) Functional Connectivity in Single and Multislice Echoplanar Imaging Using Resting-State Fluctuations. Neuroimage 7:119–132 Available at: http://www.sciencedirect.com/science/article/pii/S1053811997903153%5Cnhttp://www.sciencedirect.com/science/article/pii/S1053811997903153/pdf?md5=2fcc7183f9cd46e75aefeb6132f309de&pid=1-s2.0-S1053811997903153-main.pdf.

Löwel S, Singer W (1992) Selection of intrinsic horizontal connections in the visual cortex by correlated neuronal activity. Science (80-) 255:209–212 Available at: http://www.ncbi.nlm.nih.gov/entrez/query.fcgi?cmd=Retrieve&db=PubMed&dopt=Citation&list_uids=1372754%5Cnhttp://www.sciencemag.org/content/255/5041/209.short.

Luczak A, Bartho P, Harris KD (2013) Gating of Sensory Input by Spontaneous Cortical Activity. J Neurosci 33:1684–1695 Available at: http://www.jneurosci.org/content/33/4/1684.

Luczak A, Barthó P, Harris KD (2009) Spontaneous events outline the realm of possible sensory responses in neocortical populations. Neuron 62:413–425 Available at: http://dx.doi.org/10.1016/j.neuron.2009.03.014.

Luczak A, McNaughton BL, Harris KD (2015) Packet-based communication in the cortex. Nat Rev Neurosci 16:745–755 Available at: http://www.nature.com/nrn/journal/v16/n12/abs/nrn4026.html?lang=en?WT.ec_id=NRN-201512&spMailingID=50065588&spUserID=ODIyMzAzNzA3NwS2&spJobID=80

2749223&spReportId=ODAyNzQ5MjIzS0.

Machens CK, Wehr MS, Zador AM (2004) Linearity of cortical receptive fields measured with natural sounds. J Neurosci 24:1089–1100 Available at: http://www.ncbi.nlm.nih.gov/pubmed/14762127 [Accessed September 28, 2013].

McMullen NT, de Venecia RK (1993) Thalamocortical patches in auditory neocortex. Brain Res 620:317–322 Available at: http://www.ncbi.nlm.nih.gov/pubmed/7690303 [Accessed December 3, 2013].

Merzenich MM, Brugge JF (1973) Representation of the cochlear partition of the superior temporal plane of the macaque monkey. Brain Res 50:275–296 Available at: http://linkinghub.elsevier.com/retrieve/pii/0006899373907312 [Accessed June 15, 2014].

Miller J-EK, Ayzenshtat I, Carrillo-Reid L, Yuste R (2014) Visual stimuli recruit intrinsically generated cortical ensembles. Proc Natl Acad Sci 111:E4053-61 Available at: http://www.pnas.org/cgi/doi/10.1073/pnas.1406077111%5Cnpapers3://publication/doi/10.1073/pnas.1406077111.

Miller LM, Escabí MA, Read HL, Schreiner CE (2001) Functional convergence of response properties in the auditory thalamocortical system. Neuron 32:151–160 Available at: http://www.ncbi.nlm.nih.gov/pubmed/11604146 [Accessed December 3, 2013].

Mitchell JF, Sundberg KA, Reynolds JH (2009) Spatial Attention Decorrelates Intrinsic Activity Fluctuations in Macaque Area V4. Neuron 63:879–888 Available at: http://dx.doi.org/10.1016/j.neuron.2009.09.013.

Moerel M, De Martino F, Formisano E (2012) Processing of natural sounds in human auditory cortex: tonotopy, spectral tuning, and relation to voice sensitivity. J Neurosci 32:14205–14216 Available at: http://www.ncbi.nlm.nih.gov/pubmed/23055490 [Accessed September 12, 2013].

Moerel M, De Martino F, Formisano E (2014) An anatomical and functional topography of human auditory cortical areas. Front Neurosci 8:1–14.

Moerel M, De Martino F, Santoro R, Ugurbil K, Goebel R, Yacoub E, Formisano E (2013) Processing of natural sounds: characterization of multipeak spectral tuning in human auditory cortex. J Neurosci 33:11888–11898 Available at: http://www.ncbi.nlm.nih.gov/pubmed/23864678 [Accessed September 12, 2013].

Moerel M, De Martino F, Uğurbil K, Yacoub E, Formisano E (2015) Processing of frequency and location in human subcortical auditory structures. Sci Rep 5:17048 Available at: http://www.nature.com/srep/2015/151124/srep17048/full/srep17048.html.

Monto S, Palva S, Voipio J, Palva JM (2008) Very slow EEG fluctuations predict the dynamics of stimulus detection and oscillation amplitudes in humans. J Neurosci 28:8268–8272 Available at: http://www.ncbi.nlm.nih.gov/pubmed/18701689

[Accessed March 5, 2013].

Moore BCJ (2003) An Introduction to the Psychology of Hearing.

Moore BCJ, Glasberg BR (1996) A Revision of Zwicker's Loudness Model. Acta Acust united with Acust 82:335–345.

Morel A, Garraghty PE, Kaas JH (1993) Tonotopic organization, architectonic fields, and connections of auditory cortex in macaque monkeys. J Comp Neurol 335:437–459 Available at: http://www.ncbi.nlm.nih.gov/pubmed/7693772 [Accessed May 15, 2013].

Moreno-Bote R, Beck J, Kanitscheider I, Pitkow X, Latham P, Pouget A (2014) Information-limiting correlations. Nat Neurosci 17:1410–1417 Available at: http://www.nature.com/doifinder/10.1038/nn.3807 [Accessed September 8, 2014].

Morosan P, Rademacher J, Schleicher A, Amunts K, Schormann T, Zilles K (2001) Human primary auditory cortex: cytoarchitectonic subdivisions and mapping into a spatial reference system. Neuroimage 13:684–701 Available at: http://www.ncbi.nlm.nih.gov/pubmed/11305897 [Accessed December 4, 2013].

Motter BC (2009) Central V4 receptive fields are scaled by the V1 cortical magnification and correspond to a constant-sized sampling of the V1 surface. J Neurosci 29:5749–5757 Available at: http://www.pubmedcentral.nih.gov/articlerender.fcgi?artid=2694050&tool=pmcentrez&rendertype=abstract [Accessed November 11, 2013].

Mumford JA, Turner BO, Ashby FG, Poldrack RA (2012) Deconvolving BOLD activation in event-related designs for multivoxel pattern classification analyses. Neuroimage 59:2636–2643 Available at: http://dx.doi.org/10.1016/j.neuroimage.2011.08.076.

Murphy K, Birn RM, Handwerker DA, Jones TB, Bandettini PA (2009) The impact of global signal regression on resting state correlations: Are anti-correlated networks introduced? Neuroimage 44:893–905.

Naselaris T, Kay KN, Nishimoto S, Gallant JL (2011) Encoding and decoding in fMRI. Neuroimage 56:400–410 Available at: http://www.pubmedcentral.nih.gov/articlerender.fcgi?artid=3037423&tool=pmcentrez&rendertype=abstract [Accessed February 28, 2013].

Naselaris T, Prenger RJ, Kay KN, Oliver M, Gallant JL (2009) Bayesian reconstruction of natural images from human brain activity. Neuron 63:902–915 Available at: http://www.ncbi.nlm.nih.gov/pubmed/19778517 [Accessed October 30, 2013].

Nauhaus I, Busse L, Carandini M, Ringach DL (2009) Stimulus contrast modulates functional connectivity in visual cortex. Nat Neurosci 12:70–76 Available at: http://www.pubmedcentral.nih.gov/articlerender.fcgi?artid=2610236&tool=pmcentrez&rendertype=abstract [Accessed October 6, 2012].

Nauhaus I, Busse L, Ringach DL, Carandini M (2012) Robustness of traveling waves in

ongoing activity of visual cortex. J Neurosci 32:3088–3094 Available at: http://discovery.ucl.ac.uk/1343120/.

Nir Y, Mukamel R, Dinstein I, Privman E, Harel M, Fisch L, Gelbard-Sagiv H, Kipervasser S, Andelman F, Neufeld MY, Kramer U, Arieli A, Fried I, Malach R (2008) Interhemispheric correlations of slow spontaneous neuronal fluctuations revealed in human sensory cortex. Nat Neurosci 11:1100–1108 Available at: http://www.nature.com/doifinder/10.1038/nn.2177 [Accessed November 14, 2013].

Nirenberg S, Latham PE (2003) Decoding neuronal spike trains: how important are correlations? Proc Natl Acad Sci U S A 100:7348–7353 Available at: http://www.pubmedcentral.nih.gov/articlerender.fcgi?artid=165878&tool=pmcentrez&rendertype=abstract.

Olman C, Ronen I, Ugurbil K, Kim D-S (2003) Retinotopic mapping in cat visual cortex using high-field functional magnetic resonance imaging. J Neurosci Methods 131:161–170 Available at: http://www.ncbi.nlm.nih.gov/pubmed/14659836 [Accessed April 11, 2011].

Olulade O, Hu S, Gonzalez-Castillo J, Tamer GG, Luh W-M, Ulmer JL, Talavage TM (2011) Assessment of temporal state-dependent interactions between auditory fMRI responses to desired and undesired acoustic sources. Hear Res 277:67–77 Available at: http://www.pubmedcentral.nih.gov/articlerender.fcgi?artid=3137738&tool=pmcentrez&rendertype=abstract [Accessed June 10, 2014].

Overath T, Kumar S, von Kriegstein K, Griffiths TD (2008) Encoding of spectral correlation over time in auditory cortex. J Neurosci 28:13268–13273.

Overath T, Zhang Y, Sanes DH, Poeppel D (2012) Sensitivity to temporal modulation rate and spectral bandwidth in the human auditory system: fMRI evidence. J Neurophysiol 107:2042–2056 Available at: http://www.ncbi.nlm.nih.gov/pubmed/22298830%5Cnhttp://www.pubmedcentral.nih.gov/articlerender.fcgi?artid=PMC3331610.

Page EB (1963) Ordered Hypotheses for Multiple Treatments: A Significance Test for Linear Ranks. J Am Stat Assoc 58:216–230 Available at: http://www.tandfonline.com/doi/abs/10.1080/01621459.1963.10500843 [Accessed September 10, 2013].

Park SH, Cha K, Lee S-H (2013) Coaxial anisotropy of cortical point spread in human visual areas. J Neurosci 33:1143–56a Available at: http://www.ncbi.nlm.nih.gov/pubmed/23325251 [Accessed March 4, 2013].

Parkes LM, Schwarzbach J V, Bouts AA, Deckers RHR, Pullens P, Kerskens CM, Norris DG (2005) Quantifying the spatial resolution of the gradient echo and spin echo BOLD response at 3 Tesla. Magn Reson Med 54:1465–1472 Available at: http://www.ncbi.nlm.nih.gov/pubmed/16276507 [Accessed May 15, 2013].

Patterson RD, Uppenkamp S, Johnsrude IS, Griffiths TD (2002) The processing of

temporal pitch and melody information in auditory cortex. Neuron 36:767–776.

Perkel DH, Gerstein GL, Moore GP (1967a) Neuronal Spike Trains and Stochastic Point Processes: I. The Single Spike Train. Biophys J 7:391–418 Available at: http://dx.doi.org/10.1016/S0006-3495(67)86596-2.

Perkel DH, Gerstein GL, Moore GP (1967b) Neuronal Spike Trains and Stochastic Point Processes: II. Simultaneous Spike Trains. Biophys J 7:419–440 Available at: http://dx.doi.org/10.1016/S0006-3495(67)86597-4.

Pesaran B (2010) Neural correlations, decisions, and actions. Curr Opin Neurobiol 20:166–171 Available at: http://www.pubmedcentral.nih.gov/articlerender.fcgi?artid=2862782&tool=pmcentrez&rendertype=abstract [Accessed December 2, 2013].

Petersen RS, Panzeri S, Diamond ME (2001) Population coding of stimulus location in rat somatosensory cortex. Neuron 32:503–514.

Petkov CI, Kayser C, Augath M, Logothetis NK (2006) Functional imaging reveals numerous fields in the monkey auditory cortex. PLoS Biol 4:e215 Available at: http://www.pubmedcentral.nih.gov/articlerender.fcgi?artid=1479693&tool=pmcentrez&rendertype=abstract [Accessed October 5, 2012].

Peyrache A, Lacroix MM, Petersen PC, Buzsáki G (2015) Internally organized mechanisms of the head direction sense. Nat Neurosci 18:569–575 Available at: http://dx.doi.org/10.1038/nn.3968.

Phillips CG, Zeki S, Barlow HB (1984) Localization of function in the cerebral cortex. Past, present and future. Brain 107:327–361 Available at: http://www.ncbi.nlm.nih.gov/pubmed/6421455 [Accessed May 15, 2013].

Pickles JO (2015) Auditory pathways: Anatomy and physiology. Handb Clin Neurol 129:3–25.

Pillow JW, Shlens J, Paninski L, Sher A, Litke AM, Chichilnisky EJ, Simoncelli EP (2008) Spatio-temporal correlations and visual signalling in a complete neuronal population. Nature 454:995–999 Available at: http://www.pubmedcentral.nih.gov/articlerender.fcgi?artid=2684455&tool=pmcentrez&rendertype=abstract [Accessed September 18, 2013].

Ponce-Alvarez A, Thiele A, Albright TD, Stoner GR, Deco G (2013) Stimulus-dependent variability and noise correlations in cortical MT neurons. Proc Natl Acad Sci U S A 110:13162–13167 Available at: http://www.pnas.org/cgi/doi/10.1073/pnas.1300098110%5Cnpapers3://publication/doi/10.1073/pnas.1300098110.

Pouget A, Beck JM, Ma WJ, Latham PE (2013) Probabilistic brains: knowns and unknowns. Nat Neurosci 16:1170–1178 Available at: http://www.ncbi.nlm.nih.gov/pubmed/23955561.

Pouget A, Dayan P, Zemel R (2000) Information processing with population codes. Nat

Rev Neurosci 1:125–132 Available at: http://www.ncbi.nlm.nih.gov/pubmed/11252775.

Quian Quiroga R, Kreiman G (2010) Postscript: About grandmother cells and Jennifer Aniston neurons. Psychol Rev 117:297–299.

Rademacher J, Morosan P, Schormann T, Schleicher A, Werner C, Freund HJ, Zilles K (2001) Probabilistic mapping and volume measurement of human primary auditory cortex. Neuroimage 13:669–683 Available at: http://www.ncbi.nlm.nih.gov/pubmed/11305896 [Accessed December 4, 2013].

Raichle ME (2009) A paradigm shift in functional brain imaging. J Neurosci 29:12729–12734 Available at: http://www.ncbi.nlm.nih.gov/pubmed/19828783 [Accessed March 3, 2013].

Raichle ME (2010) Two views of brain function. Trends Cogn Sci 14:180–190 Available at: http://www.ncbi.nlm.nih.gov/pubmed/20206576 [Accessed February 28, 2013].

Raichle ME (2015) The restless brain: how intrinsic activity organizes brain function. Philos Trans R Soc B Biol Sci 370:20140172–20140172 Available at: http://rstb.royalsocietypublishing.org/cgi/doi/10.1098/rstb.2014.0172.

Raichle ME, MacLeod a M, Snyder a Z, Powers WJ, Gusnard D a, Shulman GL (2001) A default mode of brain function. Proc Natl Acad Sci U S A 98:676–682 Available at: http://www.pubmedcentral.nih.gov/articlerender.fcgi?artid=14647&tool=pmcentrez&rendertype=abstract.

Rauschecker JP (1998) Cortical processing of complex sounds. Curr Opin Neurobiol 8:516–521 Available at: http://linkinghub.elsevier.com/retrieve/pii/S0959438898800408 [Accessed December 1, 2013].

Rauschecker JP, Scott SK (2009) Maps and streams in the auditory cortex: nonhuman primates illuminate human speech processing. Nat Neurosci 12:718–724 Available at: http://www.pubmedcentral.nih.gov/articlerender.fcgi?artid=2846110&tool=pmcentrez&rendertype=abstract [Accessed March 1, 2012].

Rauschecker JP, Tian B, Hauser M (1995) Processing of complex sounds in the macaque nonprimary auditory cortex. Science 268:111–114 Available at: http://www.ncbi.nlm.nih.gov/pubmed/7701330 [Accessed December 4, 2013].

Rauschecker JP, Tian B, Pons T, Mishkin M (1997) Serial and parallel processing in rhesus monkey auditory cortex. J Comp Neurol 382:89–103 Available at: http://www.ncbi.nlm.nih.gov/pubmed/9136813 [Accessed March 21, 2014].

Read HL, Winer JA, Schreiner CE (2001) Modular organization of intrinsic connections associated with spectral tuning in cat auditory cortex. Proc Natl Acad Sci U S A 98:8042–8047 Available at: http://www.pubmedcentral.nih.gov/articlerender.fcgi?artid=35464&tool=pmcentrez

&rendertype=abstract [Accessed May 10, 2013].

Ringach DL (2009) Spontaneous and driven cortical activity: implications for computation. Curr Opin Neurobiol 19:439–444.

Romani GL, Williamson SJ, Kaufman L (1982) Tonotopic organization of the human auditory cortex. Science 216:1339–1340 Available at: http://www.ncbi.nlm.nih.gov/pubmed/7079770 [Accessed December 2, 2013].

Rombouts SARB, Stam CJ, Kuijer JPA, Scheltens P, Barkhof F (2003) Identifying confounds to increase specificity during a "no task condition": Evidence for hippocampal connectivity using fMRI. Neuroimage 20:1236–1245.

Rosazza C, Minati L (2011) Resting-state brain networks: Literature review and clinical applications. Neurol Sci 32:773–785.

Rosen S, Baker RJ (1994) Characterising auditory filter nonlinearity. Hear Res 73:231–243 Available at: http://www.ncbi.nlm.nih.gov/pubmed/8188552 [Accessed August 18, 2012].

Rothschild G, Nelken I, Mizrahi A (2010) Functional organization and population dynamics in the mouse primary auditory cortex. Nat Neurosci 13:353–360 Available at: http://www.ncbi.nlm.nih.gov/pubmed/20118927 [Accessed December 2, 2013].

Rouiller EM, Simm GM, Villa AE, de Ribaupierre Y, de Ribaupierre F (1991) Auditory corticocortical interconnections in the cat: evidence for parallel and hierarchical arrangement of the auditory cortical areas. Exp Brain Res 86:483–505 Available at: http://www.ncbi.nlm.nih.gov/pubmed/1722171 [Accessed May 8, 2013].

Rubinov M, Sporns O (2010) Complex network measures of brain connectivity: Uses and interpretations. Neuroimage 52:1059–1069 Available at: http://www.ncbi.nlm.nih.gov/pubmed/19819337 [Accessed July 14, 2010].

Saad ZS, Gotts SJ, Murphy K, Chen G, Jo HJ, Martin A, Cox RW (2012) Trouble at rest: how correlation patterns and group differences become distorted after global signal regression. Brain Connect 2:25–32 Available at: http://www.pubmedcentral.nih.gov/articlerender.fcgi?artid=3484684&tool=pmcentrez&rendertype=abstract.

Sadaghiani S, Hesselmann G, Friston KJ, Kleinschmidt A (2010) The relation of ongoing brain activity, evoked neural responses, and cognition. Front Syst Neurosci 4:20 Available at: http://www.frontiersin.org/systems_neuroscience/10.3389/fnsys.2010.00020/abstract%5Cnhttp://www.frontiersin.org/Journal/DownloadFile.ashx?pdf=1&FileId=21431&articleId=1424&Version=1&ContentTypeId=15&FileName=fnsys_2010_00020.pdf [Accessed July 14, 2014].

Sadaghiani S, Hesselmann G, Kleinschmidt A (2009) Distributed and Antagonistic Contributions of Ongoing Activity Fluctuations to Auditory Stimulus Detection. J Neurosci 29:13410–13417 Available at: http://www.jneurosci.org/cgi/doi/10.1523/JNEUROSCI.2592-09.2009.

Saenz M, Langers DRM (2014) Tonotopic mapping of human auditory cortex. Hear Res 307:42–52 Available at: http://www.ncbi.nlm.nih.gov/pubmed/23916753 [Accessed February 7, 2014].

Saitoh K, Inagaki S, Nishimura M, Kawaguchi H, Song W-J (2010) Spontaneous activity resembling tone-evoked activity in the primary auditory cortex of guinea pigs. Neurosci Res 68:107–113 Available at: http://www.ncbi.nlm.nih.gov/pubmed/20600374 [Accessed December 2, 2013].

Saka M, Berwick J, Jones M (2010) Linear superposition of sensory-evoked and ongoing cortical hemodynamics. Front Neuroenergetics 2:1–13 Available at: http://www.pubmedcentral.nih.gov/articlerender.fcgi?artid=2938927&tool=pmcentrez&rendertype=abstract [Accessed August 25, 2014].

Saka M, Berwick J, Jones M (2012) Inter-trial variability in sensory-evoked cortical hemodynamic responses: the role of the magnitude of pre-stimulus fluctuations. Front Neuroenergetics 4:10 Available at: http://www.ncbi.nlm.nih.gov/pubmed/23133415.

Sakata S, Harris KD (2009) Laminar Structure of Spontaneous and Sensory-Evoked Population Activity in Auditory Cortex. Neuron 64:404–418 Available at: http://dx.doi.org/10.1016/j.neuron.2009.09.020.

Salvador R, Suckling J, Coleman MR, Pickard JD, Menon D, Bullmore E (2005) Neurophysiological architecture of functional magnetic resonance images of human brain. Cereb Cortex 15:1332–1342 Available at: http://www.ncbi.nlm.nih.gov/pubmed/15635061.

Sanchez-Vives M V, McCormick DA (2000) Cellular and network mechanisms of rhythmic recurrent activity in neocortex. Nat Neurosci 3:1027–1034.

Santoro R, Moerel M, De Martino F, Goebel R, Ugurbil K, Yacoub E, Formisano E (2014) Encoding of natural sounds at multiple spectral and temporal resolutions in the human auditory cortex. PLoS Comput Biol 10:e1003412 Available at: http://www.ncbi.nlm.nih.gov/pubmed/24391486 [Accessed January 10, 2014].

Schneidman E (2016) Towards the design principles of neural population codes. Curr Opin Neurobiol 37:133–140 Available at: http://www.sciencedirect.com/science/article/pii/S0959438816300101.

Schneidman E, Berry MJMJ, Segev R, Bialek W (2006) Weak pairwise correlations imply strongly correlated network states in a neural population. Nature 440:1007–1012 Available at: http://www.pubmedcentral.nih.gov/articlerender.fcgi?artid=1785327&tool=pmcentrez&rendertype=abstract%5Cnhttp://www.nature.com/nature/journal/v440/n7087/abs/nature04701.html.

Schneidman E, Bialek W, Berry MJ (2003) Synergy, redundancy, and independence in population codes. J Neurosci 23:11539–11553 Available at: http://www.ncbi.nlm.nih.gov/pubmed/14684857.

Schölvinck ML, Friston KJ, Rees G (2012) The influence of spontaneous activity on stimulus processing in primary visual cortex. Neuroimage 59:2700–2708 Available at: http://dx.doi.org/10.1016/j.neuroimage.2011.10.066.

Schölvinck ML, Maier A, Ye FQ, Duyn JH, Leopold D a. (2010) Neural basis of global resting-state fMRI activity. Proc Natl Acad Sci U S A 107:10238–10243 Available at: http://www.ncbi.nlm.nih.gov/pubmed/20439733 [Accessed August 20, 2014].

Schönwiesner M, Dechent P, Voit D, Petkov CI, Krumbholz K (2014) Parcellation of Human and Monkey Core Auditory Cortex with fMRI Pattern Classification and Objective Detection of Tonotopic Gradient Reversals. Cereb Cortex:1–12 Available at: http://www.ncbi.nlm.nih.gov/pubmed/24904067 [Accessed August 25, 2014].

Schönwiesner M, Rübsamen R, von Cramon DY (2005) Hemispheric asymmetry for spectral and temporal processing in the human antero-lateral auditory belt cortex. Eur J Neurosci 22:1521–1528 Available at: http://onlinelibrary.wiley.com/doi/10.1111/j.1460-9568.2005.04315.x/full [Accessed November 21, 2013].

Schönwiesner M, Zatorre RJ (2009) Spectro-temporal modulation transfer function of single voxels in the human auditory cortex measured with high-resolution fMRI. Proc Natl Acad Sci U S A 106:14611–14616 Available at: http://www.pubmedcentral.nih.gov/articlerender.fcgi?artid=2732853&tool=pmcentrez&rendertype=abstract.

Serences JT, Saproo S (2012) Computational advances towards linking BOLD and behavior. Neuropsychologia 50:435–446 Available at: http://www.ncbi.nlm.nih.gov/pubmed/21840553 [Accessed February 28, 2013].

Shadlen MN, Newsome WT (1994) Noise, Neural Codes and Cortical Organization. Curr Opin Neurobiol 4:569–579.

Shadlen MN, Newsome WT (1998) The variable discharge of cortical neurons: implications for connectivity, computation, and information coding. J Neurosci 18:3870–3896 Available at: http://www.ncbi.nlm.nih.gov/pubmed/9570816.

Shamir M, Sompolinsky H (2004) Nonlinear population codes. Neural Comput 16:1105–1136.

Shamma SA, Fleshman JW, Wiser PR, Versnel H (1993) Organization of response areas in ferret primary auditory cortex. J Neurophysiol 69:367–383.

Shmuel A, Leopold D a (2008) Neuronal correlates of spontaneous fluctuations in fMRI signals in monkey visual cortex: Implications for functional connectivity at rest. Hum Brain Mapp 29:751–761 Available at: http://www.ncbi.nlm.nih.gov/pubmed/18465799 [Accessed July 20, 2011].

Singer W (1999) Neuronal synchrony: a versatile code for the definition of relations? Neuron 24:49–65, 111–125 Available at: http://www.ncbi.nlm.nih.gov/pubmed/10677026.

Singer W, Gray CM (1995) Visual feature integration and the temporal correlation hypothesis. Annu Rev Neurosci 18:555–586 Available at: http://www.ncbi.nlm.nih.gov/pubmed/7605074 [Accessed November 13, 2013].

Smith M a, Kohn A (2008) Spatial and temporal scales of neuronal correlation in primary visual cortex. J Neurosci 28:12591–12603 Available at: http://www.pubmedcentral.nih.gov/articlerender.fcgi?artid=2656500&tool=pmcentrez&rendertype=abstract [Accessed March 12, 2013].

Smith SM, Fox PT, Miller KL, Glahn DC, Fox PM, Mackay CE, Filippini N, Watkins KE, Toro R, Laird AR, Beckmann CF (2009) Correspondence of the brain's functional architecture during activation and rest. Proc Natl Acad Sci U S A 106:13040–13045 Available at: http://www.ncbi.nlm.nih.gov/pubmed/19620724.

Snodderly DM, Gur M (1995) Organization of striate cortex of alert, trained monkeys (Macaca fascicularis): ongoing activity, stimulus selectivity, and widths of receptive field activating regions. J Neurophysiol 74:2100–2125.

Song W-J, Kawaguchi H, Totoki S, Inoue Y, Katura T, Maeda S, Inagaki S, Shirasawa H, Nishimura M (2006) Cortical intrinsic circuits can support activity propagation through an isofrequency strip of the guinea pig primary auditory cortex. Cereb Cortex 16:718–729 Available at: http://www.cercor.oxfordjournals.org/cgi/doi/10.1093/cercor/bhj018.

Stevens WD, Spreng RN (2014) Resting-state functional connectivity MRI reveals active processes central to cognition. Wiley Interdiscip Rev Cogn Sci 5:233–245.

Stevenson IH, London BM, Oby ER, Sachs NA, Reimer J, Englitz B, David S V, Shamma SA, Blanche TJ, Mizuseki K, Zandvakili A, Hatsopoulos NG, Miller LE, Kording KP (2012) Functional connectivity and tuning curves in populations of simultaneously recorded neurons. PLoS Comput Biol 8:e1002775 Available at: http://www.pubmedcentral.nih.gov/articlerender.fcgi?artid=3499254&tool=pmcentrez&rendertype=abstract [Accessed May 15, 2013].

Striem-Amit E, Almeida J, Belledonne M, Chen Q, Fang Y, Han Z, Caramazza A, Bi Y (2016) Topographical functional connectivity patterns exist in the congenitally, prelingually deaf. Sci Rep 6:29375 Available at: http://www.nature.com/articles/srep29375.

Supèr H, van der Togt C, Spekreijse H, Lamme V a F (2003) Internal state of monkey primary visual cortex (V1) predicts figure-ground perception. J Neurosci 23:3407–3414.

Talavage TM, Sereno MI, Melcher JR, Ledden PJ, Rosen BR, Dale AM (2004) Tonotopic organization in human auditory cortex revealed by progressions of frequency sensitivity. J Neurophysiol 91:1282–1296 Available at: http://www.ncbi.nlm.nih.gov/pubmed/14614108 [Accessed April 2, 2012].

Theunissen FE, David S V, Singh NC, Hsu a, Vinje WE, Gallant JL (2001) Estimating spatio-temporal receptive fields of auditory and visual neurons from their responses

to natural stimuli. Network 12:289–316 Available at: http://www.ncbi.nlm.nih.gov/pubmed/11563531.

Theunissen FE, Elie JE (2014) Neural processing of natural sounds. Nat Rev Neurosci 15:355–366 Available at: http://www.ncbi.nlm.nih.gov/pubmed/24840800.

Theyel BB, Llano DA, Sherman SM (2010) The corticothalamocortical circuit drives higher-order cortex in the mouse. Nat Neurosci 13:84–88 Available at: http://www.nature.com/doifinder/10.1038/nn.2449.

Tsodyks M, Kenet T, Grinvald A, Arieli A (1999) Linking spontaneous activity of single cortical neurons and the underlying functional architecture. Science 286:1943–1946 Available at: http://www.ncbi.nlm.nih.gov/pubmed/10583955 [Accessed May 10, 2013].

Upadhyay J, Ducros M, Knaus T a, Lindgren K a, Silver A, Tager-Flusberg H, Kim D-S (2007) Function and connectivity in human primary auditory cortex: a combined fMRI and DTI study at 3 Tesla. Cereb Cortex 17:2420–2432 Available at: http://www.ncbi.nlm.nih.gov/pubmed/17190967 [Accessed March 14, 2012].

Upadhyay J, Silver A, Knaus T a, Lindgren K a, Ducros M, Kim D-S, Tager-Flusberg H (2008) Effective and structural connectivity in the human auditory cortex. J Neurosci 28:3341–3349 Available at: http://www.ncbi.nlm.nih.gov/pubmed/18367601 [Accessed March 1, 2012].

van den Heuvel MP, Hulshoff Pol HE (2009) Specific somatotopic organization of functional connections of the primary motor network during resting state. Hum Brain Mapp 644:NA-NA Available at: http://doi.wiley.com/10.1002/hbm.20893.

van den Heuvel MP, Hulshoff Pol HE (2010) Specific somatotopic organization of functional connections of the primary motor network during resting state. Hum Brain Mapp 31:631–644 Available at: http://www.ncbi.nlm.nih.gov/pubmed/19830684 [Accessed May 15, 2013].

Van Dijk KRA, Hedden T, Venkataraman A, Evans KC, Lazar SW, Buckner RL (2010) Intrinsic functional connectivity as a tool for human connectomics: theory, properties, and optimization. J Neurophysiol 103:297–321 Available at: http://jn.physiology.org/content/103/1/297.long [Accessed July 28, 2014].

Van Essen DC, Newsome WT, Bixby JL (1982) The pattern of interhemispheric connections and its relationship to extrastriate visual areas in the macaque monkey. J Neurosci 2:265–283 Available at: http://www.ncbi.nlm.nih.gov/pubmed/7062108.

Vincent JL, Patel GH, Fox MD, Snyder AZ, Baker JT, Van Essen DC, Zempel JM, Snyder LH, Corbetta M, Raichle ME (2007) Intrinsic functional architecture in the anaesthetized monkey brain. Nature 447:83–86 Available at: http://www.ncbi.nlm.nih.gov/pubmed/17476267.

Vincent JL, Snyder AZ, Fox MD, Shannon BJ, Andrews JR, Raichle ME, Buckner RL (2006) Coherent spontaneous activity identifies a hippocampal-parietal memory network. J Neurophysiol 96:3517–3531 Available at:

http://www.ncbi.nlm.nih.gov/pubmed/16899645.

Wessinger CM, Buonocore MH, Kussmaul CL, Mangun GR (1997) Tonotopy in human auditory cortex examined with functional magnetic resonance imaging. Hum Brain Mapp 5:18–25.

Wessinger CM, VanMeter J, Tian B, Van Lare J, Pekar J, Rauschecker JP (2001) Hierarchical organization of the human auditory cortex revealed by functional magnetic resonance imaging. J Cogn Neurosci 13:1–7 Available at: http://www.ncbi.nlm.nih.gov/pubmed/11224904.

Wilson M a, McNaughton BL (1994) Reactivation of hippocampal ensemble memories during sleep. Science 265:676–679 Available at: http://www.ncbi.nlm.nih.gov/pubmed/8036517.

Wu MC-K, David S V, Gallant JL (2006) Complete functional characterization of sensory neurons by system identification. Annu Rev Neurosci 29:477–505 Available at: http://www.ncbi.nlm.nih.gov/pubmed/16776594 [Accessed March 6, 2013].

Yacoub E, Harel N, Ugurbil K (2008) High-field fMRI unveils orientation columns in humans. Proc Natl Acad Sci U S A 105:10607–10612 Available at: http://www.pubmedcentral.nih.gov/articlerender.fcgi?artid=2492463&tool=pmcentrez&rendertype=abstract [Accessed May 15, 2013].

Young MP, Tanaka K, Yamane S (1992) On oscillating neuronal responses in the visual cortex of the monkey. J Neurophysiol 67:1464–1474 Available at: http://www.ncbi.nlm.nih.gov/pubmed/1629758 [Accessed December 2, 2013].

Yuste R, MacLean JN, Smith J, Lansner A (2005) The cortex as a central pattern generator. Nat Rev Neurosci 6:477–483 Available at: http://www.nature.com/doifinder/10.1038/nrn1686.

Zatorre RJ, Belin P (2001) Spectral and temporal processing in human auditory cortex. Cereb Cortex 11:946–953 Available at: http://www.ncbi.nlm.nih.gov/pubmed/11549617.

Zatorre RJ, Belin P, Penhune VB (2002) Structure and function of auditory cortex: music and speech. Trends Cogn Sci 6:37–46 Available at: http://www.ncbi.nlm.nih.gov/pubmed/11849614.

Zohary E, Shadlen MN, Newsome WT (1994) Correlated neuronal discharge rate and its implications for psychophysical performance. Nature 370:140–143 Available at: http://www.ncbi.nlm.nih.gov/pubmed/8022482.

Zylberberg J, Cafaro J, Turner MH, Shea-Brown E, Rieke F (2016) Direction-Selective Circuits Shape Noise to Ensure a Precise Population Code. Neuron 89:369–383 Available at: http://dx.doi.org/10.1016/j.neuron.2015.11.019.